1-1-2015

Hybrid Enhanced Epidermal Spacesuit Design Approaches

Joseph M. Jessup

HYBRID ENHANCED EPIDERMAL SPACESUIT DESIGN APPROACHES

by

Joseph M. Jessup
Bachelor of Arts and Science (BGS), University of North Dakota, 2013

Thesis

Submitted to the Graduate Faculty of the

University of North Dakota

in partial fulfillment of the requirements

for the degree of

Master of Science

Grand Forks, North Dakota
December
2015

This thesis, submitted by Joseph M. Jessup in partial fulfillment of the requirements for the Degree of Master of Science from the University of North Dakota, has been read by the Faculty Advisory Committee under whom the work has been done and is hereby approved.

Dr. Pablo DeLeon

Dr. Vadim Rygalov

Dr. Warren Jensen

Dr. Dmitri Poltovski

This thesis is being submitted by the appointed advisory committee as having met all of the requirements of the School of Graduate Studies at the University of North Dakota and is hereby approved.

Wayne Swisher
Dean of the School of Graduate Studies

December 8, 2015
Date

PERMISSION

Title Hybrid Enhanced Epidermal SpaceSuit Design Approaches

Department Space Studies

Degree Master of Science

In presenting this thesis in partial fulfillment of the requirements for a graduate degree from the University of North Dakota, I agree that the library of this University shall make it freely available for inspection. I further agree that permission for extensive copying for scholarly purposes may be granted by the professor who supervised my thesis work or, in his absence, by the Chairperson of the department or the dean of the School of Graduate Studies. It is understood that any copying or publication or other use of this thesis or part thereof for financial gain shall not be allowed without my written permission. It is also understood that due recognition shall be given to me and to the University of North Dakota in any scholarly use which may be made of any material in my thesis.

Joseph M. Jessup
December 7, 2015

TABLE OF CONTENTS

LIST OF FIGURES

LIST OF TABLES

ACKNOWLEDGMENTS

I wish to express my sincere appreciation to the members of my advisory committee for their guidance and support during my time in the master's program at the University of North Dakota.

Vadim Y. Rygalov, Ph.D., Mathematical-Physical Sciences,

thank you for always encouraging me to not let others' limitations become mine.

ABSTRACT

A Space suit that does not rely on gas pressurization is a multi-faceted problem that requires major stability controls to be incorporated during design and construction. The concept of Hybrid Epidermal Enhancement space suit integrates evolved human anthropomorphic and physiological adaptations into its functionality, using commercially available bio-medical technologies to address shortcomings of conventional gas pressure suits, and the impracticalities of MCP suits. The prototype HEE Space Suit explored integumentary homeostasis, thermal control and mobility using advanced bio-medical materials technology and construction concepts. The goal was a space suit that functions as an enhanced, multi-functional bio-mimic of the human epidermal layer that works in attunement with the wearer rather than as a separate system. In addressing human physiological requirements for design and construction of the HEE suit, testing regimes were devised and integrated into the prototype which was then subject to a series of detailed tests using both anatomical reproduction methods and human subject.

CHAPTER I

INTRODUCTION

From the earliest hominin Sahelanthropus tchadensis, to the loss of body hair and development of sweat glands in Homo ergaster and evolutionary Ice-age modifications of anatomical body surface are120a, the epidermis in particular plays a vital role for Homo sapiens. The human organism has evolved and has been continuously modified around a comparatively narrow set of planetary environmental conditions. Reduced to simplest form, Earth's atmosphere provides the elements necessary for both aerobic respiration and evolved human thermal control in its own enclosed recirculating system of material flows. Habitable atmospheric pressure, temperatures and gas mixtures are primary design principals of conventional space suits. Contemporary space suits mimic these surrounding environmental conditions for the wearer, and these artificial environmental conditions are translated as tolerable by the human physiological system as a temporary analog of habitability.

Space Suits in EVA

In essence, the modern space suit is primarily a spacecraft, which in turn relegates mobility, and comfort to secondary design consideration. Sensory, kinesthetic and motor functions which are normally taken for granted become severely limited. Each multiple layer which serves its own independent and specific function (e.g. LCU layer for thermal control) can be considered multiple barriers to movement and the

human sensory experience. Although designed for comfort and habitability, ergonomics becomes the wild card in any space suit variant, and at best the differences in the fundamental design configurations are almost nil. The current U.S. space suit is comprised of 14 layers of various materials, with just the LCU comprising the first 3. Other layering includes multiple Mylar, bladder, shape retaining layers and protective outer shell. Even with mobility refinements focused on the arms and glove segments for EVA work related activities, current suit designs resist to varying degrees any movement from the wearer that deviates from its original manufactured geometry.

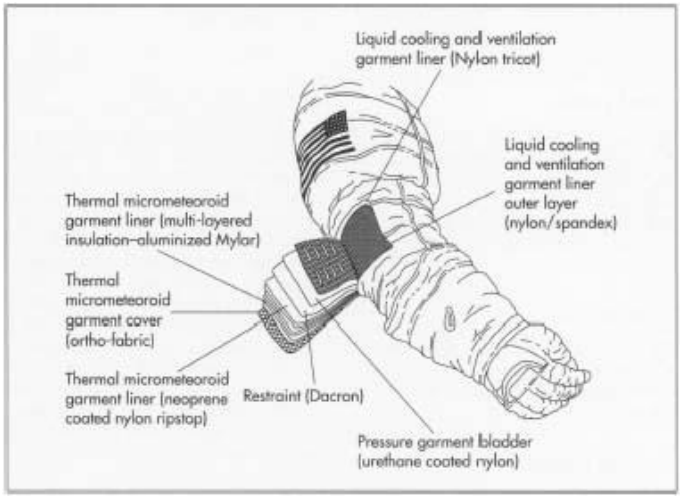

Figure 1. Conventional material layers.

Internal Gas Composition

Current space suit design utilizes atmospheric pressures down to 4.5 P.S.I with a 100% oxygen atmosphere to both maximize flexibility and provide adequate amounts of breathable oxygen content. With lowered suit pressure for mobility advantages, also come trade-offs in pre-breathe time regime, and the lower limits of hypoxia in the instance of a suit malfunction or puncture on any part of the surface area. The difference

between life and death depends on maintaining atmospheric pressure through the entire suit from boots to helmet. A single leak can compromise the entire system, with inevitable blackout of the wearer occurring in a matter of seconds. Even a slow leak and partial depressurization can cause hypoxia, with symptoms that include loss of color vision, confusion and eventual loss of consciousness.[1]

Thermal Control

Conventional space suits rely on a separate subsystem known as the Liquid Cooling Undergarment (LCU). Similar to knitted thermal underclothing, the LCU employs long continuous and parallel lengths of flexible tubing used to circulate coolant over skin surfaces. In space and low pressure atmosphere, thermal convection diminishes to the point of the human bodies' own metabolism becoming a dangerous heat source, and potential for hyperthermia. To counter this problem, the LCU is the standard solution, though it carries its own risks. The recent near-drowning of Italian Astronaut Luca Parmitano demonstrates the inherent disadvantages of an unintegrated system. As the faulty LCU leaked coolant into the spacesuits pressure garment, water migrated into Parmitano's helmet, eventually covering the nose and eyes. It was only from memory that Parmitano was able to make it back to the airlock after the EVA was terminated. Parmitano's most ominous comment was that he was not sure when his next breath would fill his lungs with water instead of air.[2]

---

[1] Ment, Gilles. "Operational Space Medicine." In *Fundamentals of Space Medicine*, 283-284. El Segundo, Calif., CA: Springer, 20011.

[2] Spotts, P. (2014, Feb 27). Near-drowning of astronaut tied to wrong diagnosis, slow response. *The Christian Science Monitor* Retrieved from http://ezproxy.library.und.edu/login?url=http://search.proquest.com/docview/1502915471?accountid=28267

Figure 2. Liquid cooling undergarment.

The disadvantages of a non-unified system become apparent with the potential injury or loss of a crewmember during what should be a relatively simple subsystem like the LCU.

Operations and Habitability

The average safe operational duration for a typical gas pressure space suit EVA is around 6 to 8.5 hours under normal working conditions[3]. The basic necessities for the three major life support functions, including thermal control and drinkable water are provided to the operator. EVA tasks are designed around the operability and limitations of the suit, rather than designing the suit around required tasks. Various design

[3] HSF." HSF. April 7, 2002. Accessed November 26, 2015. http://spaceflight.nasa.gov/shuttle/reference/faq/eva.html.

proposals for improvements have been considered for mostly mobility and donning/doffing. With each new generation of conventional gas pressure suit, a certain amount of trade-off in functionality vs. bulk must be incorporated. A rear hatch for ingress/egress is made possible with reduced visibility of the helmet component. A hard torso allows simplification of design and assembly but with added weight. The quality of space suit habitability affects operations, and inversely, strenuous operations can greatly reduce habitability.

Summary of Problems in Current Space Suit Design Approaches

Current design concepts focus on improving existing concepts, with no real departures from basic design formula. Each unintegrated system component implies a separate system with its own separate weaknesses and identifiable points of failure. It has become evident that space suit habitability using standard design principals and construction methods has reached the apex of technology, therefore it is preferable that new design approaches and construction methods are utilized that exploit advancement in materials.

Since the introduction of the conventional gas space suit, functionality has remained unchanged. In most simple terms, the physical limits of human engineered mimic of Earths' natural envelope has been reached. Air in the gaseous state required by humans cannot be engineered in any way to overcome the limitations of design and materials technology.

Potential Solution and Prototype

Mechanical counter-pressure (MCP) space suits have been considered as an alternative to conventional gas pressure suits for several decades. In theory, MCP space

suits offer the possibility for increased mobility and decreased mass for the astronaut during planetary exploration. The objective of this concept offers many advantages, but in practice offers few workable results as a practical application given current TRL's. The concept of applying surface pressure through experimental woven, braided and knitted fabrics of Spandex and Elastic is the design driver behind the MIT Biosuit concept. Many attempts to create an evenly distributed surface counter pressure have increased complexities in the fundamental concept, and created stumbling blocks for other important systems vital to homeostasis in extreme environments.[4] Mars' mean surface atmospheric pressure of 600 Pascal's (0.087 psia) implies that radiation rather than convection is the dominant heat exchange mechanism at average elevations. This raises serious problems that are currently only secondary considerations in current MCP design attempts given the metabolic heat generated by the human body even in a resting state in such low pressures. Other technical uncertainties are durability of woven materials in dusty lunar or Martian environments, and maintaining proper tension on the popliteal fossa, antecubital fossa and axilla.

A new approach to an old problem of space suit mass and mobility is essential. A design concept that works as an extension of the human integumentary system, rather than against it (literally the case with MCP) is needed.

[4] Patel, Samir S (October 20, 2005). "This suit is made for walking (on Mars)". The Christian Science Monitor. Retrieved 2015-10-14.

Integrated Thermal Control and Mechanical Counter Pressure

Special attention was paid to thermal control, specifically body core and skin surface temperature. In considering Mars as just one example of prospective applications, convective cooling models indicated the need for forced body surface cooling for any variant of non-gas inflated space suit. Further research revealed the importance of active full body perspiration monitoring and countermeasures. Integrated multi-channel thermal control was designed specifically to address body temperature, suppression of perspiration for the wearer and reduced system mass. The prospective thermal transfer efficiency of the cooling system was calculated using test samples of HEE material with embedded cooling components, and then implemented and tested on the functional prototype test suit. The initial areas of interest were the suppression body perspiration and core body temperature stability.

Target body surface temperatures are regulated to a stable < 36-37C as a countermeasure to the production of skin surface perspiration[5], a critical control function that current MCP suit proposals have not addressed. Movement by wearer would be far less restricted in the HEE concept, as the material hydrostatically shifts around joints while retaining vital surface tension on body surfaces. Physical and psychological stress factors can be expected to be reduced due to greater freedom of movement and reduced catastrophic decompression risks. The variety of different components and mass of the HEE design is far less than a conventional space suit, increasing reliability and functionality. Human-machine integration parameters would

[5] Nadel, Ethan, Robert Bullard, and J A Stolwijk. "Importance of Skin Temperature in the Regulation of Sweating." Journal of Applied Physiology 31, no. 1 (1971): 80-87. Accessed October 12, 2015. http://jap.physiology.org/content/31/1/80.long.

be enhanced, control interface limitations greatly reduced and design functionality easily expanded during the fabrication layup process. In summary, the HEE design concept is based on the design philosophy that 4.5 P.S.I pressure will be achieved and maintained from the body's own internal dissolved gas pressure, with the HEE layer being the semi-flexible barrier that keeps epidermal surface geometric stability. This is a somewhat paradoxical answer to the MCP approach of external counter pressure to human body surfaces.

Suit Materials and Functional Integration

The HEE concept represents a departure from conventional gas pressure suits not only in its design philosophy, but also the materials utilized in its construction. The foundation of the suit's functionality is the HEE layer, which is an actively constricting artificial epidermal layer that combines microprocessor controlled thermal regulation and active/passive surface tension that mimics human skin through biotechnical polymers currently used for treatment of burn victims. Hybrid Epidermal Enhancement integrates multi-functionality into a single layer during the HEE layup and construction process. A microfiber layer borrowed from dry suit technology forms the wicking contact surface, and is laminated with Shore-A 00-10 Bioflex gel which serves as both a buffer to equalize and distribute applied pressure between body surfaces as a confining layer, and as a thermal conductor that enhances HEE suit's convective cooling system.

A thermal control mechanism in the form of 100m of surgical 1/16" PVC tubing is installed over the microfiber layer followed by a laminated Bioflex℗ layer. The outermost embedded layer is a polymer 1/8" weave micro-mesh that is bonded to pneumatic actuators, forming a floating compressional confinement layer. This layup

process creates a garment that allows easy donning and activation, causing the epidermal layer to constrict evenly and maintain geometry of the body surfaces. This concept is not MCP per se, as the HEE is designed to hydrostatically balance pressure over uneven body surfaces and conform to the wearer's anatomy in response to the wearers own internal dissolved gas pressure. Hydrostatic balance is designed to be dynamically maintained during all motions of joints and limbs, as the attributes of the HEE gel limb joint segments are designed to seek voids (body surface depressions) through their semi-viscous physical nature. The properties of HEE allow efficient thermal conduction through the material adjacent to the cooling tubing, and active thermal stability via embedded sensors controlling liquid cooling flow rates. Significant integration between helmet atmospheric pressure and the unconventional HEE layer was accomplished by utilizing a composite clamshell style hard torso. The HEE suit hard torso fulfills several roles. Most importantly, its potential to compress the transitional seal of the pressurized helmet neck liner to the HEE suit layer was immediately obvious. The next logical application was to utilize the hard torso as an additional abdominal pressure containment layer over the underlying HEE. garment, as well as providing the site for application of RST Demron radiation shielding. As the fabrication of the composite torso progressed, further integration was achieved by directly mounting the LSS system backpack housing to the rear segment of the clamshell hard torso. This synthesis of design created a one piece unified hard torso and LSS unit that can be donned without assistance. Other important advantages of this configuration include excellent distribution of the backpack mass over the entire torso, and added protection for vital organs. Throughout the entire design and construction

process, multi-functionality was the foundation of HEE design. Every material and component was designed to augment other materials or components wherever possible.

CHAPTER II

METHODOLOGY

Chapter II serves in part as an introduction to the concepts behind the design. The methodology used to design and construct the prototype Hybrid Epidermal Enhancement (HEE) space suit utilizes an approach oriented around enhancing the existing capabilities of humans as a species already evolved around 1 Earth atmosphere, but with complemented protective properties. A conventional gas pressure suit is designed to counter adverse environments by replicating Earth's atmospheric conditions. HEE aims to enhance the human bodies existing resistance to adverse environments. The main design drivers that emerged were identifying critical points of human homeostatic control. Instead of a gas envelope for internal and external pressure equalization, HEE uses the body's own internal pressure to achieve hydrostatic equilibrium against a semi-flexible augmented artificial skin based on an enhanced version of classic decompression theory modelling.[6] Furthermore the countermeasure for ascertained perspiration and humidity is the through the direct suppression of perspiration activation by the eccrine and apocrine sweat glands, which are directly controlled hypothalamus, and stimulated by a combination of internal body temperature and mean skin temperature.

[6] Wienke, Bruce R. Basic decompression: theory and application. Best Pub Co, 2008.

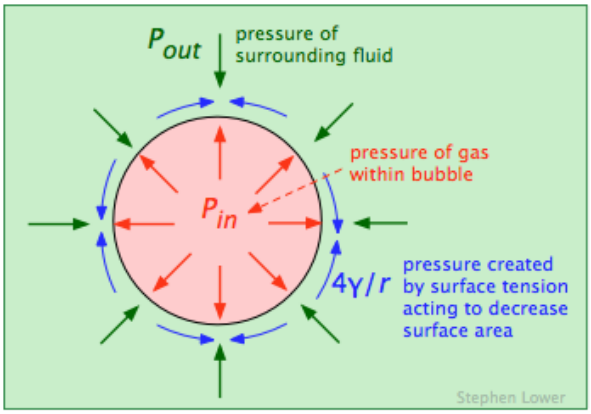

Figure 3. In equilibrium the internal pressure in the bubble is equal to the sum of the ambient pressure.
http://chemwiki.ucdavis.edu/Textbook_Maps/General_Chemistry_Textbook_Maps/Map%3A_Lower%27s_Chem1/07%3A_Solids_and_Liquids/7.4%3A_Liquids_and_their_Interfaces

To keep within the scope and limits of a thesis, the primary focus of this study is human thermal stressors, and the effect of countermeasures within the broader context of such an operational body conforming system. The results are analyzed within the operational environment and limits of the suit constriction functionality, life support system, and anthropomorphic mobility. The research and design process was iterative and in a constant state of flux as material research necessitated new and unorthodox construction techniques. Materials selection was an iterative process as well. The basic foundation of the HEE concept was the ability of a material to redistribute epidermal surface pressure against the epidermal layer in a manner that would cause a semi plastic state of hydrostatic balance in both actual pressure, and body surface geometry. This unique requirement mandated the need for unconventional materials. The basic design problem was not so much the ability to create a semi-immovable barrier against tissue expansion, as it was allowing the wearer to don the suit before functionality is implemented. With this in mind, it became apparent that the suit must have two separate

states; a relaxed state, as well as a tensional state. It was determined that the best combination of materials which could fill these requirements would be those based on prosthetic and bio- tensional state, reached through an integrated, 3-component design process. Pneumatic actuators placed longitudinally on the frontal plane of the suit constrict a layer of 1/8" polyester Micro-Mesh. The advantages of the Micro-Mesh is its ability to conform to the variable cross-sectional sizes of the human form through its hexagonal weave with minimal distension. The second mechanism of HEE is the Bioflex gel laminate layering. Its primary purpose is for further distribution of surface tensional pressure, but major integrational advantages were identified. The gel laminate consists of two different hardness levels of Bioflex gels based on the Durometer Shore Hardness Scale.[7] When layered properly the laminate in conjunction with the base micro-weave skin contact layer tends to always pull inward without wrinkles or folds. The gel laminate layer provides increased thermal transfer efficiency as it conforms around the circular cross section of 1/16" PVC cooling tube matrix. Another advantage observed was the gel's ability to contain water leaks that might arise in the coolant circulation tubing.

[7] A. W. Mix and A. J. Giacomin (2011), Standardized Polymer Durometry, Journal of Testing and Evaluation, 39(4), pp. 1–10.

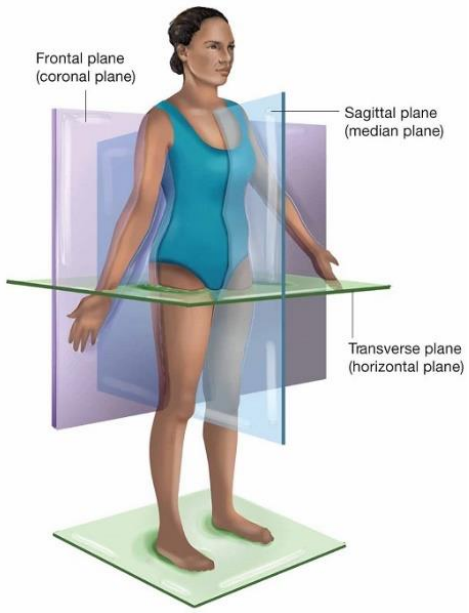

Figure 4. Anatomical planes of the human body.

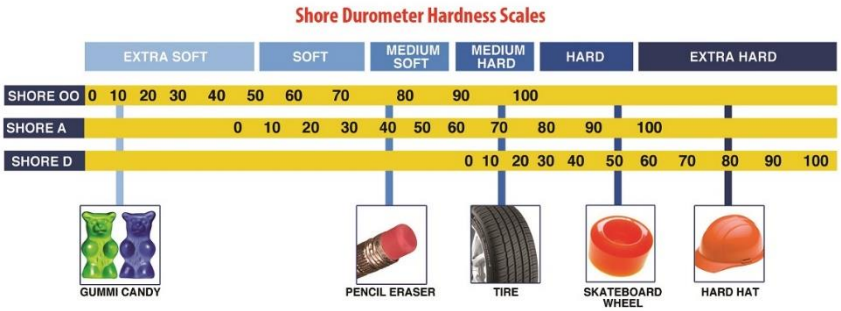

Figure 5. Shore Durometer Scale of Hardness.

A mechanism was devised to address the problem of tension on anatomical areas of depression such as the popliteal fossa, antecubital fossa and axilla. Analysis and experimentation led to the development of gel filled cells consisting of Shore 00-00 hardness gel in polyethylene liners resembling breast implants. These cells when placed snugly to the posterior of the knee or inside the elbow joint, flow in a semi fluid state seeking anatomical indentations and depressions. The flow increases in direct relation to the tension applied by the micro-mesh tensional layer. This design allows geometric variability and shape shifting that cannot be matched by 2-dimensional textiles or other types of materials currently being considered.

Although liquid cooling thermal control is required for typical EVA scenario, the HEE space suit utilizes a more advanced version of body cooling through active sensor and pump loop feedback control on multiple channels. The main considerations in such a scenario besides simple core body temperature homeostasis are wearer comfort as well as hygiene, requiring special attention and made necessary by the close fitting epidermal layer. As described on previous pages the liquid cooling works under the same thermal transfer principals as a standard Liquid Cooling Undergarment (LCU), but with some major control differences. The nature of a gas pressure suit facilitates the need for a sublimator, because much of the body's emitted humidity is circulated through the atmospheric pressure envelope as part of the oxygen circulation system.

Because HEE uses surface tension, a solid state control system capable of monitoring and reacting to body temperature in one-second intervals is utilized. In designing the thermal regulation system, several enhancements were incorporated into the liquid cooling matrix. Cooling tubing diameters were decreased, and counter-

directional coolant flow was introduced for increased thermal exchange and stability. Using a combination of sensor input and reactive pump control, the multi-channel microprocessor regulates body surface temperature similar to the human bodies own hypothalamus, in effect an enhancement of existing biological regulatory systems. The objective of this system was the minimization of perspiration and moisture, and body temperature regulation. Complete engineering and operational details are described in following sections of this document.

The designation Hybrid Epidermal Enhancement (HEE) derives from the implementation of conventionally gas pressurized helmet and actuators, and the unconventional materials and engineering used to achieve internal physiological homeostasis. The technical challenge of integrating the transition between the HEE layer and helmet was addressed through the use of a fiberglass/carbon fiber clamshell hard torso. The torso is able to open to allow easy donning without assistance. The torso halves are lined with a hydrostatic compressional layer, and provide additional abdominal rigidity in conjunction with HEE actuation. This functionality provides stability in conjunction with the integrated Portable Life Support System (PLSS) backpack. The load to the wearer is evenly distributed over the torso, and serves as the interconnect between sensor wiring and liquid cooling tubing route directly through the backpack to the suit without the need for external cables or hose. A second important function of the hard torso is the transitional interface between HEE and the atmospheric pressure of the helmet. The donut seal located at the base of the pressurized neck liner is compressed to the shoulders and upper body when the hard torso is strapped down securely.

Two workable Helmet designs were tested with varied configurations. The first design consists of an accordion polymer material encased in a segmented flexible neck. The base of the neck seats into the hard torso the neck opening with the seal accomplished upon closure of the torso halves as described previously. The second neck design uses the same pressure transition, but has a pleated layer of ballistic nylon combined with a latex rubber liner, and stationary bubble-style helmet configuration. The methodology of helmet design and construction was based on qualitatively determining the best helmet solution for such a suit. Additional technology in the form of color coded system status indicators were installed into the test helmets for evaluation as a simple HUD in peripheral vision.

Though not the central focus of research, boots and gloves were also designed and constructed using both conventional and unconventional materials. The design of the gloves incorporate a flexible liner, constricted joints, a segmented semi-flexible Cordura ballistic nylon exoskeleton around fingers, and back of hand. The gloves are lined with Bioflex and wicking liner. Compression is achieved when wrist ring is locked forward, forcing the Bioflex gel lining into hydrostatic equilibrium around the entire epidermal surface of the hand. A test glove and components underwent preliminary pressure testing in both sub-atmospheric pressures and a hard vacuum

The Boots are a composite heavy rubber material layered with ballistic nylon and lined with inflation bladders similar to standard high altitude flying boots. The main difference is that instead of pressure being relieved from the internal bladders during ascent to altitudes, pressure is actually increased via connection fitting from suit leg actuators. The cell walls are reinforced to allow for ~300-315 Mb (4.5 p.s.i) inflation

without danger of rupture. An Ecoflex liner similar to the gloves is compressed by the bladders to achieve hydrostatic equilibrium within the boot, fully compressing all surfaces of the human foot and toes. The research regime was based on component testing in context of the fully constructed and integrated system. Although individual characteristics such as analysis of thermal cooling efficiencies and relative body surface pressure were tested as both individual component variables, quantitative and qualitative testing required design and construction of a fully functional and complete space suit. Movement under varying conditions in the confines of a fully fitted suit can create variations of surface tension (relative surface pressure). Surface tension can directly influence thermal cooling efficiencies. The mass of the backpack, hard torso and helmet add extra physiological stressors that can only be properly evaluated as part of the unified and assembled system.

The purpose of this thesis is to chronical phases of physical suit construction, electronics design configurations, sensor calibration and programming, as well as human test methodology and results. The project is documented step-by step with the inclusion of supported working assumptions, materials research and application, component fabrication details and testing methods. In an attempt to present information in a logical manner understandable by the reader, this document is categorizes the evolution of the project in both theory and application, considerations for integration, surface tension and thermal control concepts, and all subsystem design approaches and operational envelopes.

Although a considerably complex project in pursuit of alternative mechanism for human homeostasis in open space, extensive effort was made to record and transliterate

operational theory put into practical working application within the bounds of a thesis document. When applicable, visual tools including diagrams and illustrations are included where pertinent text information requires the use of visuals for clarification. Testing and data collection for proof-of concept was implemented during initial materials research, active phases of suit construction, and human subject activity. Test data utilized pressure, thermal, humidity and galvanic sensors, as well as electronic scales for pressure sensor calibration. Complete details are discussed in Chapter III under section Experimental Approaches.

CHAPTER III

PROJECT DEVELOPMENT

Multi-functional Integration into Single System

The path to an experimental non-gas pressure space suit that also had largely unified system components emerged somewhat unintentionally during the initial phases of research in late 2013. The development of this project began by establishing several basic requirements for an unconventional non-pressurized space suit. The principal design driver was the realization of a workable non compressed gas space suit that (a) provides stability of internal gas pressure for the wearer, and (b) achieves this objective in a tangible manner that can be applied to real world applications outside of a research facility. This requirement implied that it must provide a mechanism to change geometry in order to be donned, as well as to provide the necessary surface tension for the user once it is in place. Ideally, such a system would also have to afford all of the protection parameters of a conventional suit, while increasing mobility several fold and decreasing system mass. This desire to devise a lightweight, low-profile design had significant influence on the evolution and final outcome of the finished suit.

From its inception it was clear that the research and development would need to be fully realized from start to finish, as this was an entirely self-funded, with no solicitation of funds from any organizations public or private. Such a proposition would require results that were more than conceptual mockups based on research restricted to

single components, and sometimes flawed or incomplete assumptions. Any viable alternative to a conventional gas pressure suit would have to provide the wearer with the full range of required functionality to maintain homeostasis in near or zero pressure space and planetary environments. Besides integumentary stability, thermal regulation for the wearer is a critical component of control that determines the success of any non-gas pressurized space suit. This realization coalesced around the first major integration of components, which in the final analysis was serendipitously based findings of material component properties testing early in the project. The characteristics of the materials and textiles that were envisioned, necessitated integration of the surface compressional layer with embedded thermal regulation matrix during the fabrication process. Thus the component termed the HEE layer was the first product of multifunctional integration, and serves as the core component of uniform epidermal surface tension, humidity control and perspiration suppression.

Figure 6. The Webb Space Activity Suit (SAS).

The next major integration in design emerged during the process of solving the problem of transition between the pressurized helmet and HEE tensional layer. This problem was researched and addressed to an extent with the Dr. Paul Webb Space Activity Suit (SAS) in the late 1960's.[8] On the Webb SAS, Positive pressure breathing was delivered by a helmet which was connected to a simple flow-through compressed air supply. The helmet sealed around the face and supplied pressure to the neck and most of the head by means of a bladder. Straps that looped under the arms held the helmet down snug to the shoulders. The air supply was worn using conventional straps, similar to a hiking backpack. The MIT Biosuit had minimal (nil) development toward resolution of the transition problem. There exists little or no documentation regarding a working helmet or seal, except for a mockup used for publicity photographs. Both the Webb SAS suit and the MIT BIOSUIT have a fixed bubble type helmet designs, with the Webb helmet functional and the MIT version a conceptual representation used for publicity photos.

Planning for the eventual construction of the PLSS backpack originally envisioned conventional straps similar to the Webb SAS design. As the HEE layer evolved it became apparent that in an environment affected by acceleration or gravitation forces, backpack straps had the potential to interfere with the HEE's embedded liquid thermal control matrix. Upon further consideration it was recognized that if a similar bubble helmet would be used, a second set of straps similar to the Webb helmet design would have to be utilized in order to achieve a hermetic seal to the body, moreover, this would be only a partial solution considering the other complexities of shoulder movement and distortions to body

[8] Webb, P. "The Space Activity Suit: An Elastic Leotard for Extravehicular Activity." *Aerospace Medicine* 39, no. 4 (1968): 376-83.

surface geometry caused by the underlying muscle, tendons and skeletal structures during even the most simple body functions, such as a deep inhalation.

The dilemma of a workable helmet seal was resolved by utilizing a two-piece clamshell style hard torso. The torso is hinged at the shoulders, slips over the wearers head, and fits snugly over the body, compressing the base of the flexible neck seal against the shoulders. The implementation of a hard torso also solved several additional engineering problems simultaneously. The straps for the PLSS backpack route through the posterior hard torso segment, follow over the shoulders, and are affixed to the inside of the anterior hard torso segment, pulling the torso halves together. Additionally, the entire PLSS backpack is rigidly mounted to the posterior segment of the hard torso. The result is an easily donnable, integrated one-piece unit that distributes the mass of the PLSS backpack over the abdomen, and seals the helmet's pressurized neck segment.

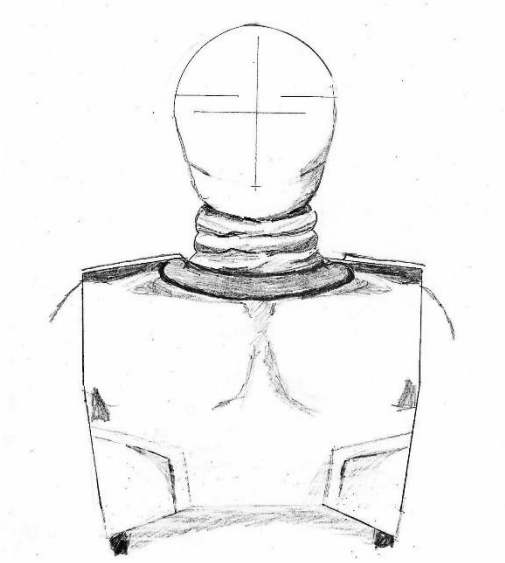

Figure 7. Design sketch of pressurized collar and compression.

Additional improvements were made by integrating torso radiation shielding, compressional Smart Foam to maintain abdominal geometric stability, and routing all sensor wiring and liquid thermal control tubes directly to the PLSS backpack. Another advantage of the torso to backpack integration was that it did away with the need for external cables and hoses. In summation, the clam shell hard torso option was the best choice to fulfil the roles of load-bearing, abdominal pressure stability, protection for vital organs as well as the solution for pressure to HEE tension transition.

Anti-expansion and Stability of Body Geometry

The approach of Hybrid Epidermal Enhancement (HEE) relates to the concept of the human integumentary systems evolved and inherent characteristics of astriction in the form of a protective external organ. Human skin by its very nature has a certain degree of surface tension that maintains stable body surface geometry. Numerous accounts documented in medical journals of skin distention as a symptom of edema, allergens, angioedema from anaphylaxis glean some insights into both elasticity and tensity of the human epidermis. A limited number of documented incidents regarding high altitude and decompression stress on humans are available in published academic sources, including NASA's *Bioastronautics Data Book*[9].

Research on decompression effects on humans was documented extensively by Emanuel M Roth his publication *Rapid (Explosive) Decompression Emergencies in Pressure-Suited Subjects*. While its focus is on decompression, and not the effects of long term vacuum exposure, including the results of decompression events involving humans.

[9] Parker, J. F. Jr., and V. R. Eds West. Bioastronautics Data Book. Second Edition. N.p.: Government Printing Office, Washington, D.C., 1973. Print.

The effects of explosive decompression are devastating on human physiology, as the description appropriately implies. The physiology of rapid decompression is examined in detail as transitional phases, in which pressure change across the chest wall, impulsive loading of the structures result in shearing of tissues similar to that found in a blast injury. Maximal expansion of the lungs and chest wall, disruption of tissue as tensile strength is exceeded. This is exacerbated with closed airways. Pulmonary hemorrhaging, edema and penetration of bubbles into the bloodstream as a high pressure gradient forms between the alveoli and pulmonary veins. Gas emboli eventually reach the bloodstream, and through arterial circulation. Exposure to the vacuum for several minutes will lead to further lung damage, and is considered a direct trauma to the lungs preceding eventual death[10].

There are several cases of humans surviving exposure to vacuum worth noting. In 1966, Jim LeBlanc, a technician testing a space suit in a vacuum simulator, was subjected to a rapid loss of suit atmospheric pressure due to a faulty hose coupling failure, disconnecting the pressure line from his suit. He recalled the sensation of saliva boiling off of his tongue just before losing consciousness. The chamber was rapidly repressurized within less than a minute by supervising engineer Cliff Hess. At partial pressure restoration LeBlanc regained consciousness, and within minutes was walking normally, with aching ears from rapid repressurization being his only complaint. In another example, a man was accidentally exposed to vacuum in an industrial chamber; it was at least three minutes before he was repressurized. He required intensive medical care, but eventually regained full function. These accounts demonstrate that ebullism is

[10] Roth, Emanuel M. *Rapid (explosive) Decompression Emergencies in Pressure-suited Subjects,*. Vol. 1223. Washington: National Aeronautics and Space Administration; for Sale by the Clearinghouse for Federal Scientific and Technical Information, Springfield, Va., 1968.

not necessarily fatal, and in at least during early stages major organs of the human body remain intact and functional.

While many studies that focus on skin surface tension are primarily the research domains of pathology and dermatology, valuable findings have been gleaned from these research fields which imply workable solutions for a space suit that can essentially non gas pressurized. Hybrid epidermal enhancement is based on several working assumptions regarding the human body, deep diving, and space operations:

1. The human body in relation to internal absorbed gas pressure is composed of several different (virtual) compartments which are subject to permeability, diffusion, and can be considered similar to reduced gradient bubble model (RGBM)[11].
2. In a state of equilibrium the internal pressure in the bubble is equal to the sum of the ambient pressure and the skin pressure due to the surface tension.
3. It is not decompression that kills; it is the rate of decompression.
4. A certain amount of super saturation of a divers (or astronauts) tissue with dissolved inert gas is allowed in keeping with Haldane's classic decompression model. Human tissue is divided in a number of hypothetical tissue compartments, with a certain limit (M-value) is

[11] Wienke, Bruce R; O'Leary, Timothy R (13 February 2002). "Reduced gradient bubble model: Diving algorithm, basis and comparisons" (PDF). Tampa, Florida: NAUI Technical Diving Operations. pp. 7–12. Retrieved 8 August, 2015.

associated with each compartment to super saturation levels of dissolved inert gas in the compartment (tissue tension). This theory suggests efficient decompression by pulling the diver as close to the surface as possible with constraint that in all tissue compartments the super saturated tissue tension remains within the limits. These same rules apply to space operations, as combined and ideal gas laws work the same, regardless of operational environment. Optimization of this theory has been demonstrated with customized decompression steps.

5. The human integumentary system, including the epidermis and its various subcutaneous layers has its own degree of inherent surface tension similar to a bubble.
6. With the introduction of thermal and humidity points of control, anti-expansion mechanisms and a customized decompression schedule, the human body can not only tolerate, but maintain homeostasis without conventional gas pressure suits, or the current MCP spacesuit criterion of simulated 4.5 P.S.I counter pressure.

The HEE concept combines several key functions designed to minimize risks by applying technologies that augment human performance in extreme space and low pressure planetary environments. The human body is already equipped with its own evolved integumentary system. This innate human physiological component provides protection against extreme terrestrial environments when augmented with compatible technologies, for example an Arctic parka or scuba diving wet suit. These are relatively simple technical solutions that enhance human body surfaces for resistance to adverse

conditions than might otherwise be fatal otherwise. The human body's epidermal layers are capable of expanding over twice normal size in cases of edema, or shorter duration allergic reactions with few or no long term side effects due to properties of elasticity of the skin. The degree hydration, or moisture in the layers of skin has a direct relationship on the degree of elasticity. Dryer skin tends to have decreased ductility due to a combination of external environmental conditions, trans epidermal water loss and changes in density of the skin fiber system.

Much of the physiological research that would be beneficial for the concept of HEE remains outside of the academic realm, and what is available and published pertains to pathology and surgery technique. Some ancillary knowledge regarding skin surface tension can be gleaned from the study of *Langer's lines*, alternatively known as relaxed skin tension lines or cleavage lines. Langer's lines are directional lines within specific regions of human skin that give an indication of underlying collagen fibers in relation to flexibility, but these directional lines are not always a precise indicator of tensile strength due to differences between individuals, and changes in direction of these lines had been known to occur in individuals. The subject of dynamic mechanical properties of skin is complex, and poorly researched, as most studies are done on human cadavers of advanced ages. Adding to these complexities is the fact that skin is a multilayered material comprising three major layers, the epidermis, dermis and hypodermis. At rest, the fibers of skin appear orientated in a random configuration; however, once a load is applied, the fibers stretch parallel to the load direction. Initially, elastin fibers are thought to stretch in a linear fashion and, as the load further increases, the collagen fibers re-orient in order to carry a greater proportion of the load. The

epidermis being the outermost layer is considered the dominant factor when determining the properties of the skin such as the tensile strength of skin, depending on the size and degree of crosslinking of the collagen framework[12.] Although currently applications using Langer's lines data is mostly applied in the medical and pathology fields, progress continues in research and understanding of their implications for biotechnical applications. Although there are variations of factors including age, and individual differences that are not entirely understood, it is foreseeable that future research will create better physiological models that will have tangible value to future studies of humans in low or zero pressure atmospheres. Even in context of the currently narrow scope of understanding in the context of human space flight, it is clear that human skin has to a degree the ability to contain the force of internal dissolved gas pressures. This makes the application of enhancing these existing capabilities even more crucial in the pursuit of a better space suit that does not require a gas envelope, and works in concert with the human body. A workable HEE concept only requires a slight degree of balanced expansion against the constraint layer, as once again the concept works inversely from a standard MCP mechanism, with pressure and final stability deriving from internal gas pressure, not from an external garment.

[12] Gallagher, A J, Ni Annaidh, and Aisling; Bruyère, Karine; Et Al. "Dynamic Tensile Properties of Human Skin." 2012 IRCOBI Conference Proceedings, 2012. http://www.ircobi.org/downloads/irc12/pdf_files/59.pdf

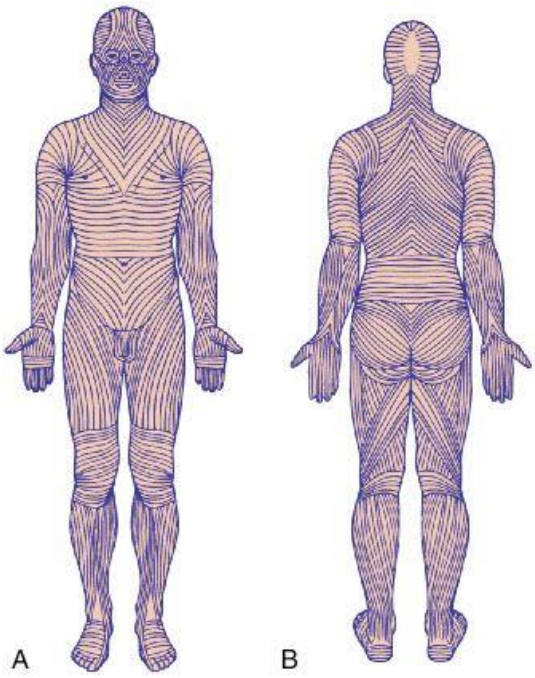

Figure 8. Lange's lines of skin tension.

Multi-channel Active Thermal Control

The primary research focus of this thesis in relation to the HEE space suit prototype is thermal control. In considering the severe temperature variations between exposure to direct solar radiation and shade, or day compared to night on a planetary environment with a marginal atmosphere, thermal control will be a critical part of space suit functionality. In a low Earth orbit EVA, temperatures differences of nearly 275°F (135°C) between the sunward facing side and deep space side, thermal convection is non-existent. Mars' average temperature is -80°F (-62°C), with great diurnal and seasonal temperature ranges, and a significant temperature gradient with altitude. The key thermal transfer component of convection is also severely diminished depending on atmospheric temperature and density at altitude. Radiation and conduction into regolith

or adjacent objects are the dominant heat transfer mechanisms on Mars. Typically on Earth or a gas pressurized space suit there are 3 mechanisms of heat transfer;

1) Radiation

The metabolic heat generated from within the body is emitted at UV wavelengths into the surrounding atmosphere.

2) Evaporation

Perspiration generated by the sweat glands is transferred to the surface of the skin. At normal atmospheric pressure a phase change transforms liquid into water vapor, while the liquid (perspiration) evaporative kinetic energy loss is felt as a decrease in skin surface temperature, and the natural result is a cooling effect, followed by subsidence of perspiration.

3) Convection

Convection is the process of air flowing over the skin and transferring body heat. This principal can be easily demonstrated in water. Convective heat loss can be minimized by staying still as possible in the water, creating a heated boundary layer next to the skin surfaces. Rapid motion in water disrupts the boundary layer of warmer water, increasing heat loss. The same effect is demonstrated in everyday situations through the use of fans for cooling, or experienced as a breeze on a hot day, with its effectiveness increased in combination with perspiration.

In a vacuum, convection has been lost as an element for thermal control, with radiation, conduction being the primary avenue of heat dissipation. The Webb SAS suit

proposed the concept of flash evaporation for cooling[13]. The porosity of the suit material fibers in a near perfect vacuum allowed evaporation of the wearer's body perspiration. The result was a near instantaneous cooling effect that removed large quantities of heat from the body. In flash evaporation, perspiration in its liquid form changed state directly into vapor while passing through the suit material, which would then have changed into ice crystals. It can be surmised that because a natural heat boundary layer between the suit elastic and skin surfaces (similar to a wetsuit), the phase change to vapor would be slow enough to inhibit the accumulation of ice crystals in the material. While this is a scientifically sound approach to cooling, the porosity of the suit material needed for this type of method cooling also leave the skin surfaces exposed the hard vacuum of space, particle bombardment, and potentially caustic or abrasive contaminants in a planetary EVA scenario.

In the 1990's Honeywell, Inc., in collaboration with Dr. Paul Webb and Clemson Apparel Research, has developed a modern prototype of the original Webb SAS pressure suit[14]. The team tested several configurations of breathable polymers for EMU (Extra-Vehicular Mobility Unit) applications. Among the characteristics being tested were water permeability as a function of temperature, O2 permeability as a function of temperature, pressure, and resistance to ultraviolet light[15]. The proposed dense polymer

[13] Woods, Michael. "Toledo Firm Develops Light-Weight Space Suit." The Blade, October 2, 1969, Second News Section sec. Accessed August 8, 2015. https://news.google.com/newspapers?nid=1350&dat=19691002&id=au1OAAAAIBAJ&sjid=tQEEAAAAIBAJ&pg=5285,1040523&hl=en.

[14] Annis, J.F. and P. Webb. "Development of a Space Activity Suit." NASA CR-1992, Washington DC: National Aeronautics and Space Administration, 1971

[15] Gorguinpour, Camron et. al (2001), LPI "Advanced Two-System Space Suit". University of California, Berkeley CB-1106. Retrieved 2012-09-23. 95 KB PDF

membrane had the advantage of transmitting perspiration in a gaseous state through diffusion, acting as a semi-permeable membrane. The side of the polymer film with the highest concentration gradient diffused through the film to establish equilibrium. The benefit of this property is that the rate of transmission for a specific density of these barrier films was a function of vapor pressure difference over film thickness, as sweat/gas arrived on the inner side of the membrane and exited as a vapor or gas[16]. Liquid could not transfer through the polymers.

There are obvious advantages to this type of cooling scenario, primarily its simplicity of design and the physical mechanisms at work are based on simple physics of pressure gradients and equilibrium similar to a cellular membrane. A higher level of protection against the hard vacuum of space, or adverse planetary environments is also afforded by such a system. This type of breathable polymer could be implemented into the HEE layer with the embedded liquid cooling system to give an even greater degree of control. With further research, the HEE's cooling could be used to control the rate of diffusion between liquid to vapor. This would essentially make this type of "breathable" membrane system function more as a humidity control layer, while giving the HEE autonomous biofeedback thermal regulation system a broader and more responsive control algorithm.

Experimental Approaches

In consideration of the complexities of verifying the HEE concept as part of a technically feasible biomimic of the human integumentary system, the experimental

[16] Ward RS, White KA. "Barrier Films That Breathe". Chemtech. Nov. 1991: 670

procedures to test the concept of HEE ultimately required design and construction of a prototype suit. The experimental approaches utilized humans-in-the-loop (HITL) design, engineering, fabrication, and testing procedures[17]. The inception of the design process began with identifying performance prerequisites of the suit to formulate the developmental steps of subsystems. A derivative objective was to ensure that with each revision of fabrication methodology or materials selection, functional parameters would be improved. Some academic research of Mechanical Counter Pressure suits including the Paul Webb Space Activity Suit (SAS) and the MIT Biosuit was considered, but eventually it was determined their operational theories, materials and functionality were substantially dissimilar to HEE. It must be noted that the while the SAS had the most useful and pertinent data in the context of HEE development, both aforementioned suit research programs helped to rule out functionality concepts, fabrication techniques and materials for HEE.

The initial concept of body surface tension stability commenced with materials research, experimental construction techniques, and fabrication samples. With the development of a particular component came requirements necessary for its integration into other components of the suit, and eventually integration into a unified system. The experimental testing as well as design approaches were a multistep and iterative process, with each revision in material application, a modified construction method was required, and often testing methods were revised or redesigned. The focus of thermal control, epidermal stability and anthropometrics testing procedures were highly dependent on the iterations of suit evolution. This evolution was necessitated by the need to replicate

[17] "DoD Modeling and Simulation (M&S) Glossary", DoD 5000.59-M, DoD, January 1998 [1]

the functional characteristics of a human organ. The integumentary system as a multi-functional barrier regulates temperature, protects the body from various kinds of damage, such as loss of water, and abrasion from outside[18]. These same elements of regulation and protection had to be replicated as a form of human enhancement by virtue of the laws of thermal exchange and mobility working as virtual analogs. Each one of the points of control had to be accounted for and implemented into the HEE layer suit design.

With each iteration or modification of a suit component, solutions to the original design prerequisites tended to improve, and in the instance of the suit's skin surface contact layer, research findings necessitated a total redesign and an additional 4 months rebuild time. The testing regime at each step went from conceptual to physical, with some instances leading to redesign of a subsystem (suit component). In summary, the modifications or additions to the original HEE space suit system include a total redesign of the HEE contact layer and glove mechanisms, addition of pneumatic actuators, addition of hard torso with integrated backpack and implementation of three different helmet configurations.

The project time line was strictly adhered to when possible during the design process. Any shortcomings or delays encountered in component prototyping entailed a modification or redesign. It was decided to fully solve all architectural dilemmas throughout the course of project development, as the later integration procedures required all technical problems to be resolved. Let it be noted that the research

[18] Mclafferty, Ella, Charles Hendry, and Alistair Farley. "The Integumentary System: Anatomy, Physiology and Function of Skin." *Nursing Standard* 27.3 (2012): 35-42. Web. Retrieved 28 Sept. 1015.

conducted was preliminary in context of the complexity of the project, research is ongoing, and all solutions are subject to later revision and modification. While the HEE space suit prototype serves as a concept demonstrator, it is merely the first generation platform and at the time of this writing, design and construction revisions are being formulated. The following sections list materials types and manufacturing techniques of each component in step by step order of fabrication and assembly of the entire Generation-I HEE space suit.

Materials and Manufacturing Techniques

HEE layer

The investigation into suitable materials for the epidermal contact layer began with the notion that the choice of textiles and materials would have a defining impact in determining design and fabrication methods that would be implemented. Several sample garments of various materials and purpose were analyzed and deconstructed as part of initial research, including a wet suit, dry suit, and various Nomex flight suits, including a Russian VKK anti-G high altitude suit. Each garment was tested for mobility, and individual manufacturing details noted for reference. To be considered as a possible basis of design, the epidermal layer had to have several unique characteristics to be viable:

1) The foundational layer would need the ability to completely constrict over all body surfaces, including axilla, antecubital fossa and popliteal fossa.

2) The material used would have to both conform to the changing local topography of the epidermis, and equalize surface tension that would be introduced from a to-be-determined actuation mechanism.
3) The material would have to be able to be able to integrate a cooling system in the form of flexible tubing, as well as have the ability to keep the surface of the skin relatively perspiration free.

The lack of gas pressurization precluded the use of a sublimator, which on a conventional space suit plays a role in helping to minimize perspiration[19].

None of the test articles offered any of the characteristics needed to serve as even a minimum conceptual analog for the envisioned HEE layer. Both the wet-suit and dry suits lacked the structural integrity to be considered, and the Nomex based suits were deficient in their ability to conform to complex anatomical shapes, even when modified. While the VKK anti-G suit shared similar disadvantages of the basic Nomex flight suits, the compression actuators did offer potential for possible future integration into the HEE prototype. After an arduous search for a suitable foundational component, a microfiber bodysuit manufactured now defunct Australian company Easy-Therm was selected, and several of the last remaining examples procured from England. The Easy-Therm suits met all criteria of a workable HEE foundation. These suits were developed as an all-purpose, unisex undersuit, originally designed to wear under scuba gear, wet/dry suits etc. as a wicking and thermal layer. They are manufactured in one piece, with a stretchable neck for ease of entry. The fabric used is a single weave 85%/70D A+

[19] **J**ones, Harry. "Spacesuit Cooling on the Moon and Mars." *SAE Technical Paper Series* (2009): n. pag. Web. 28 Dec. 2015.

Nylon and 15% 20D Elastane, which gives it stretch and durability. The most important characteristic about the Easy-Therm suit is that can completely conform to all contours of the human body, leaving no areas of body surface without contact. The suits conform to body contours in a way that no other material researched could come close to matching.

With the problem of a form fitting bodysuit resolved, research commenced for the purpose of adding the constituent materials that would comprise its functionality and structure. Following completion of testing several different types of silicon and urethane substances, a polymer was identified that had the characteristic required for such a unique application. Known as Bioflex, the material is available in several different types of hardness, and is used primarily for prosthetics and bio-medical applications[20]. For the purpose of HEE space suit construction, a similar material called Ecoflex was utilized, which is nearly identical, but lacks the medical use certifications. A technique was then developed that involved using a small rubber squeegee to apply the Ecoflex gel in 3 layers onto the microfiber suit while it was mounted over a PVC mannequin. This method forced the gel into the microfiber weave while leaving exposed a thin embedded fibrous wicking layer exposed on the epidermal interior contact surface. Two additional coats provided additional strength, and served to embed the cooling tubing into the HEE bodysuit.

[20] Lamba, Nina M. K., Kimberly A. Woodhouse, Stuart L. Cooper, and Michael D. Lelah. *Polyurethanes in Biomedical Applications*. Boca Raton: CRC, 1998. Print.

During the Ecoflex coating process, over 100 meters of 1/16" PVC tubing was embedded into the suit. It was determined longer runs of the 1/16" vs shorter runs of 1/8" cooling tubing was a better option for several reasons:

1) Using the smaller diameter in greater combined lengths added a greater degree of cooling control through the use of a greater number of individual cooling pump motors and isolated cooling loops.
2) The smaller diameter allowed a thinner more flexible HEE bodysuit, cutting the weight factor by 50%.
3) Smaller diameter tubing has a better interior diameter-to- wall thickness ration, thus minimizing the risk of crimping, or being crushed during compression mesh layer activation.

The technically accurate term involving composite materials fabrication is *layup process*. An initial 24cm^2 HEE layer test section was constructed using the impregnation of microfiber combined with a bonding process for the cooling tube integration. The layup process began by using a life-size polyethylene mannequin to create a generally correct anatomical form for the microfiber base and associated layers that would be applied. The Easy-Therm body suit was placed over the wet-sanded and prepared mannequin, with careful attention paid to correct centering and fitting of the garment. Using a flexible rubber squeegee, a thin layer of Ecoflex gel was pressed into the entire surface of the microfiber layer, causing the entire body suit to shrink down to the mannequin's polyethylene surface. The next step was applying the roughly 100 meters (330 ft.) of cooling tubing using the thermal body mapping data described in Chapter III Testing Approaches. The tubing was routed in a redundant configuration, implementing

parallel lengths over targeted areas of the body that would allow counter-circulation to evenly distribute thermal transfer in the coolant contained within the entire liquid cooling matrix. Special attention was paid to ensuring that tubing would not interfere with mobility, or be compressed or subject to wall collapse during movement. Tubing application typically allowed a minimum of 3 independent directions of flow per anatomical cooling region. The tubing was then assigned a direction a flow by designating it to a particular cooling pump motor loop in the PLSS backpack. Ends of tubes were then numbered and labelled for future connectivity. Ethylene vinyl acetate and a second coat of Ecoflex was used for tubing installation, followed by a third coat over the entire body suit. All areas that were both major sources of heat radiation as well as responsive to surface cooling were considered part of the cooling matrix; primarily the abdominal anterior and posterior, arms, legs to the knee, and head via the helmet cooling loop. Spacing between the parallel lengths of tubing was also taken into consideration to allow the most efficient heat transfer in regards to the thermal conductivity of the Ecoflex layers. The problems of surface tension behind the axilla, antecubital fossa and popliteal fossa were addressed primarily during the HEE layer fabrication. For each of these areas, a composite cell was created, incorporating 00 hardness Ecoflex gel inside a flexible polyethylene plastic resin membrane. The size of the cells were dependent on the areas being applied, with each being installed by a layer of Ecoflex 00-10 gel, followed by compression mesh joints sewn over the cell. The compression mesh wraps tightly around each limb, and in the case of the elbow, is gathered and affixed to the olecranon (tip of elbow) This configuration takes advantage of the arms geometry during flexion, where the actual distance between the olecranon

(elbow) and cubital fossa increases, creating constriction. The semi viscous properties of the gel seeks hydrostatic equilibrium of pressure against what is commonly known as the inner elbow.

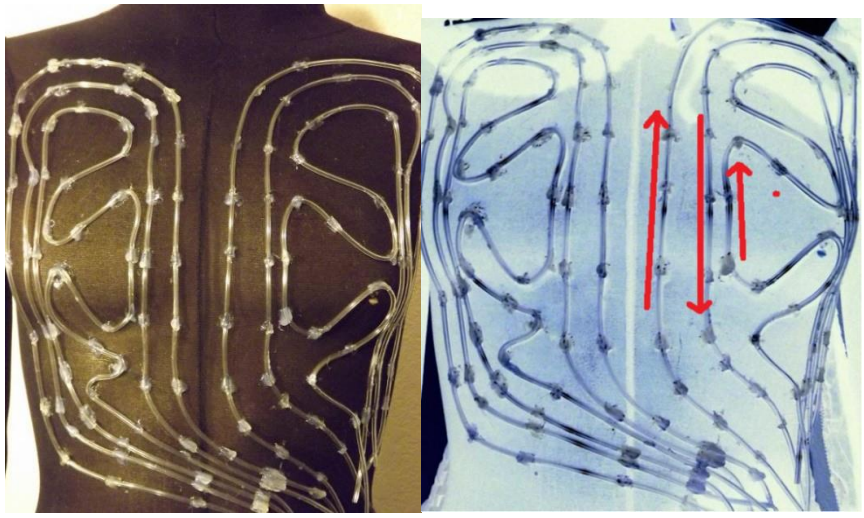

Figure 9. Parallel counter flow cooling matrix for uniform thermal transfer of body heat.

Figure 10. Cubital Fossa.

Figure 11. Semi-Viscous compression insert.

Figure 12. Cooling tubing under constricting layer.

Following completion of gel cell installation, the entire HEE under suit layer was integrated with the Micro-Mesh compression layer. This mesh layer is woven in a configuration that allows the surface area to shift with body movement geometrically on the planer 2 dimensional surface with minimal stretching or increase in actual surface area. Finally, the sensors for thermal, humidity and surface tension monitoring and control were embedded into the side of dominant laterality; which in this prototype is the left side of the body. The dominant side serves as the baseline for biometric readings responsible for controlling the HEE suit onboard cooling system. Sensor wiring and leads were carefully secured and routed for later connectivity to the PLSS backpack.

Hard torso and PLSS Enclosure

The core of the PLSS breathing apparatus consists of reengineered Soviet KIP-8 and IDA-71 rebreather systems combined into a single unit retaining part of the KIP-8 housing. Because the addition of pressurized counter lung, thermal control system and associated hardware would add extra weight and require more space, a lightweight polypropylene/polyethylene enclosure was selected to house the combined system. Serious consideration was given to the problem of supporting the mass of the backpack in both zero gravity and gravitational environments while avoiding the possible restrictions in the cooling system tubing matrix that might be incurred from conventional straps or harnesses. Integrating the backpack to the hard torso was the best solution to address the problem of load stability. The housing was fabricated from a commercially available enclosure with 3-1/4" bolts for direct attachment of the breathing apparatus to the rear segment of the torso. The remaining original straps of the rebreather were then routed through attachment point of the rear segment of the hard torso, and attached to the interiors of both anterior and posterior torso halves, which in effect distributes the backpack mass over the entire hard torso, minimizing the risk of restricting coolant circulation. The enclosure was then covered in a layer of Mylar and features a removable padded cover for protection. The hard torso was manufactured by hand using a form and fiberglass/epoxy laminate process, with metal added into the anterior half before final gel coat was applied.

Figure 13. PLSS housing fabrication.

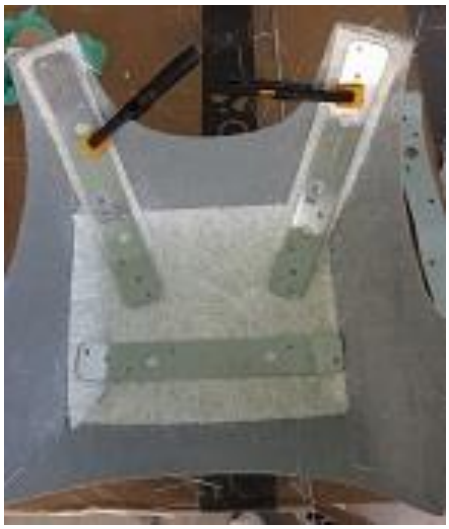

Figure 14. Hard torso fabrication and Lamination process.

Figure 15. Hard torso ballistic Nylon coating.

Figure 16. Mating PLSS housing and hard torso.

An essential feature of the hard torso is its two-piece hinged design. The torso opens similar to a clamshell with the hinge point at the top of the shoulders. This configuration allows a wearer to step under the unit, placing their head though the neck opening, while pulling the helmet ring seal through, and closing the torso halves without assistance. The upper and side friction straps are easily tightened by the wearer, creating both the hermetic helmet seal as well as the constriction over the thorax. The torso features a fibrous Smart Foam compression liner, rather than conventional closed cell liner. This circumvents the problem of air expansion in a vacuum which would be a detriment to conventional foam. The hard torso can be lined with a number of different types of radiation shielding for at least a degree of protection for internal organs, with Demron being the preferred shielding because of its low mass[21]. Other features of the hard torso include an articulated abdominal component, actuator air-line and coolant interconnects, external atmospheric pressure sensors, and wiring junction board on the anterior segment. The composite surface is covered with a layer of Dupont 1050D Cordura ballistic nylon, similar to the outer shell of the space suit garment for extra protection against abrasive elements. When fitted and secured down to the wearer, the hard torso, backpack and helmet function as a single unit, with flexible helmet collar giving the ability for head rotation, upward and downward movement with both the composite Mars prototype helmet, as well as the modified GSh-4MS helmet. The hard torso also allows free movement of the head inside the prototype bubble helmet as well.

[21] Chae, Myeong-Seon, and Bum-Jin Chung. "Radiation Exposure of an Astronaut Subject to Various Space Radiation Environments and Shielding Conditions." *Journal of the Korean Society for Aeronautical & Space Sciences* 38.10 (2010): 1038-048. Web. 8 Aug. 2015.

The input and exhaust air hoses are secured to the torso shoulders by straps, while allowing mobility it the two versions of articulated helmets.

Constriction Actuation

The basis of HEE operational design at first glance may seem similar to the Webb Space Activity Suit, or the MIT Biosuit, but there are fundamental differences in its functionality. The goal of HEE is to be several development steps ahead of the aforementioned MCP concepts through understanding of human physiological principals, and application of appropriate technological interactions. As stated previously, HEE operates with the human body in conjunction with internal dissolved gas pressure parameters, innate human homeostatic thermal regulation and the elastic properties of the human epidermal layers. The major differences in operations and functionality between HEE and mechanical counter pressure are as follows;

1) MCP attempts to replicate a pressurized atmospheric gas envelope around the wearer using constricted fabrics to apply even counter-pressure to the body surfaces[22]. In contrast, HEE uses constriction as part of the donning process. Once the suit is in place on the wearer, the contact pressure between the skin surfaces is generated from within the body, not from without, limiting tissue expansion.
2) While both MCP and HEE would use pre-breathing protocols, MCP is currently limited to the amount of surface tension that has been successfully applied; roughly 3.6 psi (190 mmHg)[x]. HEE uses a

[22] Obropta, Edward W., and Dava J. Newman. "A Comparison of Human Skin Strain Fields of the Elbow Joint for Mechanical Counter Pressure Space Suit Development." *2015 IEEE Aerospace Conference*

multistep protocol that reduces internal tissue compartment pressure, and allows for some instances of negligible skin puffiness (comparable to zero g flight), and statically counterbalances and buffers internal gas pressure through its pneumatic actuator system. The Micro-Mesh constricting layer allows for very little geometric expansion, and any expansion of body tissue that might occur during movement is transferred and counteracted against other body surface areas by the pneumatic actuators closed loop design, greatly reducing the risk of embolism.

3) HEE in combination with its accessory components is envisioned as a multi-use system, with built-in points of control and capability to maintain homeostasis in a variety of different environments including planetary, and long durations flight. The first generation HEE space suit is considered a technological demonstrator using conventional and unconventional materials for a unified non-pressurized space suit. The second and third generation HEE space suits will incorporate improved actuation systems, enhanced bio-monitoring, and remote tactile sensors transmitting spacecraft and life-support information directly to the wearer's nervous system. This is envisioned as an enhanced form of sensory perception that would for example, allow a wearer to detect micrometeorite impacts on a spacecraft hull, or sense spacecraft navigational orientation via induced vestibular stimulation. This would be a preliminary step towards man-machine sensor integration and eventually making physical human control interfaces obsolete.

Because the HEE suit was entirely self-funded with no outside assistance, there were budget constraints placed on certain components which were specifically chosen so as not to affect the functionality concepts. Out of expediency, it was decided that the pneumatic actuators for the constriction layer testing would be fabricated from the Russian VKK anti-g suit bladders. The VKK suit was completely dismantled and the bladders pressure tested for 24 hours. An off the shelf digital sphygmomanometer was modified with an addition of a pressure sensor to raise actuator inflation pressure near 3.8 psi (200mm Hg), though this is currently considered beyond minimal required pressure for the HEE concept. Materials research involved several months of testing different types of netting and meshes used in textiles and collapsible storage technologies.

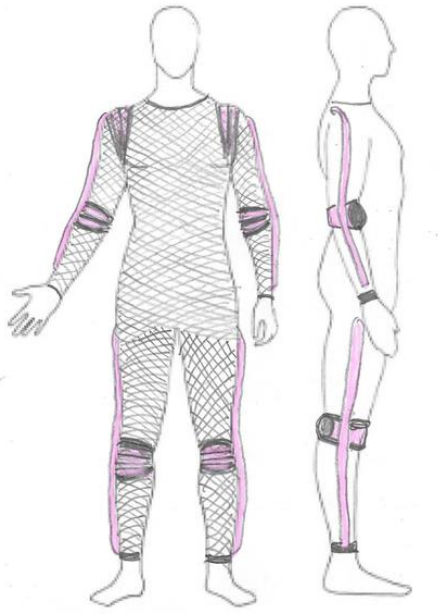

Figure 17. Compression netting preliminary design sketch.

Two configurations of micro-mesh were deemed to be the optimum material for transfer of pressure from the suits pneumatic actuators to the HEE surfaces. Both

versions of Micro-Mesh are very low stretch geometrically woven fabrics that allow distortion without losing tension. The finer 75- Denier polyester weave was used for the major anatomical surface areas, and the larger weave offering greater tensile strength was used principally around joints as its properties allow conformity to extended contours. The Micro-Mesh was first measured, cut and sewn onto the pneumatic actuators, then fitted to the HEE layer to achieve a reasonably snug fit over all surface areas. This method allowed quick installation of both the actuators and Micro-Mesh constriction layer due to the ability to adjust fit and snugness to the individual by gathering any areas that needed tightening. The mesh constriction layer was then attached to the HEE layer at interspersed points using heavy duty nylon thread. The result is a free floating mesh layer with the ability to conform around body surfaces, while at the same time allowing very little distension from outward force. Care was taken during the fitting process to ensure that in the actuators relaxed state the suit was easy to don and doff, while in the activated state all surfaces of the body are taut.

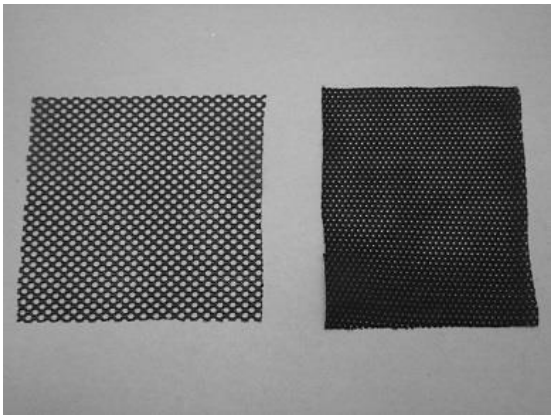

Figure 18. Polyester weave micromeshes.

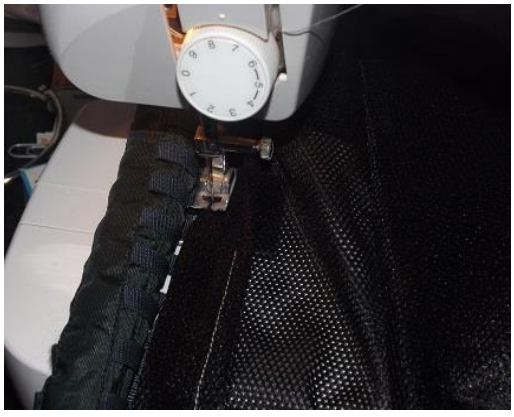

Figure 19. Air actuator installation.

Helmet variants

Helmet development for the HEE space suit consisted of 2 custom built conceptual helmets, and a heavily modified Russian GSh-4 pressurized helmet for initial pressurized neck seal testing. The rationale behind testing three variations was evaluating mobility and comfort of fixed bubble designs vs. floating helmets that move with motion of the head. These experiments also aided in refining the union between the helmets and the non- gas pressurized HEE suit layer.

The first project was to rebuild the GSh-4 helmet. An unissued helmet was purchased and completely dismantled for modification and adaptation for suit testing purposes. The major pressure components were discarded, and the modification and upgrade process included;

1) Disassembly of outer liner, latex rubber pressure bladder, as well as visor glass and seals. A new heavy duty latex and neoprene full hood was bonded to the existing visor pressure gasket, with a bellows neck seal added to the neck opening. Pliobond P-612-LV cement was used for all bonding of rubberized materials. The visor and new components were inflated to 4.5 psi and leak tested for 24 hours.
2) The oxygen hoses as well as exhaust and purge valves were removed from the helmet. The chin area was modified to accept one-way diaphragm valves for the checked flow of oxygen into the helmet, and exhaled carbon dioxide. A return line and quick disconnect housing was added for exhaust gas flow back to the PLSS system scrubber and recirculation system.

3) The visor was coated with a 15% gold Mylar film, and it was determined that the defogger system embedded inside the visor was rated at 28 volts DC, and left in place for possible future use.

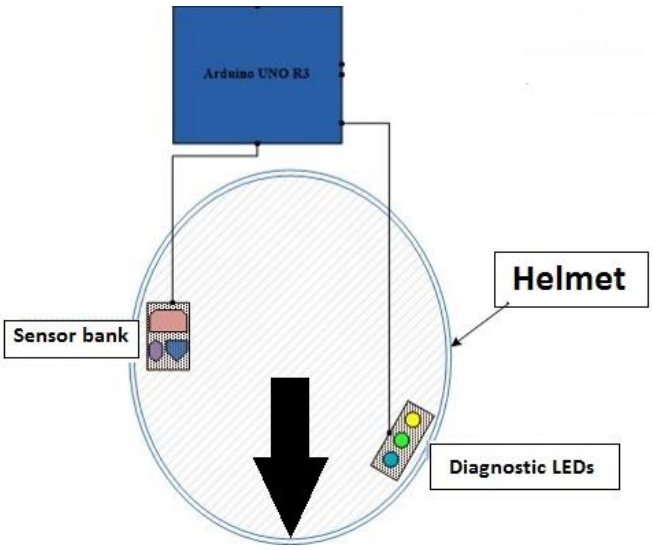

Figure 20. Pressure sensor and diagnostic LED's.

Figure 21. Closed loop breathing circuit and check valve assembly.

Monitoring of vital functions done via microcontroller built into hard torso, and include blood oximeter, CO2 monitoring and humidity sensors. Information is displayed in a straightforward manner; colored LED indicators placed just in peripheral vision

blink in a fashion similar to automotive trouble-code light. This configuration provides a simple “HUD” and no near-focus is required by the wearer for status information. For internal helmet cooling, a simple cooling cap was constructed using a knit stocking cap with 3 meters of 1/16” flexible tubing in two parallel channels of circulation in continuous flow. For initial testing, both the status display system and the cooling cap are used interchangeably between the 2 test helmets.

The second helmet variant was patterned from a standard motorcycle helmet built up and contoured with modelling clay, from which a silicon mold was created. The helmet was cast from fiberglass, inlaid epoxy weave cloth, and slow curing aviation epoxy used for the construction of experimental aircraft. The slope of the visor while envisioned to give considerable visibility for the wearer, presented challenges in forming and attaching it to the helmet itself. Because of the possible risks of the visor being damaged during pressure testing, a set of aluminum frames with a removable rubber seal was constructed for mounting the clear acrylic visor. The neck seal was construction from a neoprene and latex rubber composite, and bonded on to the opening. Hose adapters and one-way check valves of the same type as the GSh-4 helmet were installed on the sides of the helmet for closed loop respiration.

Figure 22. Floating helmet construction.

In practical application this type of helmet while having superior visibility, also had some major disadvantages. The headband needed to secure the helmet to the wearer was essentially a complex suspension device mounted to the rear, and never worked acceptably as there tended to be slippage when turning the head with the pressurized collar and neck seal in place. A second technical concern was the shape of the sloped visor seemed to be a weak point. The original acrylic visor blew out during testing. A second visor made from polycarbonate was installed which also failed during pressure testing. Visor fragments were examined under a microscope, and it was discovered that in the vacuum forming process the heat was causing a chemical reaction in the polycarbonate that formed microscopic gas bubbles embedded within the transparent material.

Figure 23. Chemical reaction (gas bubbles) in acrylic causing visor failure under pressure.

Figure 24. Completed floating helmet.

This unwanted chemical reaction caused not only minor visual distortion, but weakened the visor itself. A third visor was constructed using lower temperatures during the forming process, and this attempt was successful. The visor was transparent, was reasonably free of visual distortion and passed pressure testing. The second pending redesign of the upper portion has potential for its low weight and visibility, but the suspension mechanism for the head and transparent visor will need further development.

Thermal Control System

Because the HEE layer and associated components lack an air pocket surrounding the body, and need to remove metabolic heat from the wearer, an active thermal controller was developed specifically for the HEE space suit. The design considerations had to take into account the lack of convective heat transfer and humidity controls through air circulation and the sublimator common in conventional space suits. A design for simple closed loop liquid cooling evolved into a multi-channel computer controlled temperature regulation system, capable of both cooling and heating. Because of the increased complexity of the architecture, the HEE space suit outer shell had to be modified, adding an extra layer of Polyfill and Mylar reflective thermal blanket to stabilize both skin surface and core body temperatures. For an active feedback loop system, it was critical to limit the effects of external temperatures on the suit in order to for the microprocessors to establish a baseline stable temperature baseline. The suits intended role as a planetary surface system gained additional features that likened it closer to an open space EVA suit.

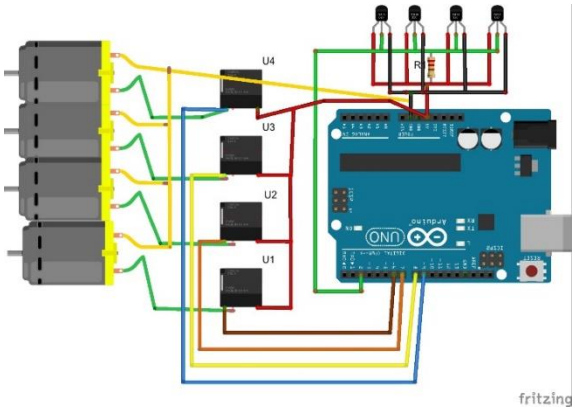

Figure 25. Langer's lines.

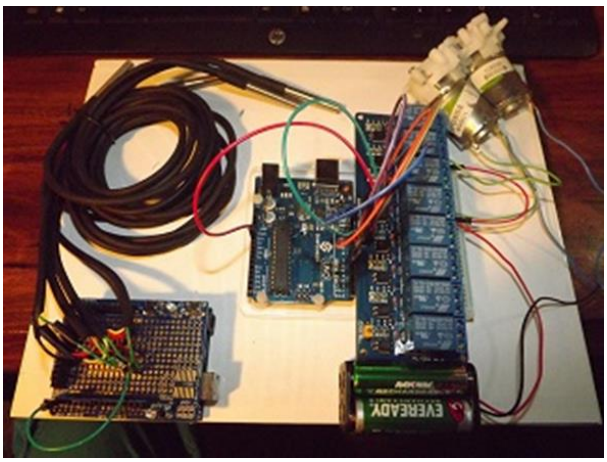

Figure 26. Assembled controller and test pump motors.

The Amtel ATmega328 running at 16 MHz was selected as the standard core processor for the 3 controllers that would be implemented in various control systems in the HEE suit. The ATmega328 uses simple C++ coding, utilizes flash memory boot loader and can be easily reconfigured by a simple power reset. All circuits were designed through Fritzing PCB design software, then bread boarded and tested before the circuit boards were assembled and soldered. The basic design of the thermal controller is a 4 channel feedback loop system consisting of 4 waterproof DS18B20 digital temperature Probes, a NO (Normally Open) relay board, four 7-12V DC pump motors, wiring loom and battery pack. 4 additional channels are enabled for future testing under higher thermal loads, for a total of eight possible coolant circulation loops. Each thermal probe is embedded into the HEE contacting the skin surfaces, and provides real time measurements to the microcontroller. The order of thermal control sensor and feedback operations are as follows:

1) The digital thermal sensors are assigned numeric values one through four. Every second the microprocessor polls a sensor in order, for a total of four seconds to transmit temperature data from all four sensors. Temperature changes are sensed instantaneously, and the sensitivity of the DS18B20 sensor is limited only by the conduction rate of its aluminum probe housing.
2) The microcontroller programming interprets the digital signal as both Celsius and Fahrenheit temperatures, with a motor activation threshold set to ~33° C., with the target body temperature programmed as a stable ~36/37 °C. The temperature settings can be adjusted to the individual's preference.
3) As the skin surface temperature rises and crosses the programmed 33° C. setting, the microcontroller activates the cooling pump motor that is associated with that particular sensor. The pump motor circulates coolant to the assigned anatomical area to cool the skin temperature, as the DS18B20 sensor keeps polling at regular intervals.
4) When the skin surface temperature reaches below 33° C, the coolant pump motor automatically switches off. The cooling channel remains at a resting state until the digital temperature sensor again detects elevated skin surface temperature, and the process repeats.

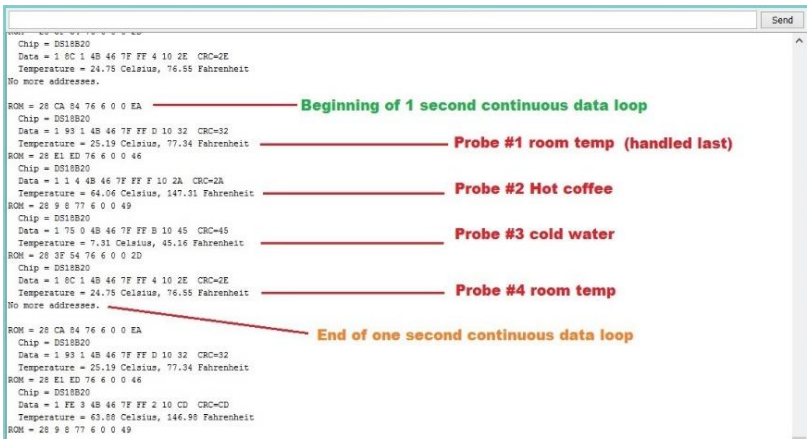

Figure 27. Terminal console data with descriptors.

Flow testing through 1/8” and 1/16” flexible tubing was performed using one of the DC pump motors to confirm quality control and determine an average flow rate. First using a test sample of HEE material, water with blue dye (food coloring) was circulated through the embedded cooling tubes to ensure the radii of the tubing bends were not restrictive, and that fluid freely flowed. Next, the test sample of HEE material with a dual cooling loop was connected to the DC motor with a one gallon water reservoir, and a one gallon transfer container from which the transferred water was measured. Several tests of two identical pump motors were implemented at both 6 volts and 12 volts DC power. A stopwatch was used to time fluid transfer on each one minute test, the measurements noted in liters, and the transfer container carefully emptied and dried before each new test was performed.

Figure 28. Flow rate testing.

Table 1. Flow Rate Tests of 6-12 Volt DC Fluid Pumping Motor.

Voltage	Test #1	Test #1	Test #1
6v	0.595 L	0.582 L	0.598 L
12v	0.951 L	0.959 L	0.948 L

The system was tested with water at different temperatures, and each channel calibrated accordingly. After complete motor, relay and thermal sensor testing, the unit was encased in a housing and mounted in a padded prototype case which is worn as a waist pack. The sensor probe wiring harness is routed through the side of the outer suit shell, and connects to the HEE layer with a multi-pin connector. The heart of the cooling system for test purposes consists of 3 cooling cartridges built into case which perform the function of a thermal phase change reactor. 1/8” tubing coiled in each cartridge for a total of ~16’ circulate the coolant in a closed loop between the suit’s cooling matrix and pump control motors. Some specialized research in coolant technology for this method

was also performed. A cooling medium consisting of an alginate polymer in a 99.5% water solution was developed, and injected into each cooling cartridge before sealing. In very early testing, the alginate augmented water attained solid and liquid forms more evenly than water, and retained its shape in gel form after a complete thaw. At this point it can only be speculated that the polymer chains in the alginate mixture distribute thermal phase changes at a more even rate in the cartridges, but at present there is only anecdotal evidence, and research into this cartridge technology in ongoing. While it was entirely possible to mount the thermal control system housing in the backpack, in the prototype suit the decision to create its own separate waist pack was based on ease of configuration and repair, as more space for debugging and calibration was afforded. Additional independently controlled cooling loops may be added into the system depending on effectiveness of current configuration in future testing regimes. The DS18B20 leads were routed into the outer space suit shell, and placed according to figure 42 (page 81) "*Thermal sensors placement"*. Special care was taken to ensure there was no binding between the leads and the HEE layer. The leads from the waist pack control box to the suit were bundled together and wrapped in protective flexible conduit.

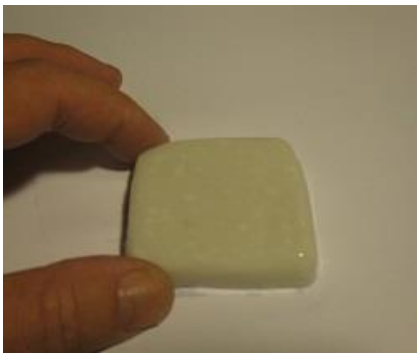

Figure 29. "Solid water" 96% by wt alginate augmented water coolant.

Figure 30. Wiring the controller, relays and pumps into enclosure.

In summation the purpose of the cooling system in context of the HEE is to cool the wearer's body temperature in non-convective environments, minimize adverse sanitary problems associated with perspiration and to reduce fatigue. Details of the test results are located in Chapter IV, under sections "Thermal Control.

Epidermal Pressure Sensors

Although the purview of the preliminary research pertaining to the HEE space suit and this thesis is primarily thermal control, this section will describe the design and implementation of the digital pressure sensor system that will be implemented for future testing in later publications. Initially, the pressure testing system is a series of force sensitive resistive (FSR) pressure sensors that use a dielectric material which translate compression into an electrically resistive digital value. These sensors can be calibrated and measured using both a digital multi-meter and a computer for more complex readings. The pressure sensor consists of a 0.5 diameter sensing area, and the FSR will vary its resistance reading depending on how much pressure is being applied to the

circular sensing area. The harder the applied force, the lower the resistance. When no pressure is being applied to the FSR its resistance will be larger than 1MΩ. The FSR can sense applied force anywhere in the range of 100g-10kg. Because of sensitivity, and each FSR varying slightly from production, each had to be carefully calibrated and evaluated before any further testing could be implemented. The calibration method is described as follows.

Figure 31. Padded waist pack thermal controller with activation switches.

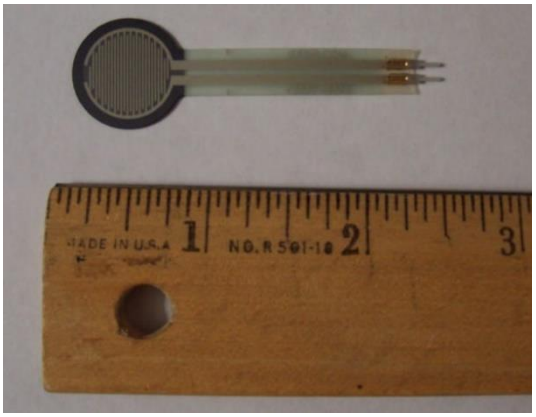

Figure 32. Force Sensitive Registor (FSR).

The first step was to test each resistor individually on a flat aluminum plate to examine the properties of each. An electronic scale was zeroed out with the empty weight of a water bottle. A table of digital resistance scales was created by filling the water bottle with weights between 28oz to 40oz in 2 inch increments. A digital interface was constructed to read the data on a Windows 8 computer via USB-Serial emulation. Each resistor was tested 3 times, and the weight applied for 1 full minute to allow settling of the dielectric material, as well as an accurate reading. Each resistors calibration reading varied within only one or two digital pulse values, but the values generally matched if a few extra seconds were added to the test. This is most likely due

to microscopic variations in each resistor, even though they are manufactured in a controlled factory environment. These minor variations had to be documented and accounted for. The digital pulse values were non-linear, and each resistor was assigned a number and its own data sheet.

Table 2. Preliminary Calibration Table Results for Five FSR Sensors (Note each Resistor has Unique Digital Pulse Incremental Values Per Force Applied).

Oz. per/0.5" Diameter	Sensor 1 Rval	Sensor 2 Rval	Sensor 3 Rval	Sensor 4 Rval	Sensor 5 Rval
28	913	902	905	890	911
30	921	918	923	912	920
32	924	922	931	915	923
34	927	928	934	921	927
36	933	930	943	932	935
38	934	933	946	935	940
40	937	936	949	938	943

It was deemed critical to create a contact surface to match the sensor area. A 0.5" diameter vinyl disk was implemented to ensure exacting contact of the test mass (bottle) within only the active sensor area of the FSR pad. Each sensor was again pressure tested using the same methodology, and digital pulse values assigned to each. It was observed that with the 0.5" diameter disk, the overall pulse value to applied pressure went down on each sensor. The disk was removed and each sensor tested using the original method. All values returned to the higher levels. It was determined that the non-sensing part bordering the sensor area of each FSR pad changed the quality of the digital pulses. The disk was reinstalled to the sensors, and readings successfully repeated with a new series of tests. The digital pulse values were transcribed to a table with the equivalent lbs./inch^2 ratios.

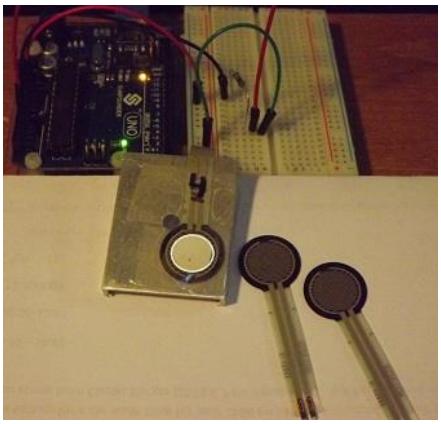

Figure 33. FSR sensor calibration with aluminum contact plate and interface.

Table 3. FSR Sensor Digital Pulse Values Per LBS./Inch^2.

Lbs./inch^2	Sensor 1 *Rval*	Sensor 2 *Rval*	Sensor 3 *Rval*	Sensor 4 *Rval*	Sensor 5 Rval	Sensor 6 *Rval*
4.5	805	784	850	810	812	843
5.0	816	798	858	838	839	865

Outer Shell

While the HEE Spacesuit serves as a protective layer for the HEE constriction and cooling layer, it also serves as an important part of the thermal regulation system, helmet to HEE transition, and as impact protection for the wearer. The original concept of the outer shell envisioned integrating the HEE layer with its cooling and constriction functions mechanism into a single garment complete with outer the outer shell. Following initial design inception, several changes were deemed necessary during fabrication. The HEE layer in relation to the outer shell was no exception, and this was due mainly to translating a design on paper into the realities of physical construction and practicalities of interrelation between the HEE layer and outer shell. The criteria for the outer shell consisted of:

1) An emphasis on protection for the underlying HEE layer, including its cooling, constriction and associated components.
2) The outer shell would be required to offer a limited degree of open space EVA protection in an emergency situation, puncture and impact resistance, as well as resistance to high speed abrasive particles.
3) The outer shell would be required to serve as an envelope of thermal stability for increased effectiveness of the liquid cooling system, while isolating the wearer and interior components from extreme temperature variations.
4) The ability to don and doff without assistance.

The HEE suit outer shell pattern was creating by completely dismantling various commercially made garments to create a workable paper pattern, and constructing an entirely new garment from suitable materials. The outer shell was designed and patterned around Dupont 1050D Cordura ballistic nylon as the primary material. Other composites such as Kevlar or epoxy weaves are also perfectly suitable, but for the first prototype suit version, Dupont ballistic nylon was deemed acceptable for ease of construction, while still providing adequate durability for a Mars surface environment.

The suit was assembled using an inexpensive Brother sewing machine, but also many hours of hand sewing where the sewing machine was incapable of penetrating multiple layers. The rational for choosing a quilted Polyfill construction method was to provide cushion and for the liquid cooling tubing minimizing crimped tubing in transitional and accelerated gravitational environments. The inner shell liner is

temporarily basted in, and the addition of Mylar layers can be easily accomplished with minimal work if required.

The layers were arranged from innermost to outermost in the following order:

1) Liner
2) Cotton/polyester foundation
3) Mylar layer
4) Polyfill layer
5) Mylar layer
6) Polyfill layer
7) Dupont 1050D Cordura ballistic nylon

Figure 34. Alternating layers of Polyfill and Mylar thermal blanket.

The basic forms of the arm and leg portions of the suit were assembled in a conventional manner, with special attention being paid to the areas of knee and elbow movement. Several configurations of perpendicular stitching patterns were tested on fully layered mockup sections of material formed into cylindrical shapes to simulate the

sleeves with all material layers included. All quilted lines on the outer shell were created by temporarily applying painter's masking tape in the appropriate patterns to be used as a stitching guide. This same technique was used to test different types of perpendicular stitching patterns. The process was repeated using varying geometrical patterns until the best flex was determined, and implemented on the sleeves. The criteria used to select the best pattern was ease of flex at the elbow joints, the least binding of layers on the inner elbow and minimal crimping of material that might interfere with the HEE layer cooling matrix.

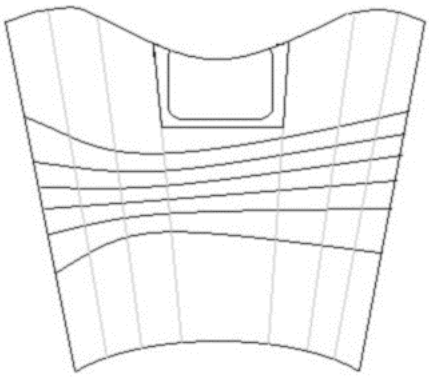

Figure 35. The basic sleeve pattern, including the quilted lateral lines, and the arc-stitched patterns implemented for maximum elbow flexibility.

Figure 36: Stitch pattern layout with low adhesion masking tape.

The arm and leg parts of the suit are equipped with full length zippers that correspond to placement of the pneumatic actuators. This configuration allows ease of donning the outer shell over the HEE layer, with zippers that close downward towards wrists and ankles, allowing easy closure without assistance. Another advantage of the zippered limbs is the geometry of the actuators remains correct while donning the suit; there is no binding between the outer shell and HEE layer. It was decided the final outer shell would be a one piece jumpsuit with full length zipper from neck to crotch to facilitate ease of wear. The upper and lower parts of the outer shell were integrated together into the aforementioned jumpsuit configuration with a full length zipper from neck to crotch.

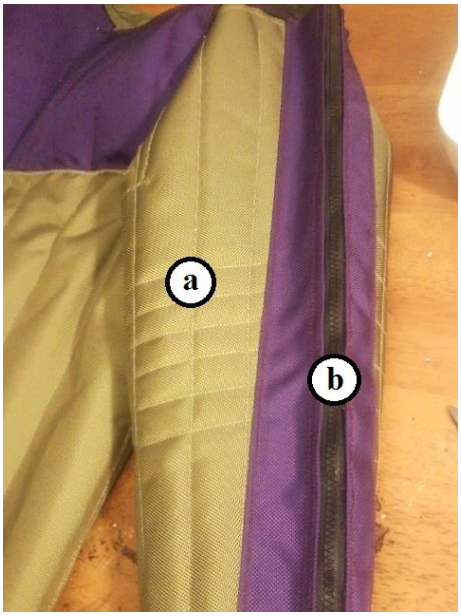

Figure 37. A) Perpendicular arc-stitched patterns for mobility. B) zippered sleeves for ease of donning/doffing.

Figure 38. Completed outer shell with individually fitted lower abdominal compression.

The Outer shell weighs a total of 2.5 kg. (5.5 lbs), features impermeable weave impregnated with polyurethane, is resistant to punctures and abrasives and can be easily cleaned. The garment can be donned and closed in less than 30 seconds without assistance, is flexible and lightweight. The Polyfill liner provides a degree of extra comfort when flexing limbs, and distributes the bulk of the hard torso around the upper abdomen. Future design considerations include integration with the underlying HEE layer, the use of carbon fiber laminates and boots and gloves as an integral part of the outer shell. It is also possible that a simplified neck seal will be included as part of the unified HEE/outer shell layer. More research into improving the actuating system as well as maintaining suit serviceability will be needed to achieve these type of improvements.

Gloves

The design and execution of a non-gas pressurized glove suitable for extra vehicular use on a space suit presents several problems that at first glance appear to be only engineering considerations that are overcame. However optimistic this seems on the surface, there are several key physiological traits of the human hand that must be recognized when designing an alternative type of glove along the lines of the HEE concept:

1) The very nature of the human hand as an evolved appendage in terms of functional requirements for fine motor coordination is constrained by the need for the same level of protection as the rest of the body creating a dilemma of mobility vs. protection.

2) Primary drivers for a non-gas pressurized glove are mobility for decreased stress to the user, and safety, which would require resistance to puncturing and catastrophic failure.
3) An alternative to a gas pressurized will require some method to constrain swelling of the hand and digits, this is a critical function due to exposed surface area of the fingers. Ambient tissue pressure must match blood pressure, or circulating blood will rush into low pressure areas.

The aforementioned research conducted in the 1990's by Honeywell, Inc., in collaboration with Dr. Paul Webb and Clemson Apparel advanced later iterations of the ECP Glove (Elastic Counter Pressure) produced substantial improvements in the utilization of semipermeable polymers and testing protocols for practical homeostasis, as well as thermal transfer of metabolic heat through evaporation. In keeping with the scope of this thesis The HEE space suit utilizes conceptual prototype mockup gloves. The impetus of this section of study was applying HEE suit construction methods and materials to a workable glove design that would benefit from the Honeywell research. Key differences originate in the types of materials used, and fabrication methods to achieve similar performance of the very successful Honeywell / Webb ECP glove study. The glove designed and built for this thesis is intended only to be a feasibility study in materials and fabrication, but basic tests in a hypobaric chamber were performed to evaluate the performance of the materials in conjunction with an air filled prosthetic hand. The test results and implications are listed in this chapter in the section

Prototype Glove construction was a multiple step process which made use of several different materials in several processes. Of primary importance was finding a suitable form that would serve as an anatomically correct representation of an average sized hand that would be the basis for glove construction. Among other criteria that needed to be satisfied was the form would need to easily separate from the materials application, as well as have the ability to be reusable for improved prototypes in the future. After searching several sources for a proper form, a rigid plastic hand that was slightly smaller than a male adults hand was chosen. The rationale behind choosing a slightly smaller size for construction is that the glove would have a fairly consistent tensional state already built into the Bioflex liner, which is the basis of most HEE suit components. The rigid plastic hand was wiped down in alcohol and sprayed with a silicon mold release.

A primary thin coat of Bioflex 010 was brushed on carefully, followed by a second coat after 1 hour. It is important that each new coat is applied before the gel is fully cured for best molecular adhesion. Between the second and third coats, there were two important steps that had to be taken. Firstly was the installation of the 1/16 inch flexible tubing that consisted of a dial pass counter flow array on the back of the hand from the knuckle area down to the wrist. Moisture suppression though thermal control was a consideration in such a confining type of material, and was applied in the same methods as the body suit HEE layer. The second step taken was the addition of constrictive bands between the joints of the fingers, and a supporting layer under the metacarpus (palm). As the second layer of Bioflex cured, bands were measured, cut and applied around each finger in segments, leaving several millimeters gap around each

joint. Each band was secured with two sets of fine thread, which was then cut after the third layer of Bioflex was brushed on, incorporating a very constrictive, yet flexible layer over the hand. A 00 hardness self-contained gel cell was formed to fit into the metacarpus in a shape that would ensure positive pressure into the palm area when the hand was relaxed. The 00 hardness gel allowed a plastic flow of material into depressions such as the palm of the hand, when clenching or grasping.

Figure 39: Completed inner liner with cooling.

It is important to note that because of differing materials characteristics between the HEE glove and the Honeywell/Webb ECP glove, the compressional glove inserts required fewer sections, as the 00 Bioflex had the capability to seek and conform to areas of lower pressure due to plasticity and flow of the gel. Finally, the final layer of Bioflex embedded another layer of constricting weave micro-mesh in areas of the hand which were subject to deformities during flexion (palmarflexion) or extension (dorsiflexion) of the hand and wrist. After curing, the inner HEE glove liner was removed from the plastic

hand that served as the form, and the liner placed onto the prosthetic hand with FSR force sensors placed into areas that were to be tested in the Paragon EHF hypobaric chamber. The prototype outer glove liner was then constructed from a PVC coated layer, with micromesh, ballistic nylon and elastic bands at each finger joint.

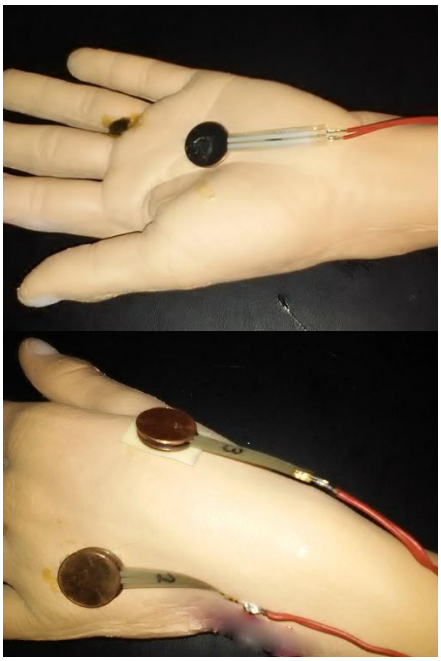

Figure 40. FSR pressure sensors placement.

Boots

For purposes of future research considerations, a boot design implementing existing and available technology was chosen as a starting point for applying the HEE concept into footwear that would be non-gas pressurized and puncture resistant, with characteristics that would make integration into the suit uncomplicated. While boot research and construction was a peripheral study of a concept prototype for the purposes of this thesis, a feasible design was developed. After careful consideration it was decided to use existing Bata Type I Extreme Cold Vapor Barrier Boots as the foundation

of the HEE prototype boot. There were several obvious advantages in the Bata Type I, one being the heavy vulcanized insulated rubber construction, making modification rather simple with dry suit adhesives, and most valuable component being the internal air bladders with manually operated relief valves. The Bata boots were designed with air bladders integrated into the construction during manufacture that function as an air filled insulating barrier heated from body warmth. At high altitudes, the atmospheric pressure differential between the internal boot pressure and ambient external pressure at altitude would cause the bladders to swell up, squeezing tight around the foot, especially during airborne and high altitude operations. The solution to the problem is the incorporation of a relief valve similar in appearance to an inner tube valve stem that is opened by turning the tip for equalization of pressure.

Two factory new pairs were purchased for testing and modification. The first objective was to reverse engineer the functional qualities of the boot by testing how reliably it could hold a workable amount of air pressure inside the bladders. A hose and clamp fashioned from wire were attached to the relief valve, and the boot coated with a water/detergent mixture to visually identify leaks in the form of air bubbles. Using an air pump with a built-in gauge, the boot was inflated to 5 P.S.I. (~35 Pascal's) atmospheric pressure, and checked for leaks. The boot successfully held the pressure for 1 hour of initial testing before air was purged from the bladders with no visual leakage or pressure loss. The boot pressure is fed from the suit actuators through a pressure line which compresses a custom molded Bioflex sheath around the entire foot. The footwear component of the HEE suit represents only a secondary area of research and design in the scope of this thesis, but further research and development is ongoing.

Testing Approaches

Thermal Control Testing Approaches

The testing procedures for the HEE layers thermoregulation abilities are composed of both qualitative and quantitative data sets. The testing is straightforward and redundant. The HEE layer is equipped with thermal sensors on the dominant limbs and torso contacting the skin surfaces, with digital signals fed to a computer which converts the digital signals into collated terminal readouts which display the temperatures of each area of the body in 1 second increments synchronously. The geometric layout of the cooling matrix is based on intensive research done by Prof. George Havenith of Loughborough University in the United Kingdom[23]. Under conditions of high ambient temperature and exercise, evaporation of sweat is typically the greatest avenue of heat loss from the body, and therefore important in maintaining body core temperature. Even in low temperatures, when protective clothing is worn, the body depends upon this mechanism to prevent overheating. Sweat production under different circumstances forms the basis for the body's ability to transfer heat via convection, which in turn is regulated by aerobic fitness, acclimatization, and efficiency of thermal transfer through evaporative processes. Numerous studies are available on global sweating, but studies on regional sweating rates are limited. The work by Dr. Havenith is one of the most concise studies on regional sweat rates, and body mapping

[23] Smith, CJ, and G. Havenith. "Body Mapping of Sweating Patterns in Male Athletes in Mild Exercise-in." *Induced Hyperthermia*. U.S. National Library of Medicine, 12 Dec. 2012. Web. 23 Nov. 2015.

of thermal transfer processes available in published academia. Design and construction of the HEE cooling matrix pattern and flow was influenced by the Havenith studies.

One of the primary areas of focus for this thesis is the suppression of perspiration by means of artificial cooling of body surfaces through conduction of heat in a confining garment instead of convection in a typical atmospheric environment of a conventional space suit. Because the HEE concept relies on hydrostatically equalized surface pressure in a confining garment, several key components found in conventional space suits would be considered extraneous for the HEE concept. As with a conventional space suit, the breathable circulating oxygen of the pressurized helmet is closed loop, but the exhaled air is returned directly to the PLSS system with each exhale, rather than circulating into the rest of the suit as part of ventilation and humidity control. One obvious advantage of returning exhaled air from the helmet directly to the PLSS is the reduced system mass required for environmental control. A second advantage is that the oxygen circulated throughout the suit is not used as part of the thermal control loop, thus not subject to perspiration and humidity contaminants as would be the case on a conventional suit. This means increased efficiency for the PLSS scrubber and filtration components, as well as a simpler design.

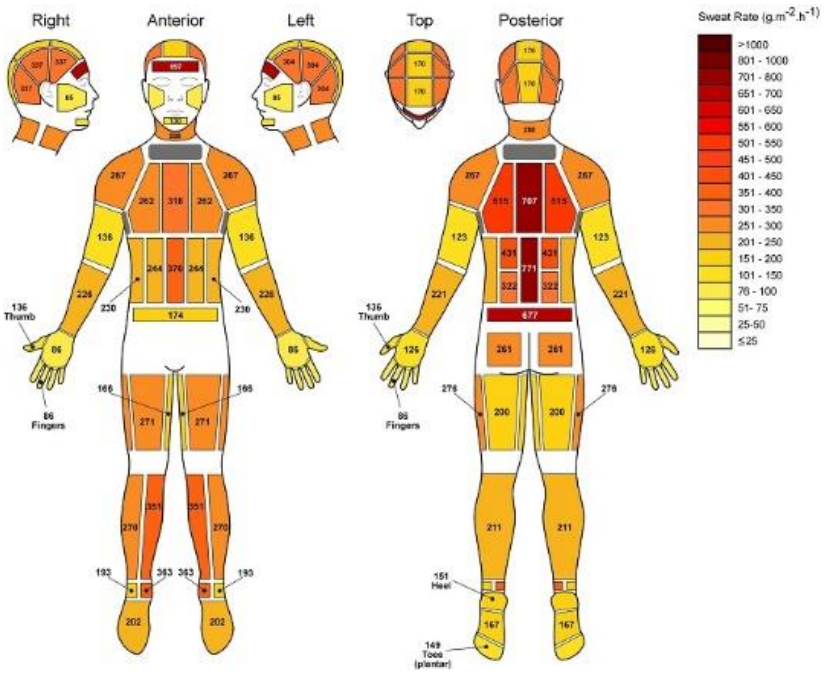

Figure 41. Surface area sweat rates calculated in grams per meter square per hour. [Havenith-Smith]

The HEE space suit's concept of a constricted garment as well as protection for skin means that there are certain trade-offs in technical approaches. Condensate and feedwater circuits are eliminated, as well as the sublimator, heat exchanger and centrifugal fan[24]. While reducing the reliability and complexity of the system, a non-gas pressurized space suit introduces new problems regarding thermal regulation of the human body. No longer is the conventional system of air circulation and atmospheric convection a major mechanism of humidity and perspiration control. While it is within the realm of technical and physiological possibility to employ limited evaporative

[24] Jones, Eric M. "Apollo Lunar Surface Journal : Apollo PLSS Images." *Apollo Lunar Surface Journal : Apollo PLSS Images*. Apollo Lunar Surface Journal, 31 Aug. 2008. Web. 06 Dec. 2015.

cooling in an open space environment through the use of knitted MCP materials, the risks and associated hazards would certainly preclude an EVA on Mars for example, where perchlorates constitute a chemical hazard to humans.

Such extravehicular activities will require extensive protection against caustic environments that would be damaging to organic tissues including skin and respiratory systems. The HEE layer replicates an artificial layer with the protective, self-healing, and thermo-stabilizing characteristics analogous to human skin. The form fitting and non-breathable qualities such a garment imply a high degree of thermal regulation for temperature stability, comfort and hygiene for the wearer. As previously stated, the tradeoff for a non-gas pressurized suit and its various components means the necessity of a biofeedback controlled multi-channel system capable of suppressing the tendency of perspiration via magnification of conduction and deterrence of vasodilation by both proactive cooling, and the introduction of an artificial secondary negative feedback system in an attempt to modify communication to the hypothalamus and minimize skin surface perspiration.

In summation, protective and constrictive qualities of the HEE space suit necessitate the need for developing an autonomous multi-channel thermal control system to;

1) Control core body and skin surface temperature across a broad range of temperatures and conditions, enabling the ability to both cool and heat the spacesuit for flexibility and adaptation to various operational environments.

2) Suppress skin perspiration in a garment that mechanically confines body surface geometry as a mimic of atmospheric pressure.
3) Add a point of control for Hygiene and personal comfort, which can greatly affect individual performance in extra vehicular activities of varying temperatures and other environmental conditions.

After samples of the HEE suit material with embedded cooling matrix was tested in a hypobaric chamber for fluid circulation efficiency and leaks under reduced pressures, it was decided to use a live human subject for thermal stability testing in normal atmospheric pressures. Because the HEE layer with embedded cooling is essentially a closed circuit system, normal ambient atmospheric pressure was deemed acceptable for initial physiological evaluations. The rationale behind a live subject was the ability to actively monitor real-time quantitative data of the 4 channel digital thermal sensors under various physical loads while monitoring humidity levels with the adjacent humidity sensors. A live human test subject also has the ability to report qualitative data regarding stamina, comfort, fatigue, and anecdotal reporting of performance details not available through quantitative methods. Appraisal of stressors included breathing rate, muscle fatigue, ability to talk normally and gradual increases in perspiration with elevated exertion levels.

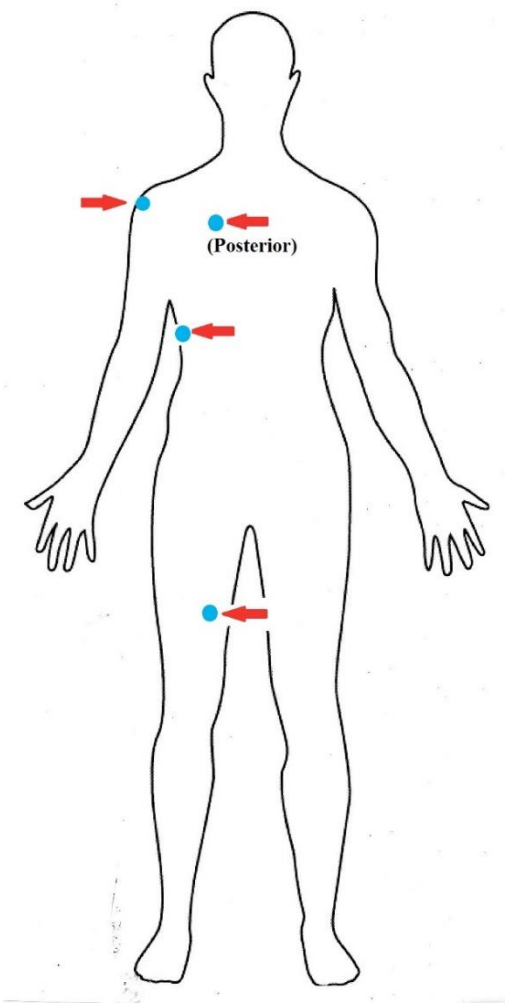

Figure 42. Thermal sensors placement.

The combined skin temperatures, sweat loss, and ratings of perceived exertion (RPE), were monitored and recorded. The reporting form consisted of a simplified Borg 6-20 Rate of Perceived Exertion (RPE) Scale[25]. While the Borg Scale was originally devised as a way to assess an individual's fitness level, by quantitatively matching perceived stressors to a numbered reporting system that includes descriptors ranging

[25] Borg G.A. Psychophysical bases of perceived exertion. *Medicine and Science in Sports and Exercise*. 1982; 14:377-381.

from 6 to 20; thus, a "relative" scale. The scale starts with "No exertion," rated as a 6, and ending with "very, very hard," which rates a 20. Moderate exertion registers 11 to 14 on the Borg scale ("fairly light" to "somewhat hard"), while more strenuous activity rates from 15 and higher ("hard" to "very, very hard"). Created by Dr. Gunnar Borg, the scale is a simple way to estimate heart rate—multiplying the Borg score by 10 gives an approximate heart rate for a particular level of activity. When this scale is applied to testing the HEE layers thermal control, special attention is paid to the reported perceived perspiration as well as actual measured sweat rates detected through the humidity sensors embedded in the suit.

Table 4. Original *Borg* Rating of *Perceived Exertion* (RPE) Example for General Perceived Exertion.

BORG 6-20 Rate of Perceived Exertion Scale (RPE)		
No Exertion	6	Little to no movement, very relaxed
Extremely Light	7	Able to maintain pace
	8	Increased breathing rate
Very Light	9	Comfortable and breathing harder
	10	Sweating perceived by wearer
Light	11	Minimal sweating, can talk easily
	12	
Somewhat Hard	13	Slight breathlessness, can talk
	14	Increased sweating, still able to hold conversation but with difficulty
Hard	15	Sweating, able to push and still maintain proper form
	16	
Very Hard	17	Can keep a fast pace for a short time period
	18	
Extremely Hard	19	Difficulty breathing, near muscle exhaustion
Maximally Hard	20	STOP exercising, total exhaustion

The experimental procedure outline developed to test the thermal control system underwent several changes as exertive tasks were executed with the system and difficulties ascertained. Initially a simple treadmill regime was prepared for testing perspiration rates through varying speeds of stride. Walking up an incline and scaling an aluminum ladder in succession were then added to analyze the effects of compound movements as a load on the cooling system controller and coolant circulation channels. The controller underwent several programming modifications intended to calibrate pump motor controller response as part of the cooling feedback loop. These programming modifications consisted of changing the skin temperature trigger signals by a degree or two, and changing pump motor run times after decreases in skin surface temperatures for optimal individual cooling efficiency.

The test methodology was designed to construct a procedure for both the individualized cooling calibration in the controller software, and as a general barometer of the HEE cooling matrix thermal regulation capabilities. Testing protocols, procedures and results are discussed later in this chapter in section *Testing Protocols,* and in Chapter IV under section *Prototype Results.*

Thermal Control Testing Procedure

Thermal control evaluations proceeded using a higher-end Lifestyle programmable treadmill that was capable of multiple speed and distance regimes, recording calories burned, time, distance and heartrate. The main purpose of the initial testing was to:

1) Establish positive circulation through the cooling channels being evaluated, including purging of any air in the cooling tubing that might affect effectiveness.
2) Identify areas of the body which would have the most cogent datasets for development of future tests.
3) Record and log real time thermal control data for preliminary evaluation, including temperatures of inlet and outlet sides of the coolant flow, actual skin surface temperature, and finally estimate and record skin surface perspiration through perceived and observed methods.

The waist pack thermal control unit was removed from the suit and interfaced with a laptop computer and diagnostic cable to take readings from the 4 DS18B20 thermal probes during walking and jogging routines. The first live tests bypassed the cooling cartridges built into the thermal control unit used an external cooling source for simplicity of testing, and priming of the cooling channels to be tested, specifically the right thigh, shoulder, side of ribcage, and back. The opposite areas of the body served as the control variable, which would not be subject to coolant flow and allowed to perspire inside the confines of the HEE layer. In this scheme, unchecked perspiration would be greatly increased in such a confined non-breathable garment, but observability of cooling effectiveness would also be easily observable on the functioning side. The external cooling unit consisted of a simple cylindrical igloo cooler with 20 pounds if ice that had been allowed to melt into a slurry. Each of the 4 HEE test cooling channels were supplied by independent sets of cooling tubing both to and from the external cooling reservoir, and connected to the HEE Thermal control unit pump motor array. The premise behind this

configuration was to allow easier priming of the HEE cooling channels for testing, as air had to be purged from the dozens of meters of cooling tubing. Each cooling channel had approximately 20 feet of extra tubing wound around scrap pieces of PVC pipe and submerged in the ice slurry.

Table 5. Perceived Motor State, Perceived Perspiration and Average Skin Surface Temperature.

		Thigh	**Shoulder**	**Side**	**Back**
		Channel 1	**Channel 2**	**Channel 3**	**Channel**
Treadmill Speed		Perspiration	Perspiration	Perspiration	Perspiration
1	**Slow stride**	Motor off **None**	Motor off **Minimal**	Motor off **Minimal**	Motor off **Minimal**
2	**Average stride**	Motor active **None**	Motor off **None**	Motor on **None**	Motor active **Slight increase**
3	**Fast walk**	Motor off **Increase**	Motor active **Increase**	Motor on **None**	Motor off **No Change**
4	**Moderate Jog**	Motor active **Decrease**	Motor active **Increase**	Motor off **Slight increase**	Motor active **Increase**
Mean skin surface Temperature		**33.20 °C**	**32.66 °C**	**32.92 °C**	**34.23 °C**

The perspiration tests required 4 complete treadmill testing cycles to adjust the motor activation trigger points (temperature thresholds) for activation. Each channel was adjusted in the software by changing the temperature for motor activation, motor run time, and motor delay. Perspiration was based qualitative perceived humidity as well as examination of inner microfiber bodysuit upon completion of final test. The 4th treadmill test recorded a definite window of temperature stabilization, but more refinement on the software control will be required as part of future research. Proposals of these future refinements are discussed in section “Analysis and Discussion”.

Figure 43. Cooling system testing on treadmill.

HEE Components Hypobaric Testing Approaches

Construction of the composite and Bioflex suit materials took into consideration the effects of low/zero atmospheric pressure environments. During the mixing and application of the Bioflex and other composite materials, special care was taken to ensure minimal gas bubbles would be present in the gels and other compounds during mixing molding and layup. The absence of trapped air bubbles meant a stronger component, with less risk of expansion or rupture in lowered pressure. The testing regime was designed to replicate decompression (depress/repress) of a realistic EVA and emergency scenario, with evaluation of composite materials and the suit's helmet neck transitional seal, gloves, and several other structural components. Initial live

testing was carried in the EHF hypobaric chamber at Paragon Space Development Corp. of Tucson Arizona under the supervision of Test Engineering Technical Lead Walter Harrington. Data Acquisition was accomplished through isolated conduits that were specially designed to house data cables though the walls of the pressure vessel, and interface with USB and standard RS-232 serial communications.

Figure 44. Paragon SDC EHF hypobaric testing chamber.

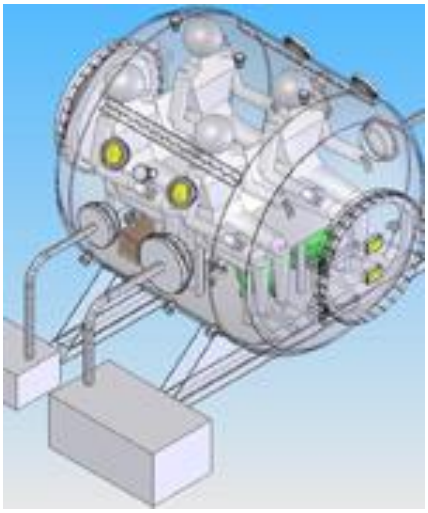

Figure 45. Paragon SDC EHF hypobaric testing chamber internal configuration.

Initial HEE layers testing consisted of both HEE individual materials component samples, and performance of an integrated HEE concept component: a complete glove with outer shell and integrated liquid cooling matrix. For sub atmospheric evaluation of materials and components, both a hard vacuum benchtop vacuum chamber and the Paragon SCD EHF testing chamber were utilized. The rational of two testing stages being that it was important to determine any off gassing by isolated HEE Bioflex materials as individual components first, and then in conjunction with Bioflex performance as part of a finished component. The proposed testing would first test exposed Bioflex materials to hard vacuum, with the before and after weights measured to the nearest thousands decimal with an Adam Equipment ACB 300 Electronic scale.

Figure 46. Partially constructed glove with exposed Bioflex and cooling matrix readied for hard vacuum testing at Paragon SDC.

The second stage of materials testing would expose a HEE suit test glove complete with functioning liquid cooling system, and FSR 402 pressure sensors in the glove. For stress testing the motor under working load, a DS18B20 thermal sensor was attached to the liquid cooling pump motor housing with surplus NASA Therma-Gap G579 thermal conducting putty. Colored water with a reservoir was al so circulated during lowered pressure sub atmospheric tests. FSR 402 pressure sensors were located according to spots that corresponded to natural surface depressions in the human hand which are subject to further distortion through movement and flexing. The pressure sensors were placed between the inner Bioflex layer and the artificial arm limb. The artificial limb was constructed of closed cell flexible foam core, with a latex skin and fitted with a PVC end cap and Schrader valve for ambient atmospheric pressurization levels.

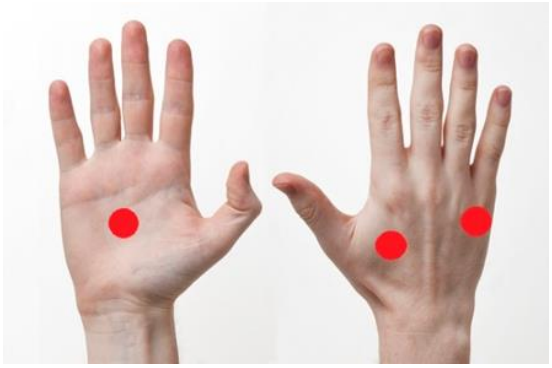

Figure 47. Initial placement of FSR 402 pressure sensors in prototype glove.

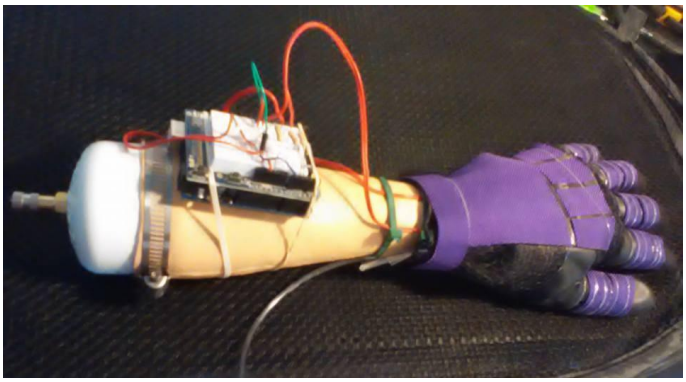

Figure 48. Pressurized test arm with glove prototype and pressure sensors (note Schrader valve left).

The GSh-4 helmet with transitional neck seal was fitted to the hard torso and upper mannequin assembly, which had been partially dismantled by removing the legs to allow it to fit into the Paragon EHF hypobaric chamber. The inflatable seal surrounding the base of the neck seal was inflated to 0.05 psi to allow a natural bend over the shoulders, and contact that resulted in a satisfactory seal at ambient atmospheric pressure. A Schrader valve with a pressure line to an Omega PX419-050A10V-EH pressure sensor and multi-meter read the helmet pressure, while an Omega PX309-030A5V read the EHF chamber pressure. The Paragon EHF facility offered several important advantages over simply testing the transitional seal in ambient atmospheric pressure. One primary asset of hypobaric testing was the lowered atmospheric pressure outside of the internal neck seal pressure identified key points of control that are to be integrated into the next iteration of transitional neck seal development. Notable specifics of neck seal deficiencies in lowered hypobaric pressure were identified, and are being addressed at the time of writing

through modification of construction and materials selection Details of testing and data logs are documented in the HEE testing procedure section.

Figure 49. Transitional neck seal in EHF chamber being readied for testing.

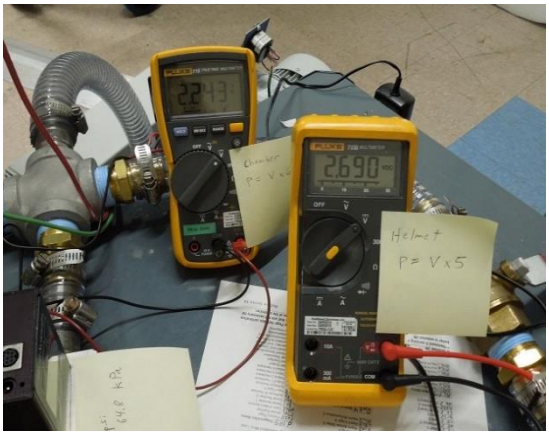

Figure 50. Multi-meters for hypobaric chamber and helmet pressure sensor readings.

HEE Testing Procedure

Initial Testing Procedures List

TASK 1. HEE Bioflex glove liner test

- Raw Bioflex glove liner with cooling matrix to be tested on rigid mannequin hand
- Bioflex glove liner to be tested in stages to close as possible to total vacuum for outgassing, materials breakdown deformities in differential pressures, and recovery state after repress.

  Micro-mesh components to be observed for tensional qualities in the design
- Webcam Monitoring of glove during depressurization
- Testing will require depress from 13.4 p.s.i.a to ~0 p.s.i.a, followed by hold time (TBD by Paragon), then repress, removal from chamber, and inspection.

Materials of construction; PVC, Bioflex orthotic gel, polyurethane tubing,Micro-mesh components on 3 fingers.

Possible SPOF: swelling or leakage of cured non-toxic Bioflex gel from faulty application

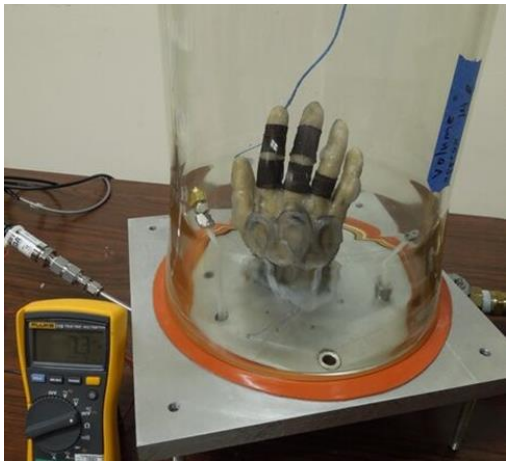

Figure 51. Bioflex glove liner in benchtop vacuum chamber.

The rigid plastic hand with HEE Bioflex liner and microfiber glove components was weighed on the Adam Equipment ACB 300 Electronic scale, with the total weight recorded at 147.02g The test was repeated with the scale being reset, the rigid plastic hand with HEE Bioflex liner and microfiber glove components reweighed, with a repeat reading of 147.02g with initial weight confirmed, the test article was place inside the benchtop vacuum chamber the multi-meter and pressure sensors activated, and video recording device started. Using a vacuum pump, pressure was reduced from ambient atmospheric pressure of 13.47 psia (2.245 V) to 12.156 psia (2.026 V) and held steady for a 5 minute observation. No effects were apparent. Pressure was then reduced from 12.156 psig to 10.5 psig (1.75V) with a 5 minute hold for continued observation, no changes were noted. Two more repress and observation cycles were completed, reducing pressures to 9 psig (1.503V) and 7.5 psig (1.255V) respectively.

The test article was removed from the benchtop vacuum chamber, and weighed twice on the Adam Equipment ACB 300 Electronic scale, with a result of 1.4701g; or virtually no change after a partial atmosphere depressurization. After being placed back into the benchtop vacuum chamber, vacuum testing of the material continued with decompression back down to 7.5 psia with a brief hold, and then down to 6.26 psig (1.043V) with no visible changes to the materials comprising the glove liner. Decompression continued to 4.2 psig (0.7V) with a brief hold for observation, and then further down to 2.1psia (0.353 V) and a hold for observation. Two small bubbles appeared between the rigid plastic hand, and the Bioflex layer on fingers #4 and #5, most likely due to a small amount of trapped air. Fingers #1 and #2 with the micro-mesh tensional layer showed no bubbles, but more importantly the Bioflex layer showed no

signs of materials degradation or reaction to lowered pressures. The final steps of decompression brought pressures down to 0.594 psig (0.099 V) with a brief hold, and then to the lowest achievable pressure of 0.048 psig (0.008 V) and longer hold time for ~10 minute observation. No outgassing of any kind was observed, and the Bioflex liner retained the same visual appearance as in normal atmospheric pressure levels. In most areas of the mock-up hand, the liner retained a drawn down surface tension against the rigid plastic where air had not been trapped while fitting the test material over the hand and fingers. The areas under the micro-mesh constricting components remained form fitted.

Figure 52. Partially completed glove liner in hard vacuum.

The benchtop vacuum chamber was repressurized and the test article place back onto the electronic scale, and weighed twice to detect any loss of volatiles that might indicate stress to the liner due to extreme low pressure environments. The final reading was measured at 146.9, for a total loss of 0.04g (40mg) with no evidence of outgassing from the Bioflex material. The glove liner was examined with a magnifier, and no signs of surface pores or openings that might have developed were found, and the original elasticity remained. Analysis and evaluation of Bioflex is discussed in section IV.

Table 6. Depress/Repress Steps with beginning and End Weights.

	Voltage (V*6=psia)	**psia**
1	2.245 V	13.47 (ambient)
2	2.026 V	12.156
3	1.75 V	10.5
4	1.503 V	9
5	1.255 V	7.5
	Repress and weigh	**1.4701 g.**
6	1.043 V	6.26
7	0.7 V	4.2
8	0.353 V	2.1
9	0.099 V	0.594
10	0.008 V	0.048
	Repress and weigh	**1.4698 g.**
	PRE WEIGHT	147.02g
	POST WEIGHT	146.98g

TASK 2 Cooling pump motor stress test in sub atmospheric pressure

- RS-360SH Micro Water Pump (DC 1.5V-12V) to be tested for flow in relation to voltage and thermal loads under reduced atmospheric pressure of 9.4 psi.
- Temperature readings of motor to be logged using Glove to be attached to cooling pump motor and fluid circulating at 6V DC for duration of test to observe any adverse effects of vacuum on the DC motor and coolant tubing wall integrity.

- Webcam monitoring of glove during depressurization
- Testing will require going from 13.4 psi to 9.4 psi , followed by hold time for observation, then repress and removal from chamber.

Materials of construction; PVC, Bioflex orthotic gel, aluminum, micro-mesh, elastic bands and DuPont Cordura 1050D.

It was imperative a cooling system motor be evaluated for its thermal properties under a load at sub-atmospheric pressures for reliability and safety before further tests on integrated HEE suit components could progress. The ability of the pump to resist overheating was the primary focus of task #2, with tuning of DC power voltages and flow rates critical to ensuring the pump was effective while operating within its limits. A single RS-360SH Micro Water Pump motor attached to the closed circuit glove cooling loop, circulating blue dyed liquid from a Pyrex beaker. The first test involved running the pump at 6V DC though a dual circuit glove cooling loop at the ambient atmospheric pressure of 13.4 psi (or 92.38 kPa). The battery pack was protected with a 1A inline fuse to protect the rechargeable battery pack from possible damage from overheating. Pump temperature was monitored through a DS18B20 temperature sensor attached to the motor casing with Therma-Gap G579 putty, with temperature data displayed through a terminal emulator and logged to a laptop computer. After 10 minutes of pump operation at 6V with simulated coolant, motor temperatures rose to over 130°F, after which the pump motor was powered off. DC power was reduced from 12V to 6V, and an extra loop of 1/6” cooling tubing introduced into the pump flow, for a total diameter of 1/8” cross-sectional flow between cooling pump input and output. The cooling pump test was repeated at a reduced voltage of 3V, and temperatures peaked and leveled off to 39.81 °C

(103.65 °F) after ~11 minutes of continuous operation. It was determined that 3V per 1/8” dia. cross-sectional flow area provided a minimum flow rate that kept the motor and battery pack from overloading. With the motor protected with an in-line fuse and flow rate improved, the cooling system was ready to be tested with the prototype glove at sub-atmospheric pressures.

Figure 53. RS-360SH Micro Water Pump.

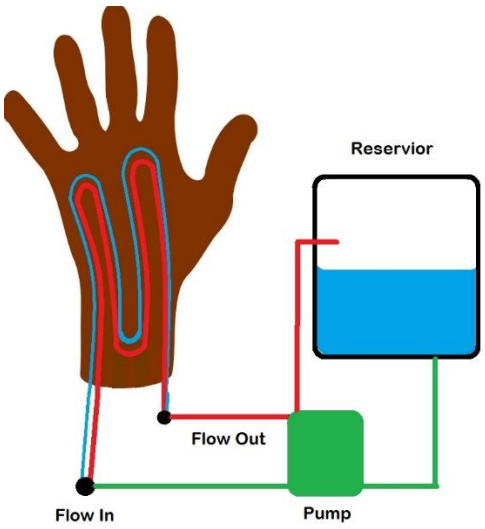

Figure 54. Cooling fluid loop for motor test.

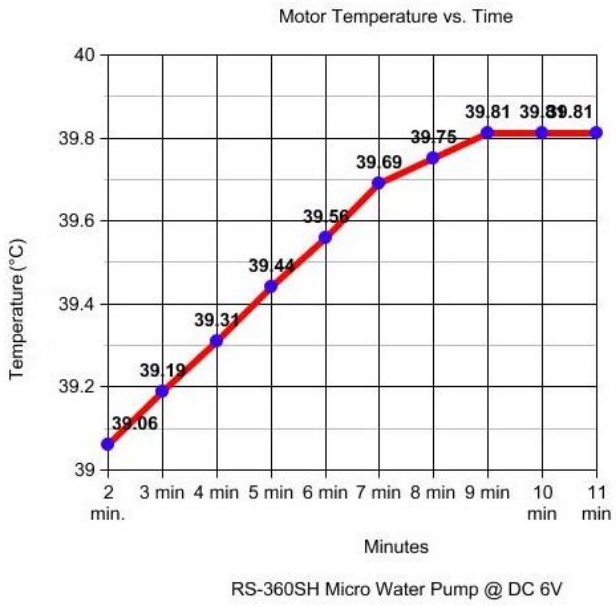

Figure 55. Motor operating temperature.

TASK 3. Prototype glove test

- Bio-flex prototype glove to be tested on prosthetic air filled hand.
- Glove will be tested for deformities in differential pressures, with surface tension logged via FSR-402 pressure sensitive resistors and data logger
- Glove to be attached to cooling pump motor and fluid circulating at 7-12V DC for duration of test to observe any adverse effects of vacuum on the DC motor and coolant tubing wall integrity.
- Webcam Monitoring of glove during depressurization
- Testing will require going from 13.4 psi to 9.4 psi, followed by hold time for observation, then repress and removal from chamber.

Materials of construction; PVC, Bioflex orthotic gel, aluminum, DuPont Cordura 1050D.

Possible SPOF: swelling or leakage of cured non-toxic Bioflex gel from faulty application.

Testing of the prototype glove proceeded under conditions that both attempted to measure glove constriction and replicate internal body pressure using a pressurized closed cell foam limb with latex skin as a simplistic analog for a human tissue surface in vivo, but lacking its isometric elastomechanical properties. The purpose of the test was to gather preliminary data on the prototype gloves ability to limit expansion of the prosthetic hand in relation to the aforementioned hypothetical bubble model of decompression. This phase of testing is considered a starting point for future research into the HEE concept, and was designed to evaluate construction techniques, and provide data for potential future development. While the hard vacuum test of the glove liner provided indices of materials suitability, the sub-atmospheric test of the integrated prototype provided a chance to inspect the assembled gloves characteristics with the cooling system operational and outer shell in place.

The artificial limb with glove was placed into the EHF hypobaric chamber along with a beaker of green dyed water, CMOS digital capture cameras and absorbent pads to contain any liquids should a cooling tube in the glove break. The cooling pump motor was started, along with the video capture camera and data logging software on the laptop. The prosthetic limb internal pressure was monitored using a pressure line from the Schrader valve on the prosthetic limbs endcap that led to an externally mounted pressure sensor with 3 way valve that allowed control and adjustment of simulated human dissolved gas pressure. The EHF internal pressure was incrementally reduced from 13.4 psi to 9.4 psi, with pressure of both the EHF and the limb's internal pressure being

verified and logged. The FSR-402 sensors also measured the glove at ambient atmospheric pressure, or the resting state of the fit around the hand, which is the compression caused by the elastic properties is the HEE glove liner's Bioflex materials.

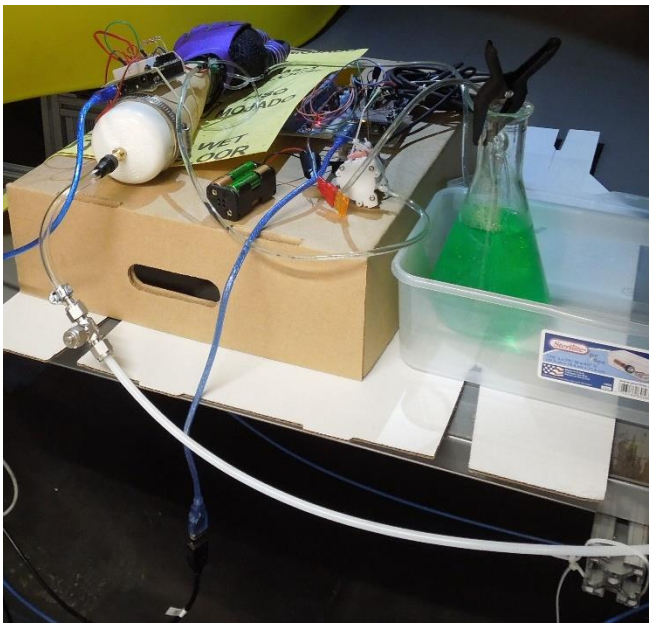

Figure 56. Pressurized limb with glove being readied in EHF chamber (note pressure line in foreground).

As pressure was reduced, it was observed that the sensors recorded increases in pressures at different rates from different sensor positions, i.e.; the palm sensor recorded little variance until sensors on the thumb area and back of hand started to rise, with the sensor on back of the hand situated near the 5th finger showing a dramatic increase on pressure with palm sensor readings increasing. It was determined that this was due to the prosthetic hand gaining relative pressure against the test chambers dropping atmospheric pressure. Although the prosthetic limb lacked the actual thicknesses and elasticity of actual human skin, the test did give some insight into how different parts of the glove

constrain the hand as pressure differentials increase at varying rates. Cooling pump motor temperatures were observed and recorded throughout depress and repress cycles, and there was no change in operating temperatures. Coolant flow rates were also monitored during the testing procedure, and there was no visible restriction of liquid flow in the closed circuit loop during lowered atmospheric pressures and glove constriction. The prosthetic test limb successfully held 13.4 psi (92.38 kPa) in the areas served by the FS-402 sensors through the duration of test period, as confirmed by the Omega pressure sensor. With the completion of lowered pressure testing, the EHF chamber was repressed back to normal atmospheric pressure at altitude, and the glove along with cooling system inspected for deformities or coolant leaks. No changes in original condition of the glove or liquid leaks on the absorbent pad were detected.

TASK 4. Neck transition seal testing

- Flexible neck transitional seal to be tested using converted Gsh-1 helmet with composite hard torso on mannequin mock-up.
- Transitional seal will be equipped with external hose, and internal pressure read with instrumentation from outside of hypobaric chamber.
- Pressure will be reduced from 13.4 psia to 9..4 psi followed by a hold TBD by Paragon, then repress and removal.
- Web cam monitoring of seal
- Decompression rate and test duration is solely at the discretion of Paragon Engineering Department.

- Pre-testing at 4.5 psi over normal atm pressure will be done to ensure integrity of helmet and neck seal before testing low pressure effects on materials in actual chamber.
- O2 bottles and LiOH scrubbers will be removed from backpack, and helmet plugged.

Materials of construction; PVC, Bioflex orthotic gel, aluminum, steel, tempered glass, vulcanized rubber, epoxy and fiberglass laminates, smart foam, DuPont Cordura 1050D

Possible SPOF*:* compression donut-seal leakage under composite hard torso.

The transitional neck seal testing required assembling the hard torso and helmet components mounted over the torso of a mannequin. As mentioned in the previous section, an upright orientation of the mock-up was necessary for tests, and due to limited interior height of the chamber, only the upper half of the suit was utilized. The assembled test components were placed in the EHF chamber, the sensors for both internal neck seal pressure and EHF atmospheric pressure attached to the pressure lines, and a video camera installed for live monitoring and recording of tests. Prior to EHF measurements, the neck seal was pressure tested on the fully assembled suit and mannequin with a hand pump and digital pressure gauge at an ambient atmospheric pressure of 14.45 psia (99.62 kPa) at an altitude of 480 ft (146.3 m). The neck seal successfully held 3.0 psi and 4.2 psi respectively. To achieve a hermetic seal, it was necessary to apply a layer of the 00 gel around the contact area of the neck seal, as well as on the HEE suit layer. This layer of 00 gel is only considered a temporary, and was applied to a circular felt ring which measured about 1” width. The configuration of the neck seal was considered a first design, and one

of its important design goals was the ability to follow the contours of the human shoulders, with an air filled ring that could compensate for geometric changes in anatomy (shoulder movement for example) through the cushion of air pressure inside the ring seal itself. The EHF sub-atmospheric tests were performed in two sessions, with an actual removal of the of the entire upper torso assembly from the chamber required to diagnose a helmet pressure drop that occurred less than 10 seconds after the start of the first depress cycle. The hard torso was opened, and the seal repositioned, the torso tightened back down over the transitional seal compression ring and the suit assembly placed back into the EHF chamber for a second depress/repress cycle. As with the previous test, the same voltage operated sensor in combination with multi-meters logged the pressures during the testing procedures. The Paragon tests revealed a problem with the design of the air filled compression ring at the base of the neck seal. The nature of the problem of the prototype is the internal pressure of the compression ring causes it to tend to go into a more rigid state incapable of bending absent of a crease, and this problem is discussed in length along with current design changes that substitute open cell composite foam compression ring for the prototype air filled ring. The Paragon SDC EHF chamber tests were critical in evaluation and redesign and construction of the second prototype transitional neck seal.

Figure57. Helmet internal pressure monitoring line detail.

Figure 58. Transitional neck seal in EHF Hypobaric chamber as captured from video camera during depress cycle.

Figure 59. Gel seal ring on prototype transitional seal (note Schrader valve for ring inflation.).

CHAPTER IV

ANALYSIS AND DISCUSSION

Prototype Testing Summary

In initial evaluations, the testing regimes of the HEE space suit took into account materials, technological concepts and technical applications with the goals of improvements on existing MCP or proposed MCP type planetary suit designs. The entire process of HEE design, from conceptualization to fabrication, construction and testing was based addressing key limitations, shortcomings and assumptions in the so called Mechanical Counter Pressure space suit concept. Considerations took into account fundamental MCP design considerations, but more importantly expanded the criteria for a workable MCP concept. These criteria included:

1) Required total pressure level consistent with respiratory homeostasis applied to human body, rather than an attempt at replicating the exacting physical characteristics of gas pressure as it applies to humans on Earth.
2) Minimal reduction in mobility envelope under modified gravity conditions.
3) Thermal regulations for human body under diminished heat transfer conditions.

4) Enhanced protection from adverse environmental conditions including toxic localized chemistry, dust from pulverized impact glass, caustic/abrasive combinations.
5) Anything else that can directly affect the health of the wearer or performance of a suit and its associated components.

The HEE suit testing protocols were based the application of materials and techniques that were very different from the knitted fabric examples of the Web SAS prototype and the MIT conceptual Biosuit. The HEE suit actively constricting artificial epidermal layer through biomedical materials required thorough evaluation to determine suitability of Bioflex and other associated materials. Initial controlled tests at Paragon SDC's hypobaric facilities demonstrated that the HEE Bioflex materials skin contact liner will withstand a hard vacuum with no detectable materials degradation. In repeated hard vacuum exposures, the Bioflex displayed resistance to extreme low pressures with no observable release of volatiles from the materials, or formation of bubbles within its structure due to any defects in application. The minute post recompression weight loss of only 0.04g after repeated depress/repress cycles can reasonably be attributed to loss of surface humidity on the exterior of the Bioflex material, as well as the contact surface between the glove interior and plastic test hand. Future improvements to HEE layer construction with Bioflex include the addition of a fibrous flocking material or microfiber weave embedded in multiple layers within the Bioflex during suit fabrication for added strength.

The thermal control testing indicate that the biofeedback controlled liquid cooling system when put into application, workable, and with further improvements in pumping

motor selection, as well as liquid cooling resolution; i.e., variable speed motors and even tighter patterns of cooling circulation tubing embedded in the HEE layer. The cooling circulation potentially has applications for adaptation to both hot and cold environments. With the evaluation of materials which constitute the glove liners suggesting viability of materials, the sub atmospheric glove prototype testing gave promising results during initial testing, which is discussed further in this section.

In principal, with some refinement in materials construction and design, the flexible neck seal offers enhanced visual mobility through the use of a smaller and more mobile helmet that can fit snug around the head. For practical purposes of discussion, this type of design is referred to as a floating helmet throughout this paper. The helmet is not rigidly attached to the upper abdomen through use of a locking ring or other type of hardware typically seen on conventional gas pressurized suits. Other advantages are lighter weight, smaller profile around the head, and better visibility.

Bio-sensors embedded in contact layer allows automatic control as an artificial extension of the autonomic nervous system

Fiberglass hard torso clamshell (placed outside the epidermal layer) with constriction functionality working in conjunction with epidermal layer

Segmented neck interface transitions helmet pressure to hard torso clamshell and underlying artificial epidermal layer. Closing the torso unit seals the segmented neck over the HEE layer.

Thermal Control

The primary objective of the human stress testing of the HEE garment was to characterize the flow rates and skin temperature characteristics of a suited

subject in the HEE cooling garment under various workloads. The data collected from the test was used as for initial calibration of the suits liquid cooling pump array goal of defining acceptable workloads and flow rates for further stress human factors testing with the integrated HEE/Cooling layer. The data will also be used toward the on-going effort to design, build and test a second prototype thermal cooling matrix with the goals of be used to validate analysis models, as well the creation of a second generation prototype with variable that features, among other things, variable speed motors and a higher resolution cooling gradient. The subsystems testing included motor loads under varying voltages, sub atmospheric pressures, tubing diameters and flow rates. The Paragon EHF chamber facility was an important factor in determining robustness and operating temperatures of the circulation pump motors. The next step in the process was integrating the motor array to several specific cooling loops, in the case of this paper, the right thigh, shoulder, back and side.

Testing of Liquid cooling system involved an exercise regime on a treadmill using the preprogrammed walking and running modes. Currently the thermal control system is being tuned, and evaluated for minor changes in trigger points in the software. The testing reveals the need for a priming bulb which is currently being installed inline on the cold side of the coolant flow at the pump motor outputs. The 100 meters of cooling tubing needed priming at each individual cooling channel due to the use of 1/8” supply tubing feeding the 1/16” HEE circulation tubing. A solution is currently being worked out that uses a small reservoir of a few ounces situated at the pump inlets. Testing and tuning of suit is ongoing, and more cooling channels can be added if finer degrees of control are needed. The initial data compiled from the live trials indicated a need for thermal probes

which are able to react to temperature changes faster. The current DS18B90 sensors are housed in a miniature aluminum tube and sealed for moisture resistance, which is conducting skin surface heat to the thermal sensor housed internally slower than required, but this was compensated with programming changes by adding a longer motor activation and cutoff durations.

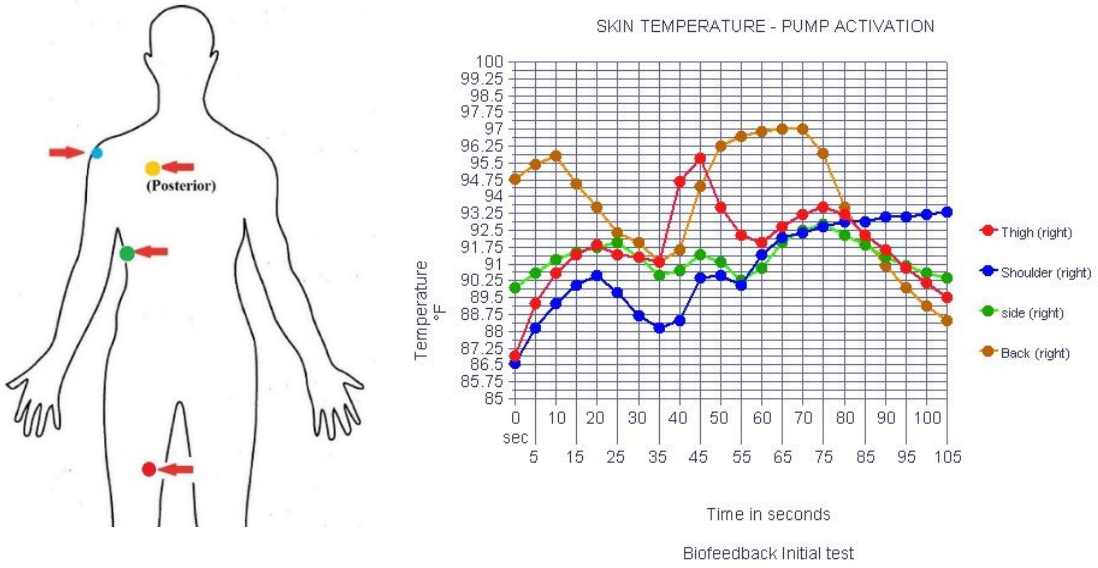

Figure 60. Color coded temperature sensor placement (L) with the four areas of skin temperature variations reacting according to motor activation. This graph indicates a period of thermal control between 10 and 90 seconds, but the variations are too great, and beyond the limits of program code changes.

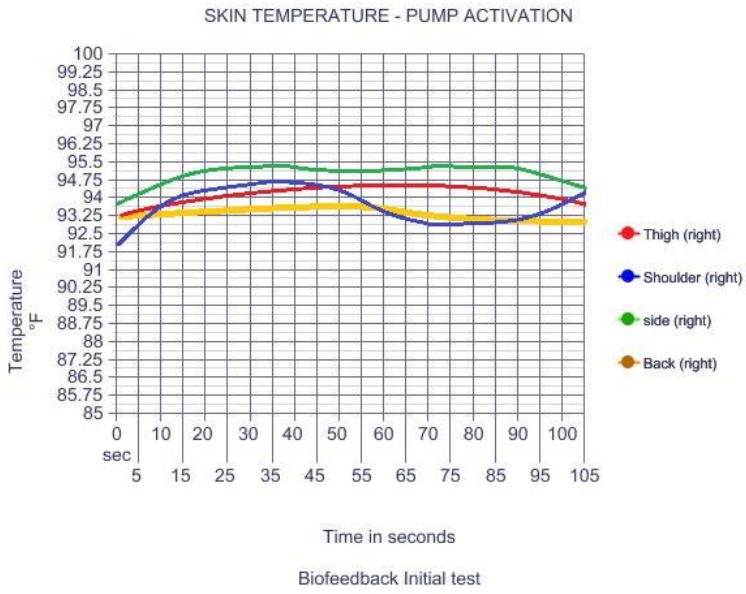

Figure 61. A flatter temperature gradient is the goal of using variable speed pump motors in place of fixed speed motors using only on/off states.

Calibration and treadmill data retrieved from a 10 minute fast walk did manage to stabilize skin surface temperature to a more suitable range, but the temperature variations between peaks and valleys need to be narrowed into a flatter profile during extended durations. This will be addressed with the addition of variable speed pumping motors and the same type of thermal sensor with a sealed silicon membrane in place of the aluminum housing.

Neck Seal

The paragon EHF hypobaric testing of the flexible neck seal in its current configuration revealed several potential advantages over traditional ringed type seals, but also indicated the need for an added point of control in the air filled variant, or a compressible donut seal of radically different material. Principally, in a static external atmospheric pressure condition, the neck seal when compressed by the torso against the

HEE constrictive layer will hold 4.5 PSI. When exposed to a reduction in external ambient atmospheric pressure, the pneumatic donut seal expands in size due to its own relative increase of air pressure, thus becoming more rigid, and unable to form a natural arc over the shoulders and maintain a hermetic seal. The design changes currently being considered as well as implemented are more a matter of simple modifications of the original concept than complete re-engineering. These iterations in the forthcoming prototypes include:

1) An added point of control with the introduction of an extra pneumatic line from the donut seal to a micro solenoid pressure valve routed into the exhaust side of the helmet pressurization line in the PLSS. This would allow an automatic regulation of the donut seal internal pressure based on a detected helmet seal leak, and react accordingly to create a more rigid or pliable contact surface the HEE layer under the hard torso.
2) A compound curve in the shape of the donut seal to better conform to the geometry of the shoulder region of contact. This type of shape would allow for further refinement in suit integration, as the helmet, neck seal and torso with PLSS backpack would be unified into a single donnable component of the suit. Other advantages of the further refinement would be the introduction of a greater hermetic seal contact area, allowing the inner surface of the hard torso to work in unison with the donut seal in maintaining an air tight seal. In this scenario, the seal contact would be enlarged inside the hard torso creating a greater surface area for added reliability and less shifting during a wearers movements.

3) Investigations into different type of material in place of an air regulated donut seal, which include preliminary research into compressed polymers taking the place of air pressure. One disadvantage to this possibility is that there would be a possibility of component swelling in lowered atmospheric pressure with no method of control depending on what type of material used. Heat dissipation might be another concern in this design.

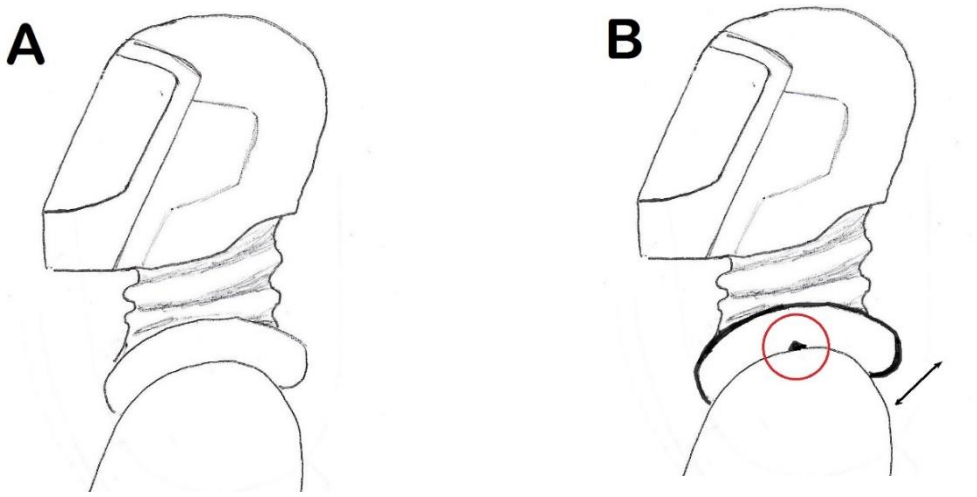

Figure 61. Flexible neck seal in two different conditions. Sketch A represents static ambient air pressure with effective hermetic seal. Sketch B represents increased donut seal relative pressure resulting in a stiffer seal, less conformity to shoulder curvature, and resulting leak indicated by red circle**.**

Glove

The prototype glove testing was done in two stages; analysis of the Bioflex glove liner in a hard vacuum, and sub atmospheric testing of the glove liner with outer shell installed and liquid cooling operational to observe epidermal counter pressure characteristics. The HHE liner testing indicated its ability to keep its shape, and the

prototype glove shell was built around it. The placement of the force sensitive resistors in the palm, the area between the thumb and forefinger, and under the 4th knuckle, was designed to collect initial data of surface pressure between the pressurized prosthetic had assembly and the gloves liner on the recessed areas of the hand which would require the most attention, the palm being the primary focus. Several depress/repress cycles were accomplished with the DC pump cooling motors running and active cooling fluid circulation. Decompression to 4.5 psi below local atmospheric pressure (9.4 psi) was accomplished and log files taken in the form of digital resistance readings were compiled while the coolant flow, hypobaric pressure and prosthetic arm internal pressure were observed.

Table 7. Recalibrated Digital Values to Pressure. The Elongated Wire Leads of Different Lengths on the Pressure Sensors Required Manual Recalibration for Correct Glove Pressure Readings. Readings Starting with Anything Other than 0 Indicate Glove Existing Glove Tension to the Hand Before a Reduction in External Atmospheric Pressure.

Palm		**Dorsal Thumb**		**Korsal Knuckle**	
0	no force	844	13.1 oz.	300	9.800 oz.
25	.5 oz.	875	16.8 oz.	313	9.87 oz.
50	.11 oz.	900	17.0 oz.	325	9.93 oz.
75	8 oz.	925	28.7 oz.	350	11 oz.
100	17.5 oz.	950	31.8 oz.	375	11.9 oz.
125	26.2 oz.	1000	31.90 oz.	400	12.5 oz.
150	33 oz.	1022	31.98 oz.	425	12.6 oz.

Depress times averaged 4-5 minutes to achieve a 5 psi reduction in hypobaric chamber pressure, and various pressure holds of were conducted between changes in atmospheric pressure to verify integrity of the prosthetic test arms ability to hold a greater atmospheric pressure, in this case 13.4 psi (92.38 kPa) for glove constraint analysis. It should be noted that prosthetic hand was in a neutral (resting) configuration, and this served as only a rough approximation of an actual human hand for this type of preliminary testing. As pressure dropped during decompression, it was observed that slight drops in one sensors recorded surface pressure often corresponded to increases in a sensors pressure reading in a different area of the glove mock up. These minor changes in pressure correlated between the Palm and Dorsal (knuckle) sensors consistently during depress cycles. Examination of the log files shows a consistent slight loss of pressure on one sensor always being compensated for by a nearly equal amount of increased pressure by its counterpart, as internal relative pressure inside the prosthetic hand increases resistance against the HEE glove liner. This implies both the glove conforming to the prosthetic hand by pulling more elastic areas taut, thereby settling into a natural envelopment on the prosthetic hand, as well as a constraining effect as the mock-up hand swells slightly to limits imposed by the glove.

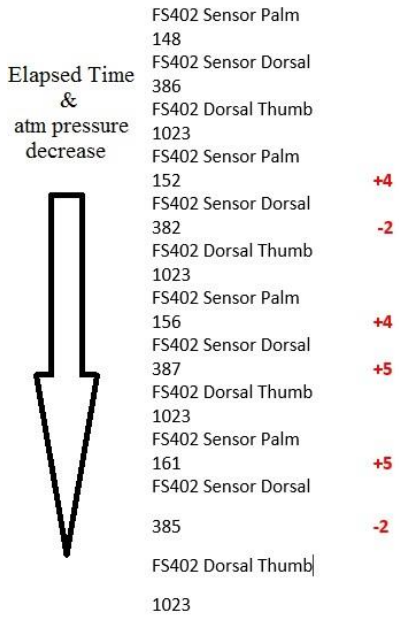

Figure 63. Consistent pressure decreases compensated by an opposing sensor during depress.

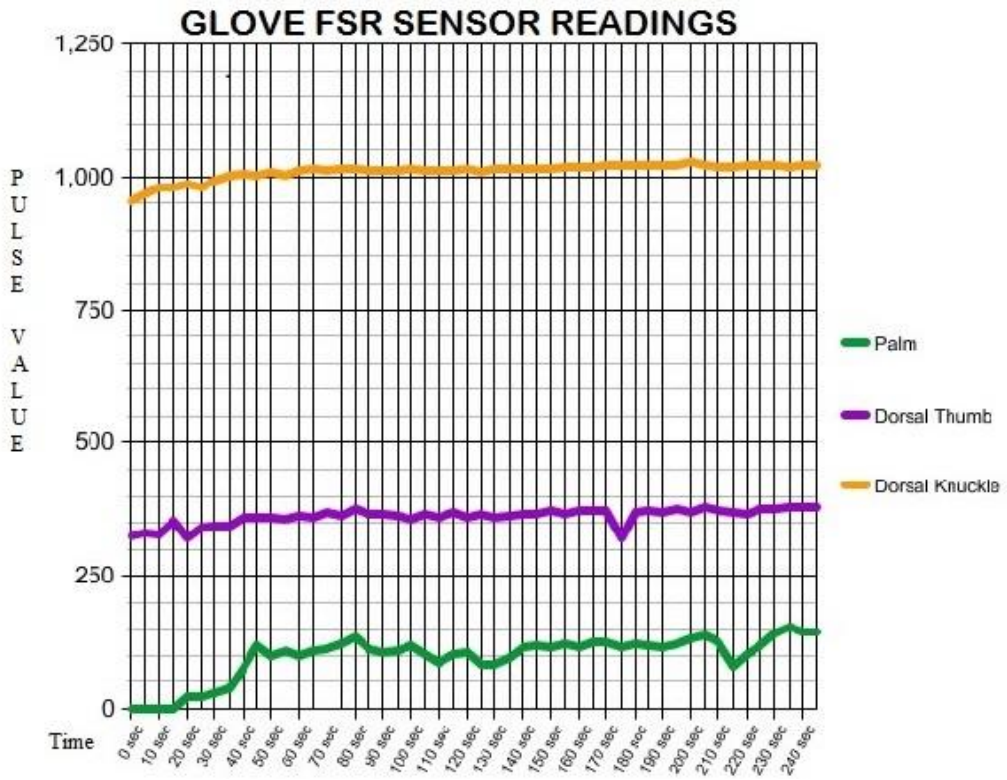

Figure 64. Typical profile of sensor values through a 4 minute period of pressure reduction.

The consistent compensation of sensor pressure decreases between sensors embedded in the HEE layer and prosthetic limb indicate that a type of hydrostatic equilibrium is at work. In this model, the ability to create exacting atmospheric pressure analog over all body surface areas as pursued by the classic definition of MCP Space Suit is relegated to a secondary consideration. The potential to achieve hydrostatic equilibrium in context of the Buehlmann ZH L16 algorithm, which splits the body into 16 tissues (compartments) and gives them a range of half-times, from several minutes to several hours of decompression durations. These tissues do not represent any specific physiological tissues in the body, and the half-times are simply chosen to give a representative spread of likely values of perfusion, diffusion in relation to off gassing and fast tissues, which accumulate gas loads quickly[26].

The HEE decompression development model proposes all theoretical ZH L16 compartments are encompassed by a 17th unifying virtual compartment consisting of the epidermis, or whole body skin surface. This concept, while outside the scope of this thesis, is currently being developed as an extension of modified decompression theory adapted specifically to HEE principals of homeostasis.

[26] *Bühlmann, Albert A (1984). Decompression-Decompression Sickness. Berlin New York: Springer-Verlag. ISBN 0-387-13308-9.*

CHAPTER V

CONCLUSIONS

1. Initial hypobaric testing demonstrate that these alternative materials and methods of construction are resistant to damage or deformations through a wide range of altered pressure environments. No adverse effects on the test glove HEE layer or associated components (compression mesh embedded in the digits was observed noted. With further refinement, the HEE garment comprised of microfiber suit, Bioflex, cooling tubing, and floating compression netting can be integrated into a single layer. The technique for an improved version has already been formulated, which will cut fabrication time in half. This new method involves laminating the micromesh and Bioflex into a unified material before HEE layer fabrication The addition of skin surface contact layer for further perspiration suppression (or/and potential minimal sweat absorption) in the form of a neoprene membrane liner has been determined to the be a possible solution for higher efficiency through an added boundary layer. The HEE layer garment has potential applications for medical emergency uses as well, including treatment of hypothermia and heatstroke victims.

2. Added points of control to flexible neck seal in the form of compression ring pressure regulation in relation to external atmospheric pressure, as well as the other design improvements discussed in section IV merit further research.
3. Further investigation into tension actuation, hydrostatic equilibrium, and modified decompression protocols are recommended, which fall into the category of design considerations not discussed in detail within the scope of this thesis. Also more research is needed into skin surface tensional properties and epidermal tissue expansion, which are areas of research not easily academically accessed at present.
4. Research into a greater resolution and control for suit cooling is being considered. This increase in control resolution would most likely involve replacing the 1/16” cooling tubing with some kind of thermal layer that can perform a similar function in multiple temperature gradients with solid state controllers. This type of material most likely will be unavailable for some time.
5. Funding efforts have to be extended further toward governmental and non-governmental funding sources, including private industry materials technology and medical sectors.

APPENDICES

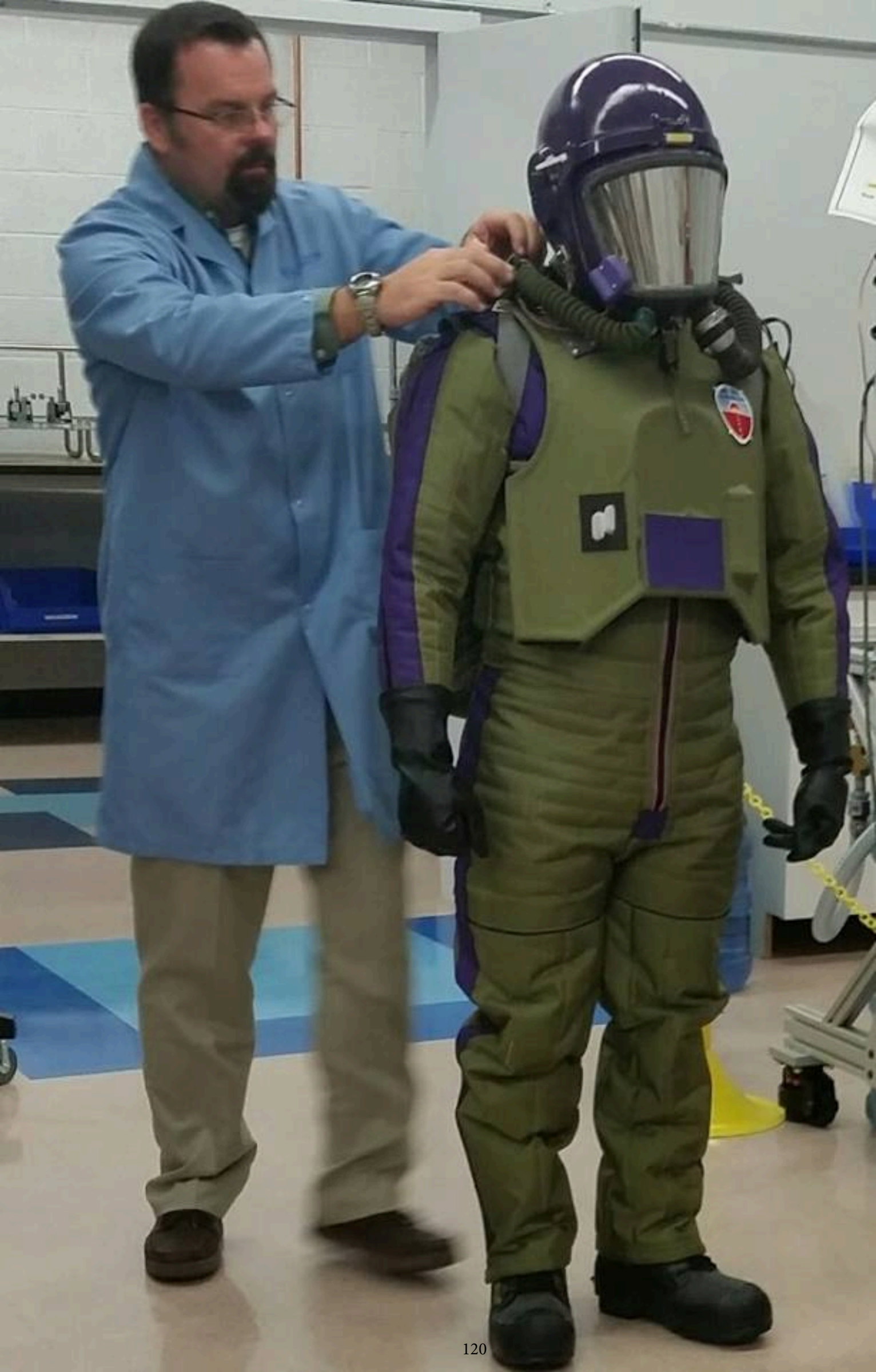

APPENDIX A

ARDUINO CODE

Arduino Code

Thermal control code

```
//The relays will be plugged in onto digital IO Pins: 2, 3, 4, 5

#include <OneWire.h> //Include the OneWire Library

OneWire ds(2); // on pin 10 (a 4.7K resistor is necessary)
//Declare a byte variable to know which thermometer reading are we taking
byte Thermometer;
//Declare the 4 relays
int relay1=6;
int relay2=7;
int relay3=8;
int relay4=9;

void setup(void) {
  //define the baud rate at which you are going to communicate with your serial monitor
  Serial.begin(9600);
    // set the digital pin as output for the relays:
  pinMode(relay1, OUTPUT);
  pinMode(relay2, OUTPUT);
  pinMode(relay3, OUTPUT);
  pinMode(relay4, OUTPUT);
}

void loop(void) {
    byte i;
    byte present = 0;
    byte type_s;
    byte data[12];
    byte addr[8];
    float celsius, fahrenheit;

    if ( !ds.search(addr)) {
      Serial.println("No more addresses.");
```

```
  Serial.println();
  ds.reset_search();
  delay(250);
  return;
}

Serial.print("ROM ="); //Save the Hardware address of the thermometer
for ( i = 0; i < 8; i++) {
  Serial.write(' ');
  Serial.print(addr[i], HEX);
}

if (OneWire::crc8(addr, 7) != addr[7]) {
  Serial.println("CRC is not valid!");
  return;
}
Serial.println();

//The last ROM Byte indicates the thermometer
Thermometer=addr[7];
// the first ROM byte indicates which chip
switch (addr[0]) {
case 0x10:
Serial.println(" Chip = DS18S20"); // or old DS1820
type_s = 1;
break;
case 0x28:
Serial.println(" Chip = DS18B20");
type_s = 0;
break;
case 0x22:
Serial.println(" Chip = DS1822");
type_s = 0;
break;
default:
Serial.println("Device is not a DS18x20 family device.");
return;
}

ds.reset();
ds.select(addr);
ds.write(0x44, 1); // start conversion, with parasite power on at the end

delay(2000); // maybe 750ms is enough, maybe not
// we might do a ds.depower() here, but the reset will take care of it.
```

```
present = ds.reset();
ds.select(addr);
ds.write(0xBE); // Read Scratchpad

Serial.print(" Data = ");
Serial.print(present, HEX);
Serial.print(" ");
for ( i = 0; i < 9; i++) { // we need 9 bytes
data[i] = ds.read();
Serial.print(data[i], HEX);
Serial.print(" ");
}
Serial.print(" CRC=");
Serial.print(OneWire::crc8(data, 8), HEX);
Serial.print(" Thermometer=");
Serial.print(Thermometer);
Serial.println();

// Convert the data to actual temperature
// because the result is a 16 bit signed integer, it should
// be stored to an "int16_t" type, which is always 16 bits
// even when compiled on a 32 bit processor.
int16_t raw = (data[1] << 8) | data[0];
if (type_s) {
raw = raw << 3; // 9 bit resolution default
if (data[7] == 0x10) {
// "count remain" gives full 12 bit resolution
raw = (raw & 0xFFF0) + 12 - data[6];
}
} else {
byte cfg = (data[4] & 0x60);
// at lower res, the low bits are undefined, so let's zero them
if (cfg == 0x00) raw = raw & ~7; // 9 bit resolution, 93.75 ms
else if (cfg == 0x20) raw = raw & ~3; // 10 bit res, 187.5 ms
else if (cfg == 0x40) raw = raw & ~1; // 11 bit res, 375 ms
//// default is 12 bit resolution, 750 ms conversion time
}
celsius = (float)raw / 16.0;
fahrenheit = celsius * 1.8 + 32.0;
Serial.print(" Temperature = ");
Serial.print(celsius);
Serial.print(" Celsius, ");
Serial.print(fahrenheit);
Serial.println(" Fahrenheit");
```

```
  //--------------------------------------------------------------------------
  if (Thermometer==0xEA) //EA is the last byte of your ROM on your first
Thermometer
  {
   if (celsius>=33)
   {
    digitalWrite(relay1, LOW);
    Serial.println(" Relay1 is turned ON");
   }
   else if (celsius<=30)
   {
    digitalWrite(relay1, HIGH);
    Serial.println(" Relay1 is turned OFF");
   }
  }
  //--------------------------------------------------------------------------
  if (Thermometer==0x46)
  {
   if (celsius>=33)
   {
    digitalWrite(relay2, LOW);
    Serial.println(" Relay2 is turned ON");
   }
   else if (celsius<=30)
   {
    digitalWrite(relay2, HIGH);
    Serial.println(" Relay2 is turned OFF");
   }
  }
  //--------------------------------------------------------------------------
  if (Thermometer==0x49)
  {
   if (celsius>=33)
   {
    digitalWrite(relay3, LOW);
    Serial.println(" Relay3 is turned ON");
   }
   else if (celsius<=30)
   {
    digitalWrite(relay3, HIGH);
    Serial.println(" Relay3 is turned OFF");
   }
  }
  //--------------------------------------------------------------------------
  if (Thermometer==0x2D)
  {
```

```
    if (celsius>=33)
    {
      digitalWrite(relay4, LOW);
      Serial.println(" Relay4 is turned ON");
    }
    else if (celsius<=30)
    {
      digitalWrite(relay4, HIGH);
      Serial.println(" Relay4 is turned OFF");
    }
   }
}
```

Glove pressure sensor control code

```
//HEE FSR 3 Channel Config

int FSR_Pin = A0; //analog pin 0
int FSR_Pin1 = A1; //analog pin 1
int FSR_Pin2 = A2; //analog pin 2

void setup(){
  Serial.begin(9600);
}

void loop(){
  int FSRReading = analogRead(FSR_Pin);
  int FSRReading1 = analogRead(FSR_Pin1);
  int FSRReading2 = analogRead(FSR_Pin2);
  Serial.println("FS402 Sensor 0");
  Serial.println(FSRReading);
  delay(5000);
  Serial.println("FS402 Sensor 1");
  Serial.println(FSRReading1);
  delay(5000);
  Serial.println("FS402 Sensor 2");
  Serial.println(FSRReading2);
  delay(5000); //just here to slow down the output for easier reading
}
```

Data Log Files

Raw glove data capture

FS402 Sensor Palm
0
FS402 Sensor Dorsal
331
FS402 Dorsal Thumb
966
FS402 Sensor Palm
0
FS402 Sensor Dorsal
328
FS402 Dorsal Thumb
981
FS402 Sensor Palm
0
FS402 Sensor Dorsal
355
FS402 Dorsal Thumb
981
FS402 Sensor Palm
23
FS402 Sensor Dorsal
322
FS402 Dorsal Thumb
988
FS402 Sensor Palm
21
FS402 Sensor Dorsal
340
FS402 Dorsal Thumb
979
FS402 Sensor Palm
29
FS402 Sensor Dorsal
344
FS402 Dorsal Thumb
992
FS402 Sensor Palm
39
FS402 Sensor Dorsal
345
FS402 Dorsal Thumb
1003

FS402 Sensor Palm
78
FS402 Sensor Dorsal
360
FS402 Dorsal Thumb
1005
FS402 Sensor Palm
119
FS402 Sensor Dorsal
359
FS402 Dorsal Thumb
1001
FS402 Sensor Palm
100
FS402 Sensor Dorsal
361
FS402 Dorsal Thumb
1008
FS402 Sensor Palm
109
FS402 Sensor Dorsal
356
FS402 Dorsal Thumb
1004
FS402 Sensor Palm
101
FS402 Sensor Dorsal
362
FS402 Dorsal Thumb
1012
FS402 Sensor Palm
108
FS402 Sensor Dorsal
359
FS402 Dorsal Thumb
1015
FS402 Sensor Palm
112
FS402 Sensor Dorsal
368
FS402 Dorsal Thumb
1013
FS402 Sensor Palm
123
FS402 Sensor Dorsal
364
FS402 Dorsal Thumb

1017
FS402 Sensor Palm
135
FS402 Sensor Dorsal
376
FS402 Dorsal Thumb
1016
FS402 Sensor Palm
112
FS402 Sensor Dorsal
365
FS402 Dorsal Thumb
1013
FS402 Sensor Palm
106
FS402 Sensor Dorsal
365
FS402 Dorsal Thumb
1013
FS402 Sensor Palm
108
FS402 Sensor Dorsal
362
FS402 Dorsal Thumb
1012
FS402 Sensor Palm
118
FS402 Sensor Dorsal
366
FS402 Dorsal Thumb
1015
FS402 Sensor Palm
103
FS402 Sensor Dorsal
366
FS402 Dorsal Thumb
1012
FS402 Sensor Palm
88
FS402 Sensor Dorsal
361
FS402 Dorsal Thumb
1012
FS402 Sensor Palm
102
FS402 Sensor Dorsal
369

FS402 Dorsal Thumb
1011
FS402 Sensor Palm
107
FS402 Sensor Dorsal
361
FS402 Dorsal Thumb
1015
FS402 Sensor Palm
84
FS402 Sensor Dorsal
365
FS402 Dorsal Thumb
1010
FS402 Sensor Palm
84
FS402 Sensor Dorsal
359
FS402 Dorsal Thumb
1016
FS402 Sensor Palm
95
FS402 Sensor Dorsal
362
FS402 Dorsal Thumb
1016
FS402 Sensor Palm
115
FS402 Sensor Dorsal
365
FS402 Dorsal Thumb
1014
FS402 Sensor Palm
119
FS402 Sensor Dorsal
366
FS402 Dorsal Thumb
1016
FS402 Sensor Palm
117
FS402 Sensor Dorsal
372
FS402 Dorsal Thumb
1017
FS402 Sensor Palm
122
FS402 Sensor Dorsal

367
FS402 Dorsal Thumb
1018
FS402 Sensor Palm
116
FS402 Sensor Dorsal
372
FS402 Dorsal Thumb
1019
FS402 Sensor Palm
124
FS402 Sensor Dorsal
372
FS402 Dorsal Thumb
1020
FS402 Sensor Palm
126
FS402 Sensor Dorsal
374
FS402 Dorsal Thumb
1021
FS402 Sensor Palm
116
FS402 Sensor Dorsal
370
FS402 Dorsal Thumb
1021
FS402 Sensor Palm
122
FS402 Sensor Dorsal
370
FS402 Dorsal Thumb
1021
FS402 Sensor Palm
120
FS402 Sensor Dorsal
374
FS402 Dorsal Thumb
1021
FS402 Sensor Palm
117
FS402 Sensor Dorsal
370
FS402 Dorsal Thumb
1021
FS402 Sensor Palm
122

FS402 Sensor Dorsal
376
FS402 Dorsal Thumb
1021
FS402 Sensor Palm
131
FS402 Sensor Dorsal
371
FS402 Dorsal Thumb
1020
FS402 Sensor Palm
139
FS402 Sensor Dorsal
380
FS402 Dorsal Thumb
1021
FS402 Sensor Palm
126
FS402 Sensor Dorsal
373
FS402 Dorsal Thumb
1020
FS402 Sensor Palm
82
FS402 Sensor Dorsal
368
FS402 Dorsal Thumb
1018
FS402 Sensor Palm
102
FS402 Sensor Dorsal
365
FS402 Dorsal Thumb
1022
FS402 Sensor Palm
120
FS402 Sensor Dorsal
376
FS402 Dorsal Thumb
1022
FS402 Sensor Palm
142
FS402 Sensor Dorsal
375
FS402 Dorsal Thumb
1022
FS402 Sensor Palm

153
FS402 Sensor Dorsal
378
FS402 Dorsal Thumb
1020
FS402 Sensor Palm
146
FS402 Sensor Dorsal
379
FS402 Dorsal Thumb
1022
FS402 Sensor Palm
146
FS402 Sensor Dorsal
378
FS402 Dorsal Thumb
1021
FS402 Sensor Palm
145
FS402 Sensor Dorsal
380
FS402 Dorsal Thumb
1023
FS402 Sensor Palm
149
FS402 Sensor Dorsal
380
FS402 Dorsal Thumb
1022
FS402 Sensor Palm
165
FS402 Sensor Dorsal
389
FS402 Dorsal Thumb
1023
FS402 Sensor Palm
180
FS402 Sensor Dorsal
389
FS402 Dorsal Thumb
1022
FS402 Sensor Palm
180
FS402 Sensor Dorsal
394
FS402 Dorsal Thumb
1023

FS402 Sensor Palm
150
FS402 Sensor Dorsal
377
FS402 Dorsal Thumb
1023
FS402 Sensor Palm
146
FS402 Sensor Dorsal
385
FS402 Dorsal Thumb
1023
FS402 Sensor Palm
143
FS402 Sensor Dorsal
377
FS402 Dorsal Thumb
1023

FS402 Sensor Palm
148
FS402 Sensor Dorsal
386
FS402 Dorsal Thumb
1023
FS402 Sensor Palm
152
FS402 Sensor Dorsal
382
FS402 Dorsal Thumb
1023
FS402 Sensor Palm
156
FS402 Sensor Dorsal
387
FS402 Dorsal Thumb
1023
FS402 Sensor Palm
161
FS402 Sensor Dorsal
385
FS402 Dorsal Thumb
1023
FS402 Sensor Palm
152
FS402 Sensor Dorsal
388

FS402 Dorsal Thumb
1023
FS402 Sensor Palm
142

Raw thermal data capture and relay actuation

Data = 1 E8 1 4B 46 7F FF 8 10 97 CRC=97 Thermometer=234
 Temperature = 30.50 Celsius, 86.90 Fahrenheit
ROM = 28 E1 ED 76 6 0 0 46
 Chip = DS18B20
 Data = 1 E5 1 4B 46 7F FF B 10 BE CRC=BE Thermometer=70
 Temperature = 30.31 Celsius, 86.56 Fahrenheit
ROM = 28 9 8 77 6 0 0 49
 Chip = DS18B20
 Data = 1 3 2 4B 46 7F FF D 10 B3 CRC=B3 Thermometer=73
 Temperature = 32.19 Celsius, 89.94 Fahrenheit
ROM = 28 3F 54 76 6 0 0 2D
 Chip = DS18B20
 Data = 1 2E 2 4B 46 7F FF 2 10 7F CRC=7F Thermometer=45
 Temperature = 34.88 Celsius, 94.77 Fahrenheit
 Relay4 is turned ON
No more addresses.

OOOOOOOOOOOO
ROM = 28 CA 84 76 6 0 0 EA
 Chip = DS18B20
 Data = 1 FD 1 4B 46 7F FF 3 10 B6 CRC=B6 Thermometer=234
 Temperature = 31.81 Celsius, 89.26 Fahrenheit
ROM = 28 E1 ED 76 6 0 0 46
 Chip = DS18B20
 Data = 1 F3 1 4B 46 7F FF D 10 D3 CRC=D3 Thermometer=70
 Temperature = 31.19 Celsius, 88.14 Fahrenheit
ROM = 28 9 8 77 6 0 0 49
 Chip = DS18B20
 Data = 1 9 2 4B 46 7F FF 7 10 F8 CRC=F8 Thermometer=73
 Temperature = 32.56 Celsius, 90.61 Fahrenheit
ROM = 28 3F 54 76 6 0 0 2D
 Chip = DS18B20
 Data = 1 34 2 4B 46 7F FF C 10 5B CRC=5B Thermometer=45
 Temperature = 35.25 Celsius, 95.45 Fahrenheit
 Relay4 is turned ON
No more addresses.

```
ooooooooooo
ROM = 28 CA 84 76 6 0 0 EA
 Chip = DS18B20
 Data = 1 9 2 4B 46 7F FF 7 10 F8  CRC=F8 Thermometer=234
 Temperature = 32.56 Celsius, 90.61 Fahrenheit
ROM = 28 E1 ED 76 6 0 0 46
 Chip = DS18B20
 Data = 1 FD 1 4B 46 7F FF 3 10 B6  CRC=B6 Thermometer=70
 Temperature = 31.81 Celsius, 89.26 Fahrenheit
ROM = 28 9 8 77 6 0 0 49
 Chip = DS18B20
 Data = 1 E 2 4B 46 7F FF 2 10 D7  CRC=D7 Thermometer=73
 Temperature = 32.88 Celsius, 91.18 Fahrenheit
ROM = 28 3F 54 76 6 0 0 2D
 Chip = DS18B20
 Data = 1 37 2 4B 46 7F FF 9 10 61  CRC=61 Thermometer=45
 Temperature = 35.44 Celsius, 95.79 Fahrenheit
 Relay4 is turned ON
No more addresses.

000000000000000000
ROM = 28 CA 84 76 6 0 0 EA
 Chip = DS18B20
 Data = 1 10 2 4B 46 7F FF 10 10 47  CRC=47 Thermometer=234
 Temperature = 33.00 Celsius, 91.40 Fahrenheit
 Relay1 is turned ON
ROM = 28 E1 ED 76 6 0 0 46
 Chip = DS18B20
 Data = 1 4 2 4B 46 7F FF C 10 A7  CRC=A7 Thermometer=70
 Temperature = 32.25 Celsius, 90.05 Fahrenheit
ROM = 28 9 8 77 6 0 0 49
 Chip = DS18B20
 Data = 1 11 2 4B 46 7F FF F 10 F0  CRC=F0 Thermometer=73
 Temperature = 33.06 Celsius, 91.51 Fahrenheit
 Relay3 is turned ON
ROM = 28 3F 54 76 6 0 0 2D
 Chip = DS18B20
 Data = 1 2C 2 4B 46 7F FF 4 10 53  CRC=53 Thermometer=45
 Temperature = 34.75 Celsius, 94.55 Fahrenheit
 Relay4 is turned ON
No more addresses.

 Chip = DS18B20
 Data = 1 14 2 4B 46 7F FF C 10 F3  CRC=F3 Thermometer=234
 Temperature = 33.25 Celsius, 91.85 Fahrenheit
 Relay1 is turned ON
```

ROM = 28 E1 ED 76 6 0 0 46
 Chip = DS18B20
 Data = 1 8 2 4B 46 7F FF 8 10 A3 CRC=A3 Thermometer=70
 Temperature = 32.50 Celsius, 90.50 Fahrenheit
ROM = 28 9 8 77 6 0 0 49
 Chip = DS18B20
 Data = 1 13 2 4B 46 7F FF D 10 E7 CRC=E7 Thermometer=73
 Temperature = 33.19 Celsius, 91.74 Fahrenheit
 Relay3 is turned ON
ROM = 28 3F 54 76 6 0 0 2D
 Chip = DS18B20
 Data = 1 23 2 4B 46 7F FF D 10 1B CRC=1B Thermometer=45
 Temperature = 34.19 Celsius, 93.54 Fahrenheit
 Relay4 is turned ON
No more addresses.

000000000000000000000000
ROM = 28 CA 84 76 6 0 0 EA
 Chip = DS18B20
 Data = 1 10 2 4B 46 7F FF 10 10 47 CRC=47 Thermometer=234
 Temperature = 33.00 Celsius, 91.40 Fahrenheit
 Relay1 is turned ON
ROM = 28 E1 ED 76 6 0 0 46
 Chip = DS18B20
 Data = 1 1 2 4B 46 7F FF F 10 A4 CRC=A4 Thermometer=70
 Temperature = 32.06 Celsius, 89.71 Fahrenheit
ROM = 28 9 8 77 6 0 0 49
 Chip = DS18B20
 Data = 1 15 2 4B 46 7F FF B 10 DE CRC=DE Thermometer=73
 Temperature = 33.31 Celsius, 91.96 Fahrenheit
 Relay3 is turned ON
ROM = 28 3F 54 76 6 0 0 2D
 Chip = DS18B20
 Data = 1 19 2 4B 46 7F FF 7 10 AC CRC=AC Thermometer=45
 Temperature = 33.56 Celsius, 92.41 Fahrenheit
 Relay4 is turned ON
No more addresses.

000000000000000000000000
ROM = 28 CA 84 76 6 0 0 EA
 Chip = DS18B20
 Data = 1 F 2 4B 46 7F FF 1 10 C1 CRC=C1 Thermometer=234
 Temperature = 32.94 Celsius, 91.29 Fahrenheit
ROM = 28 E1 ED 76 6 0 0 46
 Chip = DS18B20
 Data = 1 F8 1 4B 46 7F FF 8 10 C3 CRC=C3 Thermometer=70

```
 Temperature = 31.50 Celsius, 88.70 Fahrenheit
ROM = 28 9 8 77 6 0 0 49
 Chip = DS18B20
 Data = 1 F 2 4B 46 7F FF 1 10 C1  CRC=C1 Thermometer=73
 Temperature = 32.94 Celsius, 91.29 Fahrenheit
ROM = 28 3F 54 76 6 0 0 2D
 Chip = DS18B20
 Data = 1 15 2 4B 46 7F FF B 10 DE  CRC=DE Thermometer=45
 Temperature = 33.31 Celsius, 91.96 Fahrenheit
 Relay4 is turned ON
No more addresses.

00000000000000000000000
ROM = 28 CA 84 76 6 0 0 EA
 Chip = DS18B20
 Data = 1 D 2 4B 46 7F FF 3 10 D6  CRC=D6 Thermometer=234
 Temperature = 32.81 Celsius, 91.06 Fahrenheit
ROM = 28 E1 ED 76 6 0 0 46
 Chip = DS18B20
 Data = 1 F3 1 4B 46 7F FF D 10 D3  CRC=D3 Thermometer=70
 Temperature = 31.19 Celsius, 88.14 Fahrenheit
ROM = 28 9 8 77 6 0 0 49
 Chip = DS18B20
 Data = 1 8 2 4B 46 7F FF 8 10 A3  CRC=A3 Thermometer=73
 Temperature = 32.50 Celsius, 90.50 Fahrenheit
ROM = 28 3F 54 76 6 0 0 2D
 Chip = DS18B20
 Data = 1 D 2 4B 46 7F FF 3 10 D6  CRC=D6 Thermometer=45
 Temperature = 32.81 Celsius, 91.06 Fahrenheit
No more addresses.

00000000000000000000000
ROM = 28 CA 84 76 6 0 0 EA
 Chip = DS18B20
 Data = 1 2D 2 4B 46 7F FF 3 10 7E  CRC=7E Thermometer=234
 Temperature = 34.81 Celsius, 94.66 Fahrenheit
 Relay1 is turned ON
ROM = 28 E1 ED 76 6 0 0 46
 Chip = DS18B20
 Data = 1 F6 1 4B 46 7F FF A 10 EB  CRC=EB Thermometer=70
 Temperature = 31.37 Celsius, 88.47 Fahrenheit
ROM = 28 9 8 77 6 0 0 49
 Chip = DS18B20
 Data = 1 A 2 4B 46 7F FF 6 10 F9  CRC=F9 Thermometer=73
 Temperature = 32.63 Celsius, 90.72 Fahrenheit
ROM = 28 3F 54 76 6 0 0 2D
```

```
 Chip = DS18B20
 Data = 1 12 2 4B 46 7F FF E 10 F1  CRC=F1 Thermometer=45
 Temperature = 33.13 Celsius, 91.62 Fahrenheit
 Relay4 is turned ON
No more addresses.

000000000000000000000000
ROM = 28 CA 84 76 6 0 0 EA
 Chip = DS18B20
 Data = 1 36 2 4B 46 7F FF A 10 77  CRC=77 Thermometer=234
 Temperature = 35.38 Celsius, 95.68 Fahrenheit
 Relay1 is turned ON
ROM = 28 E1 ED 76 6 0 0 46
 Chip = DS18B20
 Data = 1 7 2 4B 46 7F FF 9 10 9D  CRC=9D Thermometer=70
 Temperature = 32.44 Celsius, 90.39 Fahrenheit
ROM = 28 9 8 77 6 0 0 49
 Chip = DS18B20
 Data = 1 10 2 4B 46 7F FF 10 10 47  CRC=47 Thermometer=73
 Temperature = 33.00 Celsius, 91.40 Fahrenheit
 Relay3 is turned ON
ROM = 28 3F 54 76 6 0 0 2D
 Chip = DS18B20
 Data = 1 2B 2 4B 46 7F FF 5 10 47  CRC=47 Thermometer=45
 Temperature = 34.69 Celsius, 94.44 Fahrenheit
 Relay4 is turned ON
No more addresses.

00000000000000000000000000000000
ROM = 28 CA 84 76 6 0 0 EA
 Chip = DS18B20
 Data = 1 23 2 4B 46 7F FF D 10 1B  CRC=1B Thermometer=234
 Temperature = 34.19 Celsius, 93.54 Fahrenheit
 Relay1 is turned ON
ROM = 28 E1 ED 76 6 0 0 46
 Chip = DS18B20
 Data = 1 8 2 4B 46 7F FF 8 10 A3  CRC=A3 Thermometer=70
 Temperature = 32.50 Celsius, 90.50 Fahrenheit
ROM = 28 9 8 77 6 0 0 49
 Chip = DS18B20
 Data = 1 D 2 4B 46 7F FF 3 10 D6  CRC=D6 Thermometer=73
 Temperature = 32.81 Celsius, 91.06 Fahrenheit
ROM = 28 3F 54 76 6 0 0 2D
 Chip = DS18B20
 Data = 1 3B 2 4B 46 7F FF 5 10 13  CRC=13 Thermometer=45
 Temperature = 35.69 Celsius, 96.24 Fahrenheit
```

```
 Relay4 is turned ON
No more addresses.

0000000000000000000000000000
ROM = 28 CA 84 76 6 0 0 EA
 Chip = DS18B20
 Data = 1 18 2 4B 46 7F FF 8 10 F7  CRC=F7 Thermometer=234
 Temperature = 33.50 Celsius, 92.30 Fahrenheit
 Relay1 is turned ON
ROM = 28 E1 ED 76 6 0 0 46
 Chip = DS18B20
 Data = 1 4 2 4B 46 7F FF C 10 A7  CRC=A7 Thermometer=70
 Temperature = 32.25 Celsius, 90.05 Fahrenheit
ROM = 28 9 8 77 6 0 0 49
 Chip = DS18B20
 Data = 1 6 2 4B 46 7F FF A 10 8B  CRC=8B Thermometer=73
 Temperature = 32.38 Celsius, 90.27 Fahrenheit
ROM = 28 3F 54 76 6 0 0 2D
 Chip = DS18B20
 Data = 1 3F 2 4B 46 7F FF 1 10 3D  CRC=3D Thermometer=45
 Temperature = 35.94 Celsius, 96.69 Fahrenheit
 Relay4 is turned ON
No more addresses.

0000000000000000000000000000
ROM = 28 CA 84 76 6 0 0 EA
 Chip = DS18B20
 Data = 1 15 2 4B 46 7F FF B 10 DE  CRC=DE Thermometer=234
 Temperature = 33.31 Celsius, 91.96 Fahrenheit
 Relay1 is turned ON
ROM = 28 E1 ED 76 6 0 0 46
 Chip = DS18B20
 Data = 1 10 2 4B 46 7F FF 10 10 47  CRC=47 Thermometer=70
 Temperature = 33.00 Celsius, 91.40 Fahrenheit
 Relay2 is turned ON
ROM = 28 9 8 77 6 0 0 49
 Chip = DS18B20
 Data = 1 B 2 4B 46 7F FF 5 10 EF  CRC=EF Thermometer=73
 Temperature = 32.69 Celsius, 90.84 Fahrenheit
ROM = 28 3F 54 76 6 0 0 2D
 Chip = DS18B20
 Data = 1 41 2 4B 46 7F FF F 10 ED  CRC=ED Thermometer=45
 Temperature = 36.06 Celsius, 96.91 Fahrenheit
 Relay4 is turned ON
No more addresses.
```

```
00000000000000000000000000
ROM = 28 CA 84 76 6 0 0 EA
 Chip = DS18B20
 Data = 1 1B 2 4B 46 7F FF 5 10 BB  CRC=BB Thermometer=234
 Temperature = 33.69 Celsius, 92.64 Fahrenheit
 Relay1 is turned ON
ROM = 28 E1 ED 76 6 0 0 46
 Chip = DS18B20
 Data = 1 17 2 4B 46 7F FF 9 10 C9  CRC=C9 Thermometer=70
 Temperature = 33.44 Celsius, 92.19 Fahrenheit
 Relay2 is turned ON
ROM = 28 9 8 77 6 0 0 49
 Chip = DS18B20
 Data = 1 15 2 4B 46 7F FF B 10 DE  CRC=DE Thermometer=73
 Temperature = 33.31 Celsius, 91.96 Fahrenheit
 Relay3 is turned ON
ROM = 28 3F 54 76 6 0 0 2D
 Chip = DS18B20
 Data = 1 42 2 4B 46 7F FF E 10 EC  CRC=EC Thermometer=45
 Temperature = 36.13 Celsius, 97.02 Fahrenheit
 Relay4 is turned ON
No more addresses.

00000000000000000000000000
ROM = 28 CA 84 76 6 0 0 EA
 Chip = DS18B20
 Data = 1 20 2 4B 46 7F FF 10 10 BB  CRC=BB Thermometer=234
 Temperature = 34.00 Celsius, 93.20 Fahrenheit
 Relay1 is turned ON
ROM = 28 E1 ED 76 6 0 0 46
 Chip = DS18B20
 Data = 1 19 2 4B 46 7F FF 7 10 AC  CRC=AC Thermometer=70
 Temperature = 33.56 Celsius, 92.41 Fahrenheit
 Relay2 is turned ON
ROM = 28 9 8 77 6 0 0 49
 Chip = DS18B20
 Data = 1 1A 2 4B 46 7F FF 6 10 AD  CRC=AD Thermometer=73
 Temperature = 33.63 Celsius, 92.52 Fahrenheit
 Relay3 is turned ON
ROM = 28 3F 54 76 6 0 0 2D
 Chip = DS18B20
 Data = 1 42 2 4B 46 7F FF E 10 EC  CRC=EC Thermometer=45
 Temperature = 36.13 Celsius, 97.02 Fahrenheit
 Relay4 is turned ON
No more addresses.
```

00000000000000000000000000
ROM = 28 CA 84 76 6 0 0 EA
 Chip = DS18B20
 Data = 1 23 2 4B 46 7F FF D 10 1B CRC=1B Thermometer=234
 Temperature = 34.19 Celsius, 93.54 Fahrenheit
 Relay1 is turned ON
ROM = 28 E1 ED 76 6 0 0 46
 Chip = DS18B20
 Data = 1 1B 2 4B 46 7F FF 5 10 BB CRC=BB Thermometer=70
 Temperature = 33.69 Celsius, 92.64 Fahrenheit
 Relay2 is turned ON
ROM = 28 9 8 77 6 0 0 49
 Chip = DS18B20
 Data = 1 1C 2 4B 46 7F FF 4 10 AF CRC=AF Thermometer=73
 Temperature = 33.75 Celsius, 92.75 Fahrenheit
 Relay3 is turned ON
ROM = 28 3F 54 76 6 0 0 2D
 Chip = DS18B20
 Data = 1 38 2 4B 46 7F FF 8 10 5F CRC=5F Thermometer=45
 Temperature = 35.50 Celsius, 95.90 Fahrenheit
 Relay4 is turned ON
No more addresses.

00000000000000000000000000
ROM = 28 CA 84 76 6 0 0 EA
 Chip = DS18B20
 Data = 1 20 2 4B 46 7F FF 10 10 BB CRC=BB Thermometer=234
 Temperature = 34.00 Celsius, 93.20 Fahrenheit
 Relay1 is turned ON
ROM = 28 E1 ED 76 6 0 0 46
 Chip = DS18B20
 Data = 1 1D 2 4B 46 7F FF 3 10 82 CRC=82 Thermometer=70
 Temperature = 33.81 Celsius, 92.86 Fahrenheit
 Relay2 is turned ON
ROM = 28 9 8 77 6 0 0 49
 Chip = DS18B20
 Data = 1 18 2 4B 46 7F FF 8 10 F7 CRC=F7 Thermometer=73
 Temperature = 33.50 Celsius, 92.30 Fahrenheit
 Relay3 is turned ON
ROM = 28 3F 54 76 6 0 0 2D
 Chip = DS18B20
 Data = 1 23 2 4B 46 7F FF D 10 1B CRC=1B Thermometer=45
 Temperature = 34.19 Celsius, 93.54 Fahrenheit
 Relay4 is turned ON
No more addresses.

```
00000000000000000000000000000000
ROM = 28 CA 84 76 6 0 0 EA
 Chip = DS18B20
 Data = 1 18 2 4B 46 7F FF 8 10 F7  CRC=F7 Thermometer=234
 Temperature = 33.50 Celsius, 92.30 Fahrenheit
 Relay1 is turned ON
ROM = 28 E1 ED 76 6 0 0 46
 Chip = DS18B20
 Data = 1 1D 2 4B 46 7F FF 3 10 82  CRC=82 Thermometer=70
 Temperature = 33.81 Celsius, 92.86 Fahrenheit
 Relay2 is turned ON
ROM = 28 9 8 77 6 0 0 49
 Chip = DS18B20
 Data = 1 14 2 4B 46 7F FF C 10 F3  CRC=F3 Thermometer=73
 Temperature = 33.25 Celsius, 91.85 Fahrenheit
 Relay3 is turned ON
ROM = 28 3F 54 76 6 0 0 2D
 Chip = DS18B20
 Data = 1 16 2 4B 46 7F FF A 10 DF  CRC=DF Thermometer=45
 Temperature = 33.38 Celsius, 92.07 Fahrenheit
 Relay4 is turned ON
No more addresses.

00000000000000000000000000000000
ROM = 28 CA 84 76 6 0 0 EA
 Chip = DS18B20
 Data = 1 12 2 4B 46 7F FF E 10 F1  CRC=F1 Thermometer=234
 Temperature = 33.13 Celsius, 91.62 Fahrenheit
 Relay1 is turned ON
ROM = 28 E1 ED 76 6 0 0 46
 Chip = DS18B20
 Data = 1 1F 2 4B 46 7F FF 1 10 95  CRC=95 Thermometer=70
 Temperature = 33.94 Celsius, 93.09 Fahrenheit
 Relay2 is turned ON
ROM = 28 9 8 77 6 0 0 49
 Chip = DS18B20
 Data = 1 F 2 4B 46 7F FF 1 10 C1  CRC=C1 Thermometer=73
 Temperature = 32.94 Celsius, 91.29 Fahrenheit
ROM = 28 3F 54 76 6 0 0 2D
 Chip = DS18B20
 Data = 1 C 2 4B 46 7F FF 4 10 FB  CRC=FB Thermometer=45
 Temperature = 32.75 Celsius, 90.95 Fahrenheit
No more addresses.

00000000000000000000000000000000
ROM = 28 CA 84 76 6 0 0 EA
```

Chip = DS18B20
Data = 1 B 2 4B 46 7F FF 5 10 EF CRC=EF Thermometer=234
Temperature = 32.69 Celsius, 90.84 Fahrenheit
ROM = 28 E1 ED 76 6 0 0 46
Chip = DS18B20
Data = 1 1F 2 4B 46 7F FF 1 10 95 CRC=95 Thermometer=70
Temperature = 33.94 Celsius, 93.09 Fahrenheit
Relay2 is turned ON
ROM = 28 9 8 77 6 0 0 49
Chip = DS18B20
Data = 1 C 2 4B 46 7F FF 4 10 FB CRC=FB Thermometer=73
Temperature = 32.75 Celsius, 90.95 Fahrenheit
ROM = 28 3F 54 76 6 0 0 2D
Chip = DS18B20
Data = 1 3 2 4B 46 7F FF D 10 B3 CRC=B3 Thermometer=45
Temperature = 32.19 Celsius, 89.94 Fahrenheit
No more addresses.

00000000000000000000000000000
ROM = 28 CA 84 76 6 0 0 EA
Chip = DS18B20
Data = 1 5 2 4B 46 7F FF B 10 8A CRC=8A Thermometer=234
Temperature = 32.31 Celsius, 90.16 Fahrenheit
ROM = 28 E1 ED 76 6 0 0 46
Chip = DS18B20
Data = 1 20 2 4B 46 7F FF 10 10 BB CRC=BB Thermometer=70
Temperature = 34.00 Celsius, 93.20 Fahrenheit
Relay2 is turned ON
ROM = 28 9 8 77 6 0 0 49
Chip = DS18B20
Data = 1 9 2 4B 46 7F FF 7 10 F8 CRC=F8 Thermometer=73
Temperature = 32.56 Celsius, 90.61 Fahrenheit
ROM = 28 3F 54 76 6 0 0 2D
Chip = DS18B20
Data = 1 FC 1 4B 46 7F FF 4 10 9B CRC=9B Thermometer=45
Temperature = 31.75 Celsius, 89.15 Fahrenheit
No more addresses.

000000000000000000000000
ROM = 28 CA 84 76 6 0 0 EA
Chip = DS18B20
Data = 1 FF 1 4B 46 7F FF 1 10 A1 CRC=A1 Thermometer=234
Temperature = 31.94 Celsius, 89.49 Fahrenheit
ROM = 28 E1 ED 76 6 0 0 46
Chip = DS18B20
Data = 1 21 2 4B 46 7F FF F 10 C CRC=C Thermometer=70

Temperature = 34.06 Celsius, 93.31 Fahrenheit
Relay2 is turned ON
ROM = 28 9 8 77 6 0 0 49
Chip = DS18B20
Data = 1 7 2 4B 46 7F FF 9 10 9D CRC=9D Thermometer=73
Temperature = 32.44 Celsius, 90.39 Fahrenheit
ROM = 28 3F 54 76 6 0 0 2D
Chip = DS18B20
Data = 1 F6 1 4B 46 7F FF A 10 EB CRC=EB Thermometer=45
Temperature = 31.37 Celsius, 88.47 Fahrenheit
No more addresses.

Dataset Temperatures

Data Set: 1
30.50, 31.81, 32.56, 33.00, 33.25, 33.00, 32.94, 32.81, 34.81, 35.38, 34.19, 33.50, 33.31, 33.69, 34.00, 34.19, 34.00, 33.50, 33.13, 32.69, 32.31, 31.94

Average (Mean):

Count:	**22**
Sum:	**730.51**
Average:	**730.51 / 22 = 33.205**

Data Set: 2
30.31, 31.19, 31.81, 32.25, 32.50, 32.06, 31.50, 31.19, 31.37, 32.44, 32.50, 32.25, 33.00, 33.44, 33.56, 33.69, 33.81, 33.81, 33.94, 33.94, 34.00, 34.06

Average (Mean):

Count:	**22**
Sum:	**718.62**
Average:	**718.62 / 22 = 32.664**

Data Set: 3
32.19, 32.56, 32.88, 33.06, 33.19, 33.31, 32.94, 32.50, 32.63, 33.00, 32.81, 32.38, 32.69, 33.31, 33.63, 33.75, 33.50, 33.25, 32.94, 32.75, 32.56, 32.44

Average (Mean):

Count:	**22**
Sum:	**724.27**
Average:	**724.27 / 22 = 32.921363636364**

Data Set: **4**
34.88, 35.25, 35.44, 34.75, 34.19, 33.56, 33.31, 32.81, 33.13, 34.69, 35.69, 35.94, 36.06, 36.13, 36.13, 35.50, 34.19, 33.38, 32.75, 32.19, 31.75, 31.37

Average (Mean):

Count:	**22**
Sum:	**753.09**
Average:	**753.09 / 22 = 34.231363636364**

BIBLIOGRAPHY

1 Ment, Gilles. "Operational Space Medicine." In *Fundamentals of Space Medicine*, 283-284. El Segundo, Calif., CA: Springer, 20011.

2 Spotts, P. (2014, Feb 27). Near-drowning of astronaut tied to wrong diagnosis, slow response. *The Christian Science Monitor* Retrieved from http://ezproxy.library.und.edu/login?url=http://search.proquest.com/docview/1502915471?accountid=28267

3 HSF." HSF. April 7, 2002. Accessed November 26, 2015. http://spaceflight.nasa.gov/shuttle/reference/faq/eva.html.

4 Patel, Samir S (October 20, 2005). "This suit is made for walking (on Mars)". The Christian Science Monitor. Retrieved 2015-10-14.

5 Nadel, Ethan, Robert Bullard, and J A Stolwijk. "Importance of Skin Temperature in the Regulation of Sweating." Journal of Applied Physiology 31, no. 1 (1971): 80-87. Retrieved October 12, 2015. http://jap.physiology.org/content/31/1/80.long.

6 Wienke, Bruce R. *Basic decompression: theory and application*. Best Pub Co, 2008.

7 A. W. Mix and A. J. Giacomin (2011), Standardized Polymer Durometry, *Journal of Testing and Evaluation*, **39**(4), pp. 1–10.

8 Webb, P. "The Space Activity Suit: An Elastic Leotard for Extravehicular Activity." *Aerospace Medicine* 39, no. 4 (1968): 376-83.

9 Parker, J. F. Jr., and V. R. Eds West. Bioastronautics Data Book. Second Edition. N.p.: Government Printing Office, Washington, D.C., 1973. Print.

10 Roth, Emanuel M. *Rapid (explosive) Decompression Emergencies in Pressure-suited Subjects*,. Vol. 1223. Washington: National Aeronautics and Space Administration; for Sale by the Clearinghouse for Federal Scientific and Technical Information, Springfield, Va., 1968.

11 Wienke, Bruce R; O'Leary, Timothy R (13 February 2002). "Reduced gradient bubble model: Diving algorithm, basis and comparisons" (PDF). Tampa, Florida: NAUI Technical Diving Operations. pp. 7–12. Retrieved 8 August, 2015.

12 Gallagher, A J, Ni Annaidh, and Aisling; Bruyère, Karine; Et Al. "Dynamic Tensile Properties of Human Skin." 2012 IRCOBI Conference Proceedings, 2012. http://www.ircobi.org/downloads/irc12/pdf_files/59.pdf

13 Woods, Michael. "Toledo Firm Develops Light-Weight Space Suit." The Blade, October 2, 1969, Second News Section sec. Accessed August 8, 2015. https://news.google.com/newspapers?nid=1350&dat=19691002&id=au1OAAAAIBAJ&sjid=tQEEAAAAIBAJ&pg=5285,1040523&hl=en.

14 Annis, J.F. and P. Webb. "Development of a Space Activity Suit." NASA CR-1992, Washington DC: National Aeronautics and Space Administration, 1971

15 Gorguinpour, Camron et. al (2001), LPI "Advanced Two-System Space Suit". University of California, Berkeley CB-1106. Retrieved 2012-09-23. 95 KB PDF

16 Ward RS, White KA. "Barrier Films That Breathe". Chemtech. Nov. 1991: 670.

17 "DoD Modeling and Simulation (M&S) Glossary", DoD 5000.59-M, DoD, January 1998 [1]

18 Mclafferty, Ella, Charles Hendry, and Alistair Farley. "The Integumentary System: Anatomy, Physiology and Function of Skin." *Nursing Standard* 27.3 (2012): 35-42. Web. Retrieved 28 Sept. 1015.

19 Jones, Harry. "Spacesuit Cooling on the Moon and Mars." *SAE Technical Paper Series* (2009): n. pag. Web. 28 Dec. 2015.

20 Lamba, Nina M. K., Kimberly A. Woodhouse, Stuart L. Cooper, and Michael D. Lelah. *Polyurethanes in Biomedical Applications*. Boca Raton: CRC, 1998. Print.

21 Chae, Myeong-Seon, and Bum-Jin Chung. "Radiation Exposure of an Astronaut Subject to Various Space Radiation Environments and Shielding Conditions." *Journal of the Korean Society for Aeronautical & Space Sciences* 38.10 (2010): 1038-048. Web. 8 Aug. 2015.

22 Obropta, Edward W., and Dava J. Newman. "A Comparison of Human Skin Strain Fields of the Elbow Joint for Mechanical Counter Pressure Space Suit Development." *2015 IEEE Aerospace Conference* (2015): n. pag. Web. 15 Nov. 2015.

23 Smith, CJ, and G. Havenith. "Body Mapping of Sweating Patterns in Male Athletes in Mild Exercise-in." *Induced Hyperthermia*. U.S. National Library of Medicine, 12 Dec. 2012. Web. 23 Nov. 2015.

24 Jones, Eric M. "Apollo Lunar Surface Journal : Apollo PLSS Images." *Apollo Lunar Surface Journal : Apollo PLSS Images*. Apollo Lunar Surface Journal, 31 Aug. 2008. Web. 06 Dec. 2015.

25 Borg G.A. Psychophysical bases of perceived exertion. *Medicine and Science in Sports and Exercise*. 1982; 14:377-381.

26 *Bühlmann, Albert A (1984). Decompression-Decompression Sickness. Berlin New York: Springer- Verlag. ISBN 0-387-13308-9.*